UNIVERSITÀ DEGLI STUDI DI TORINO

DIPARTIMENTO DI: NEUROSCIENZE

DOTTORATO DI RICERCA IN NEUROSCIENZE

CICLO XXXII

TITOLO DELLA TESI

Automatic assessment of movement disorders using ICT approaches for the monitoring and rehabilitation of Parkinson's disease

TESI PRESENTATA DA: Claudia Ferraris

TUTOR: Prof. Leonardo Lopiano

CO-TUTOR: Prof. Alessandro Mauro

COORDINATORE DEL DOTTORATO: Prof. Marco Sassoè

ANNI ACCADEMICI: 2016-2020

SETTORE SCIENTIFICO-DISCIPLINARE DI AFFERENZA: MED/26, ING-INF/06

Abstract

The continuous increase of life expectancy and the consequent aging of the population are radically changing the lifestyles and future prospects of world societies, with significant consequences on economic and social strategies. One of the sectors most impacted by demographic change is the healthcare sector, whose primary role is gaining growing interest, especially for the evaluation of the effects of these phenomena on the future sustainability of healthcare services. The estimates, provided by the latest reports of the World Health Organization (WHO), on the topic of global aging, indicate that the population over 65 will double by 2050, while the older population segment, i.e. the number of people over 80, will triple in the same period. The phenomenon of population aging is intrinsically accompanied by an increase in the number of individuals suffering from neurological diseases, generally "age-related", as demonstrated by numerous epidemiological studies. This raises further questions about sustainability in terms of costs and resources, and it is increasingly evident that only a multidisciplinary approach to the problem, even with the involvement of technological disciplines, can represent the only way to efficiently and effectively address the challenges of the near future. Already today, neurological diseases represent one of the most important causes of disability: among these, Parkinson's disease (PD) is the one with the highest growth rate in the number of cases diagnosed in recent years.

Parkinson's disease is a chronic and long-term pathology, mainly characterized by a progressive motor disability that has a strong negative, emotional and social impact on the quality of life of the individual and family. Adequate treatments of the disease are essential to control motor symptoms: this allows the individual to carry out the simplest daily activities while maintaining a lifestyle as independent and normal as possible. Drug therapy plays a major role in disease management; but equally important are the rehabilitation programs that aim at optimizing residual motor functions: both of these treatments are defined and adapted on the basis of the assessment of motor impairment severity. Traditional assessment methods include specific clinical tests and standardized rating scales, through which the patient status is analyzed and evaluated. In general, these scales are based on qualitative criteria and the score assigned to the patient's performance is often influenced by the skill and ability of the rater in detecting anomalies that are often imperceptible to the human eye. In addition, these scales are characterized by coarse scores, insensitive to slight alterations. Furthermore, the presence of at least one clinician is mandatory, who observes and judges the impairment: this

makes the assessments infrequent and generally limited to scheduled visits, delaying timely actions for example in case of symptoms worsening or fluctuations in the response to drug therapy.

This PhD thesis was developed in this context, trying to address the previously mentioned issues by adopting a multidisciplinary approach that involves Information and Communication Technologies (ICT). This has led to the development of innovative, cost-effective and non-invasive technological solutions that can become tools to support traditional clinical practice in defining new pathways and health services for the management of Parkinson's disease. Specifically, the designed solutions aim to objectively and automatically quantify the human body movement during the execution of some traditional motor assessment tasks commonly used to establish the severity of motor impairment and the best treatment of the symptoms. To this end, a combined approach of vision-based systems (using 3D optical sensors), Computer Vision techniques and Machine Learning methods was adopted. Algorithms dedicated to hand and body tracking enabled the accurate acquisition of body movements while performing standardized motor tasks for upper limb, lower limb and posture analysis. The objective evaluation through functional parameters, specific for each motor task, allowed to quantify the typical features of the movement and its minimal alterations due to motor symptoms, making it possible to monitor the progression on the basis of measurements of physical quantities as well as on the qualitative judgement only. Supervised learning methods made it possible to obtain an automated evaluation of movements strictly correlated to the standard clinical assessment, making the system comparable to a "clinical evaluator". Furthermore, the integration of natural human-computer interfaces, developed with the same methodological approach, made it possible to deploy the system "at patient's home", a step towards new patient management strategies based on "remote monitoring". Finally, it is important to consider that the versatility of the methodology makes these solutions easily adaptable to rehabilitation programs in home environments, to other pathologies characterized by movement disorders or applications for active aging: therefore, in general, to all those application contexts where it is important to evaluate the decline or improvement of motor functions.

Sommario

Il continuo allungamento della aspettativa di vita ed il conseguente invecchiamento della popolazione stanno cambiando radicalmente gli stili di vita e le prospettive future delle società a livello mondiale, con conseguenze significative sulle strategie economiche e sociali. Uno dei settori maggiormente impattato dal cambiamento demografico è quello sanitario, il cui ruolo di primaria importanza riscuote un sempre più crescente interesse, soprattutto per la valutazione degli effetti di questi fenomeni sulla futura sostenibilità dei servizi sanitari e di assistenza. Le stime degli ultimi rapporti dell'Organizzazione Mondiale della Sanità (OMS) sul tema dell'invecchiamento mondiale, indicano che la popolazione sopra i 65 anni raddoppierà entro il 2050, mentre il segmento più vecchio della popolazione, cioè il numero di persone con più di 80 anni, triplicherà nello stesso periodo. Il fenomeno dell'invecchiamento della popolazione è intrinsecamente accompagnato da un aumento del numero di soggetti colpiti da patologie neurologiche, in generale correlate all'età, come dimostrato da diversi studi epidemiologici. Questo pone ulteriori interrogativi riguardo alla sostenibilità in termini di costi e risorse, e risulta sempre più evidente che solo un approccio multidisciplinare al problema, anche con il coinvolgimento delle discipline tecnologiche, possa rappresentare l'unica strada per affrontare in modo efficiente ed efficace le sfide del prossimo futuro. Già oggi, le patologie neurologiche rappresentano una delle più importanti cause di disabilità: tra queste, la malattia di Parkinson (PD) sembra essere quella con il più alto tasso di crescita, come numero di casi diagnosticati, negli ultimi anni.

La malattia di Parkinson è una patologia cronica ed a lungo termine, caratterizzata principalmente da una progressiva disabilità motoria che ha un forte impatto negativo, emotivo e sociale sulla qualità di vita dell'individuo e della famiglia. Adeguato trattamenti della patologia sono fondamentali per il controllo della sintomatologia motoria: questo permette all'individuo di svolgere le più semplici attività quotidiane mantenendo uno stile di vita il più possibile indipendente e normale. La terapia farmacologica riveste un ruolo di primo piano nella gestione della patologia; ma altrettanto importanti sono i programmi riabilitativi che mirano all'ottimizzazione delle funzioni motorie residue: entrambi i trattamenti vengono definiti ed adattati in base alla valutazione della gravità della compromissione motoria. Le tecniche di valutazione tradizionale comprendono test clinici specifici e scale di valutazione standardizzate attraverso le quali viene giudicato lo stato del paziente. In generale, queste scale si basano su criteri di valutazione qualitativa ed il

punteggio assegnato alla prestazione del paziente è spesso influenzato dall'esperienza e dall'abilità del valutatore nel cogliere anomalie spesso impercettibili all'occhio umano. Inoltre, queste scale sono caratterizzate da punteggi grossolani, insensibili a lievi alterazioni e richiedono obbligatoriamente la presenza del medico che osserva e giudica la prestazione motoria: questo rende le valutazioni poco frequenti e generalmente limitate alle visite periodiche, ritardando azioni tempestive ad esempio nel caso di peggioramento dei sintomi o fluttuazioni nella risposta alla terapia farmacologica.

Questa tesi di Dottorato è stata sviluppata in questo contesto, cercando di affrontare le tematiche precedentemente menzionate con un approccio multidisciplinare che includesse le Tecnologie per l'Informazione e le Comunicazioni (TIC). Questo ha portato allo sviluppo di soluzioni tecnologiche innovative, dai costi contenuti e non invasive, che possono diventare strumenti di supporto alla pratica clinica tradizionale nella definizione di nuovi percorsi e servizi sanitari per la gestione della malattia di Parkinson. Nello specifico, le soluzioni progettate mirano a quantificare oggettivamente e automaticamente il movimento del corpo durante l'esecuzione di alcuni compiti motori di valutazione tradizionali utilizzati per stabilire la gravità della compromissione motoria ed il miglior trattamento della sintomatologia. Un approccio combinato di sistemi di visione (utilizzando sensori ottici 3D), tecniche di Visione Artificiale e metodi di Machine Learning è stato adottato con questa finalità. Algoritmi dedicati hanno permesso la cattura accurata del movimento di mano e corpo durante l'esecuzione di compiti motori standardizzati per l'analisi degli arti superiori, inferiori e della postura. La valutazione oggettiva mediante parametri funzionali, specifici per ciascun compito motorio, ha permesso di quantificare le caratteristiche tipiche del movimento e le sue minime alterazioni dovute ai sintomi motori, rendendo possibile una valutazione della progressione basato su misure di grandezze fisiche oltre che sul giudizio qualitativo. I metodi di apprendimento supervisionato hanno permesso di ottenere una valutazione automatizzata del movimento strettamente correlata alla valutazione clinica standard, rendendo il sistema paragonabile ad un "valutatore clinico". Inoltre, l'integrazione di interfacce uomo-macchina di tipo naturale, realizzate con la stessa metodologia, hanno permesso di distribuire il sistema "a casa del paziente", un primo passo verso nuove strategie di gestione del paziente basata sul "monitoraggio remoto". Infine, è importante considerare che la versatilità della metodologia rende queste soluzioni facilmente adattabili a programmi riabilitativi in ambiente domiciliare, ad altre patologie caratterizzate da disturbi del movimento o applicazioni per l'invecchiamento attivo: quindi, in generale, a tutti quei

contesti applicativi in cui è importante valutare il decadimento o il miglioramento delle funzioni motorie.

To my family and

to my parents, the brightest stars in the sky,

that guide my steps and inspire my hearth

Acknowledgements

Many people have contributed to this work and all of them deserve to be thanked. First of all, I thank Prof. Mauro, who convinced me to start this "adventure": years ago I would not have thought of this possibility, even if the desire to create something useful in the medical field was the main reason why I started my studies in computer science many years ago. I would also like to thank my colleagues of IEIIT-CNR, and in particular Dr. Nerino, Dr. Chimienti and Dr. Pettiti, who have supported me over these years, finding the necessary funding to continue and complete the research project. Finally, I would like to thank the neurologists of San Giuseppe Hospital in Piancavallo (VB) and the Department of Neurosciences, whose clinical contribution was fundamental and, obviously, all the "patients" and their families, who patiently participated with interest, curiosity and hope in the realization of all this.

But above all, a big thanks goes to my family, in particular to my husband Roberto and my daughter Martina, who have always supported and encouraged me, but also endured me in the most difficult and complicated time: without them it would not have been possible to achieve this goal. And finally, I would like to thank my parents who are no longer here today but who follow my steps from heaven, inspiring and supporting me as they have always done in their lives.

Thank you all!!!

List of Abbreviations

WHO	World Health Organization (OMS in Italian)
PD	Parkinson's disease
ICT	Information and Communication Technologies (TIC in Italian)
AAL	Active and Assisted Living
EIP AHA	European Innovation Partnership on Active and Healthy Ageing
ASD	Autism Spectrum Disorders
MS	Multiple Sclerosis
MOCAP	Motion capture
BSN	Body Sensor Network
HMI	Human-Machine Interface
GP_i	Internal Globus Pallidus
GP_e	External Globus Pallidus
UPDSBB	UK Parkinson's Disease Society Brain Bank
MAO-B	Monoamine Oxidase B
DBS	Deep Brain Stimulation
IPG	Internal Pulse Generator
H&Y	Hoehn and Yahr
UPDRS	Unified Parkinson's Disease Rating Scale
ADL	Activities Daily Living
MDS	Movement Disorder Society
IR	Infrared
DOF	Degrees of Freedom
ToF	Time of Flight
SDK	Software Development Kit
IMU	Inertial Management Unit
AI	Artificial Intelligence
CNN	Convolutional Neural Network
GPU	Graphical Processing Unit
HC	Healthy Controls
GUI	Graphical User Interface
HCI	Human Computer Interaction
AR	Augmented Reality
CV	Coefficient of Variation
PCA	Principal Component Analysis
NB	Naïve-Bayes
LDA	Linear Discriminant Analysis
MNR	Multinomial Logistic Regression
KNN	K-Nearest Neighbours
SVM	Support Vector Machine
LOOCV	Leave-One-Out cross validation
CoM	Center of Mass
CoP	Center of Pressure
PIGD	Postural Instability and Gait Difficulty
AP	Antero Posterior

ML	Medio-Lateral
ICC	Intra Class Correlation
PSSUQ	Post-Study System Usability Questionnaire
MCI	Mild Cognitive Impairment

List of Figures

Figure 1: Steps and mechanisms involved in picking up an object 5
Figure 2: Regions of the frontal lobe and main functions. 6
Figure 3: The anatomical structure of the basal ganglia and the related structures. 18
Figure 4: Direct (left) and indirect (right) pathways of basal ganglia from coronal view. 19
Figure 5: The UPDSBB diagnostic criteria used in clinical practice. 22
Figure 6: Evolution of the response to Levodopa with PD progression. 24
Figure 7: Deep Brain Stimulation: main components and brain areas treated. 25
Figure 8: An example of MDS-UPDRS item (Finger-Tapping motor task) 28
Figure 9: Example of environment dedicated to motion analysis with an optoelectronic system. 34
Figure 10: Optoelectronic system with passive markers 35
Figure 11: Optoelectronic system with active markers 35
Figure 12: Helen-Hayes marker set or Davis protocol 36
Figure 13: Types of BTS optoelectronic systems with technical specifications 38
Figure 14: The Microsoft Kinect© (on the left) and its main inside elements 40
Figure 15: Images generated by the RGB-Depth camera. 41
Figure 16: The skeletal tracking algorithm. 42
Figure 17: The Microsoft Kinect v.2 (left) and 3D reconstruction of the scene (right) 43
Figure 18: The alternatives to Microsoft Kinect: Astra Pro (left), D415 (centre), D435 (right) 45
Figure 19: The Nuitrack skeletal model 46
Figure 20: The Leap Motion (left) and the hand skeletal model (right) 46
Figure 21: The Kinect Azure (left), the depth image (centre) and the IR image (right) 47
Figure 22: The skeletal model of Kinect Azure 48
Figure 23: Multi-persons tracking with OpenPose 49
Figure 24: Schema of the proposed approach for upper limb assessment 52
Figure 25: The acquisition system: configurations with notebook (left) and mini-pc (right) 53
Figure 26: Hand Tracking algorithm: static open hand (left); dynamic semi-closed hand 56
Figure 27: Glove with reflective markers for the optoelectronic system 56
Figure 28: Example of FT task: 3D trajectory (top) and speed (bottom) captured by the two systems 58
Figure 29: Tracking errors of Leap Motion tracker (blue line) 59
Figure 30: Example of the Leap Motion failures in little-finger trajectory during the Pronation-Supination 60
Figure 31: Example of GUIs for the gestural human-interaction with the acquisition system 62
Figure 32: Example of 3D trajectory of an healthy subject (FT task) 63
Figure 33: Example of 3D trajectories (FT task) for different level of impairment. 65
Figure 34: 2D representation of the 3D reference points used for PS (left), OC (centre) and FT (right) tasks 65
Figure 35: Detection of elementary movements (OC tasks) 66
Figure 36: Example of descending speed in central and final periods 67
Figure 37: Example of "freezing" detection 68
Figure 38: Example of "partial movement" detection (incomplete hand closure) 68
Figure 39: Example of "hesitation" detection 68
Figure 40: Frequency Analysis to detect rhythm variations in the motor performance 69
Figure 41: Relationship of parameters for Finger Tapping task 71
Figure 42: Guttman Monotonicity Coefficients between pairs of parameters 72
Figure 43: Guttman Monotonicity Coefficients between parameters and UPDRS severity scores 72
Figure 44: Radar chart of significant selected parameters versus UPDRS (Finger Tapping task) 76
Figure 45: Radar chart of significant selected parameters versus UPDRS (Hand Movements task) 77
Figure 46: Radar chart of significant selected parameters versus UPDRS (Pronation-Supination task) 77
Figure 47: Schema of the training phase for supervised classifiers 79
Figure 48: Schema of the prediction phase of supervised classifiers 79
Figure 49: Example of classifiers prediction for the GOOD and BAD performance of Figure 48 79
Figure 50: Example of performance with LEFT and RIGHT hand (Finger Tapping) 84
Figure 51: Example of performance with LEFT and RIGHT hand (Hand Movements) 85
Figure 52: Example of performance with LEFT and RIGHT hand (Pronation Supination) 86
Figure 53: Schema of the proposed approach for the assessment of body movement 92
Figure 54: The system configuration with mini-pc (left) and the visual feedback on monitor (right) 93
Figure 55: Position of 3D joints in real space (Left); position of 2D joints on color image (Right) 93

Figure 56: 3D position of joints (left) and CoM_{body} (right) on point cloud (3D reconstruction of body) 95
Figure 57: Markers configuration for validation procedure 96
Figure 58: Example of ANG_{KNEE} and ANG_{TRUNK} trajectories 98
Figure 59: Examples of GUIs to select tasks and legs 100
Figure 60: Segments involved in angular measures for LA, AC and Po tasks 101
Figure 61: Radar charts of normalized kinematic parameters for LA (a), AC (b), Po (c) and PS_{COM} (d) 105
Figure 62: Example of CoM_{body} trajectories during the $Phase_1$ and $Phase_2$ of Po task (i.e., PS_{COM}) 109
Figure 63: Worsening of CoM_{body} parameters between $Phase_1$ and $Phase_2$ 110
Figure 64: Infrastructure of the remote-monitoring platform 115
Figure 65: The main window of the Patient subsystem 116
Figure 66: The GUI window to enter time of drug intake (left) and the perceived dyskinesia level (right) 116
Figure 67: Guided mode window with list of tasks to be performed 117
Figure 68: Main window of Clinician subsystem 118
Figure 69: Comparison between left and right hand (in the same acquisition session) 119
Figure 70: Comparison over time between left and right hands performance (different acquisition sessions) 119
Figure 71: Trend of kinematic parameters over time 120
Figure 72: Results of the PSSUQ questionnaire on the system usability 122
Figure 73: Linear trends of "per week" data aggregation (Finger Tapping task) 124
Figure 74: Linear trends for "time bands" data aggregation (Finger Tapping task) 125
Figure 75: Linear trends for "time bands" data aggregation (Hand Movements task) 125
Figure 76: Linear trends for "time bands" data aggregation (Pronation Supination task) 126
Figure 77: Example of abnormal behaviours during Pronation-Supination task with right hand 127
Figure 78: Example of clinical and instrumental assessment for FT task 129
Figure 79: Example of clinical and instrumental assessment for CO task 129
Figure 80: Example of clinical and instrumental assessment for PS task 129

List of Tables

Table 1: List of the original articles published during the research activity 15
Table 2: The H&Y rating scale with description of the progressive forms of disabilities. 27
Table 3: List of MDS-UPDRS items considered and analysed. 31
Table 4: Comparison between Kinect v.1 and Kinect v.2: hardware components 43
Table 5: Comparison between Kinect v.1 and Kinect v.2: software components 44
Table 6: Accuracy of the tracking algorithm for the three tasks 57
Table 7: Accuracy of the Leap Motion tracking algorithm for the three tasks 58
Table 8: Characteristics of PD and HC groups 60
Table 9: Contribution (%) of parameters to the major PCA components 73
Table 10: Significant Parameters for Finger Tapping task (FT) 74
Table 11: Significant Parameters for Hand Movements task (OC) 74
Table 12: Significant Parameters for Pronation-Supination task (PS) 75
Table 13: Accuracies for binary (Healthy vs PD) and multiclass (Healthy vs UPDRS) classifications 82
Table 14: Segments, joints and anthropometric data for CoM body estimation 95
Table 15: Correspondence between skeletal model and markers 97
Table 16: Mean and standard deviation of correlation coefficients 97
Table 17: Characteristics of PD and HC groups 98
Table 18: Significant parameters for LA task (with respect to Leg Agility scores) 103
Table 19: Significant parameters for AC task (with respect to Arise from Chair scores) 103
Table 20: Significant parameters for Po task (with respect to Posture scores) 103
Table 21: Significant parameters for PS_{COM} task (with respect to PIGD scores) 103
Table 22: Distribution of severity UPDRS scores for PD subjects 107
Table 23: Accuracies of classifiers for binary (Healthy vs PD) and multiclass (UPDRS severity) problems 107
Table 24: ICC between system and neurological assessment 108
Table 25: Average difference of postural parameters between $Phase_1$ and $Phase_2$ for HC and PD subjects 110
Table 26: ICC values between the scores of reference neurologist from videos (N) and system (SY) 121
Table 27: Results of the questionnaire on the technological skills 121
Table 28: Results on the ability to wear gloves 122
Table 29: Failure rate and number of valid sessions for week 123

Contents

Abstract ..... **III**
Sommario ..... **V**
Acknowledgements ..... **IX**
List of Abbreviations ..... **X**
List of Figures ..... **XII**
List of Tables ..... **XIV**
Contents ..... **XV**
1) Introduction **2**
1.1 Motor function and complex movements: the role of the brain 5
1.2 Qualitative and quantitative analysis of human movement 7
1.3 Background and related work on quantitative analysis of human movement 8
1.4 Motivation and thesis outline 13
2) Parkinson's Disease **16**
2.1 History 16
2.2 Epidemiology 17
2.3 Pathophysiology 18
2.4 Symptomatology and Clinical Diagnosis 20
2.5 Disease Management 22
2.6 Clinical Rating Scale 26
2.7 Contribution of the thesis on Parkinson's Disease 29
3) Vision-based systems for motion analysis **32**
3.1 Historical evolution of vision-based systems 32
3.2 Marker-based motion capture: the optoelectronic systems 33
3.3 Marker-free motion capture: the 2D camera-based systems 38
3.4 Marker-free motion capture: the 3D camera-based systems 39
3.5 The future: Deep Learning approaches (OpenPose) 48
3.6 Thesis Motivation on RGB-Depth cameras 49
4) Quantitative assessment of hand motor function using vision-based systems **51**
4.1 Schema of the proposed approach 51
4.2 Data Acquisition 53
4.3 Performance Analysis 62
4.4 Classification 78
4.5 Example of automatic assessment 83
4.6 Issues and Limitations 87

4.7 Summary and Discussion 88
5) Quantitative assessment of body motor function using vision-based systems 90
5.1 Schema of the proposed approach 90
5.2 Data Acquisition 92
5.3 Performance Analysis 100
5.4 Classification 105
5.5 Focus on the analysis of postural stability 108
5.6 Limitations 111
5.7 Summary and Discussion 111
6) New perspectives in management of neurological diseases 114
6.1 Technology at "patient's home" 114
6.2 Experimental Protocol 120
6.3 Usability 121
6.4 Main results of the first experimental test: analysis of aggregated data 123
6.5 Main Results of the second experimental test: anomalies and fluctuations 126
6.6 Summary and Discussion 130
7) Conclusions and Future Work 131
7.1 Thesis Contributions 131
7.2 Future Work 133
7.3 The future of Telemedicine 134
References 135

Chapter 1

Introduction

In recent years, many developed and developing countries have experienced major changes in the demographic composition of their populations that have conditioned and will increasingly influence economic and social policies in the near future[1]. "Silver Tsunami" is one of the metaphorical terms used to describe the global demographic transition towards an elderly population caused by the concomitance of two factors: increase in longevity and decrease in birth rate[2]. As confirmed by the latest reports from the World Health Organization (WHO) focusing on health and aging issues, projections indicate that the "over 65" world population will double by 2050, while the "over 80", the oldest segment of the population, will triple in the same period[3,4].

There are many conflicting opinions on the effects of the transition to a global older population: while this demographic change is considered, with a very positive flavor, as a new opportunity for economic growth (the so-called "Silver Economy"), on the other side, with a totally negative feeling, is only considered as a big problem to be faced in terms of costs and resources. The opportunities of the Silver Economy are closely linked to active healthy aging, which allows people to travel, work, learn new things, improve interests and knowledges, live independently for many years to come.

In Europe, for example, these issues have focused the attention of policy makers and economic operators in various fields such as research and innovation, industry, home automation, pharmacology, health services, also favoring the creation of new professionals and jobs[5]. Several projects have been funded by the European Commission under the H2020 program, the Active and Assisted Living Program (AAL) and the European Innovation Partnership on Active and Healthy Ageing (EIP AHA) to promote research synergies and innovation focused on active and healthy aging, with a particular focus on economic and social effects. On the contrary, another line of thinking only looks at the dark side of demographic changes, namely the economic burden for the public pension and health systems[6]. In particular, the public health system is one of the most affected by this trend and its sustainability is much debated and source of uncertainty.

The demand for health services depends on the number of people in need of care: this is determined not only by the size but also by the state of health of the population, which is

directly related to age and the percentage of elderly people in the overall population. Although the population lives longer, the population is not necessarily healthier: this is also a hotly debated issue. Changes in the disability rate are considered a measure of population health associated with aging. Some experts estimate a decrease in the prevalence of disability with increasing life expectancy; others see an increase in overall disability; still others argue that while medical advances will slow the progression of chronic diseases with severe disabilities, chronic diseases with mild disabilities will increase[7]. In particular, there is a worldwide "epidemiological transition" linked to the aging of population: it is characterized by the increase in chronic, neurological and neurodegenerative diseases. The increase in these pathologies and related disabilities represents one of the main epidemiological trends of the last century[8,9].

Among these, Parkinson's disease appears to be the one with the fastest growth in terms of prevalence and disability. Prevalence reflects both the incidence and the duration of the disease: the incidence is related to risk factors, of which "age" is the most important; duration is linked to longevity, which implies a longer disease duration[10]. Disability is associated with the progressive loss of independence in basic and daily activities: it is closely linked to symptoms severity and to the identification of the most appropriate treatments to contain their effects[11].

More in general, the ability to treat people with chronic and long-term diseases is the key to prolong life with good quality, but how will countries cope with the challenges and heavy burden of care and assistance? The answer seems to be linked to a "revolution" of the health system, in which ICT will increasingly become part of clinical practice, playing a key role in defining new strategies for disease management and patient care. Considering ICT as a strategic tool will allow healthcare professionals and patients to benefit from the opportunities offered by innovative and widespread technologies which, until a few years ago, were confined to other productive sectors[12]. One of the most promising and revolutionary proposal for the future of the health system is telemedicine, a very broad term that includes different definitions and applications (such as telehealth, tele-diagnosis, remote monitoring, tele-rehabilitation) that share the concept of "distance"[13]. As indicated by WHO[14], a more general definition of telemedicine is "*The delivery of health care services, where distance is a critical factor, by all health care professionals using information and communication technologies for the exchange of valid information for diagnosis, treatment and prevention of disease and injuries, research and evaluation, and for the continuing education of health care providers, all in the interests of advancing the health of individuals*

and their communities". It is therefore clear that this transformation process must be based on a multidisciplinary approach that involves both health and technological skills, in order to identify the most appropriate solutions to problems and needs related to specific pathological conditions. For example, ICT solutions are widely used in autism spectrum disorders (ASD) through the use of virtual interaction environments, special communication devices (including robots), avatars and tele-rehabilitation applications, in order to evaluate responses of autistic children to specific behaviors, to teach and practice skills[15]. ICT solutions are also used for tele-rehabilitation in multiple sclerosis (MS), in order to extend traditional rehabilitation treatments beyond the hospital, to provide the same rehabilitation programs to geographically disadvantaged subjects and to improve the general quality of treatments[16]. The same happens for dementia and related cognitive pathologies, in which ICT solutions are used to provide technological aids, to develop ambient-assisted living systems, tools for the assessment and practice of cognitive functions, to maintain social relationships[17]. These are just a few examples of ICT application domains: the potential is practically infinite, but the mutual knowledge of health needs and technological possibilities is fundamental to design truly useful solutions.

In the context of PD, one of the most important clinical needs is the assessment of typical motor symptoms, which cause various forms of disability from the onset of the disease. Traditional clinical evaluation of motor symptoms is based on observation and judgement of their effects on movements, applying the qualitative criteria established by the standard and international evaluation scales. However, these qualitative criteria implicitly require to consider some physical quantities (such as amplitudes and velocities of movements), potentially measurable and quantifiable but certainly not for the human eye. The quantitative and automatic assessment of motor symptoms is recognized as one of the main challenges for a different management of PD in the near future. The key point lies in the design and development of ICT solutions capable of supporting clinical practice with objective measurements of specific physical quantities strictly correlated to the severity of motor impairment and well correlated to traditional clinical evaluations. In this way, it would be possible to keep the progression of symptoms under control, detect early alterations in motor function, measure the effects of pharmacological and rehabilitative treatments, quantify the response to therapy and customize the dosage, create platforms for remote monitoring and rehabilitation to follow up people outside health facilities. This process would generate significant benefits both for healthcare professionals, who could follow up patients with

greater continuity, and for patients who could be followed up at a distance in more familiar environments.

This thesis aims to develop some technological solutions for the objective and automatic assessment of motor function in Parkinson's disease, trying to address part of the opportunities and issues previously mentioned. The quantitative assessment of motor function represents the starting point for designing, for example, remote monitoring platforms and for defining new decentralized pathways for motor rehabilitation, applicable not only to Parkinson's disease but, more generally, to other clinical scenarios and pathological.

1.1 Motor function and complex movements: the role of the brain

Almost all of our activities involve motor function, even when we don't think about it explicitly: every time we talk, smile, walk, we are using motor function. In general, we can consider motor function as the ability to perform voluntary movements in response to external stimuli. Everything that we observe, listen to, perceive around us generates a reaction which, in most cases, results in natural and autonomous movements of the body or part of it[18]. But even the simplest movement is actually a very complex task, if we consider all the components involved and the mechanisms activated to achieve it [Figure 1].

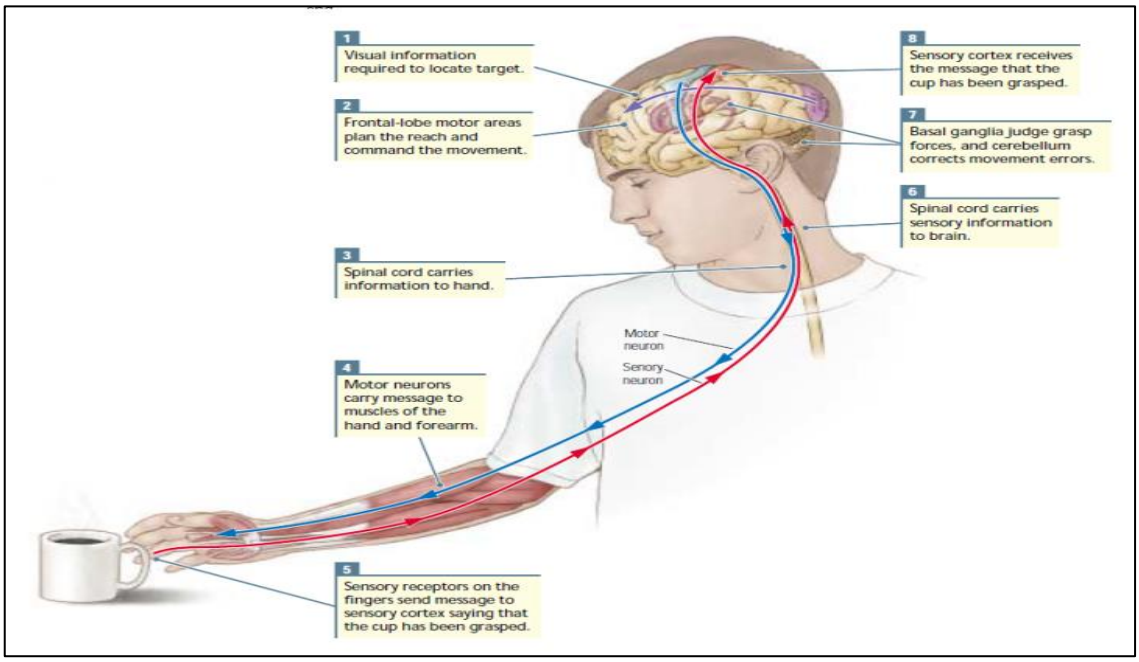

Figure 1: Steps and mechanisms involved in picking up an object
[Image source: 18]

Motor function is supported by the motor system, a complex integration of central and peripheral components of the nervous system that have a hierarchical organization. Central components include the neocortex which, in human brain, represents the largest part of the cerebral cortex, the brainstem and the spinal cord[18]. Peripheral structures involve skeletal muscles and neural connections with muscle tissue[19].

The cerebral cortex is part of the anterior brain: its main functions are processing sensory information, controlling motor functions, performing high-order functions such as reasoning and problem solving. It is divided into four lobes for each cerebral hemispheres. In particular, the frontal lobes are responsible for planning and initiating the sequence of steps that will produce precise movements[18]. The frontal lobe area is further divided into multiple parts, including the prefrontal cortex, premotor cortex and primary motor cortex [Figure 2]. The prefrontal cortex acts as a planner for complex tasks: it does not indicate the precise movements to be performed but rather it specifies the final goal of the movements, sending appropriate instructions to the premotor cortex. The premotor cortex organizes complex sequences of movements to be performed: damage in the premotor cortex prevents the generation and coordination of the sequences and, therefore, the achievement of the final goal. Although the premotor cortex is responsible for coordinating and organizing the overall task, it does not specify how each individual movement should be performed. This is the function of the primary motor cortex that is responsible for performing skillful movements.

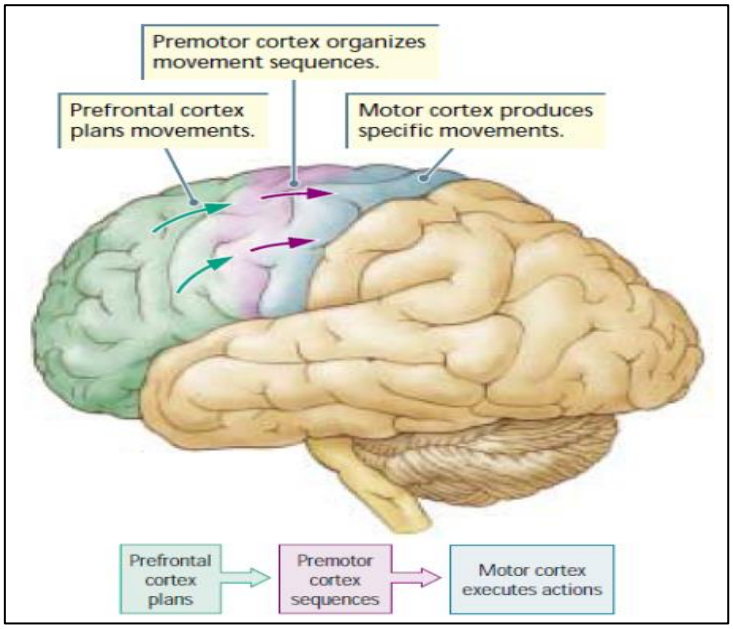

Figure 2: Regions of the frontal lobe and main functions.
[Image source: 18]

The brainstem is a small component of the brain. Despite this, it plays a crucial role in the transport of motor and sensory information from the brain to the body and from the body to the brain. Among other functions, the brainstem is important for posture, for the ability to stand upright and for the coordination of limb movements. The brainstem is directly connected to the spinal cord. The spinal cord is a structure of nervous tissue that extends from the brainstem to the lumbar region of the spine: it is the main pathway between the brain and the peripheral nervous system. The primary functions are the transmission of nerve signals from the motor cortex to the rest of the body and the independent generation of reflexive movements. Two other regions of the brain, the basal ganglia and the cerebellum, play an active role in controlling movement: the evidence is that any damage to these structures generates forms of motor impairment. The cerebellum, located in the posterior brain, is directly involved in the control of movements: it improves motor skills by using a timing mechanism and a continuous evaluation of the actual movements compared to those expected, to calculate the appropriate corrections and adjust the right action. The basal ganglia are a collection of nuclei in the forebrain connected to the motor cortex and the midbrain, which have a strong connection with the cerebral cortex, thalamus and brainstem and are involved in the control of voluntary movements. The basal ganglia are involved in motor control by regulating, for example, the force associated with a specific movement. Consequently, any damage to the basal ganglia produces involuntary and unwanted movements when excessive force is exerted (hyperkinetic disorders), or insufficient voluntary movements when poor force is exerted (hypokinetic disorders). The basal ganglia are made up of different components that have a complex anatomical and neurochemical organization: dysfunctions in specific components or mechanisms related to the basal ganglia are at the origin of a wide spectrum of neurological disorders, behavioral control and motor impairment[20]. In particular, PD falls into the category of hypokinetic disorders[18]: damage to specific components of the basal ganglia causes the loss of motor ability to produce normal movements, but these aspects will be further discussed in Chapter 2 where a more detailed description of the characteristics of Parkinson's disease is presented.

1.2 Qualitative and quantitative analysis of human movement

The severity of motor impairment (or disability) in pathological conditions is generally based on specific qualitative criteria, as established by international rating scales, to evaluate the effect of symptoms on human body movement. This involves a qualitative analysis of movement (or performance) in completing well-defined tasks in order to assign scores or

judgements. But what is the meaning of qualitative analysis? According to Knudson (2002)[21], the qualitative analysis is the "*systematic observation and introspective judgement of the quality of the human movement for the purpose of providing the most appropriate intervention to improve performance"*. There are three key elements that emerge from this definition: observation, intervention and performance. Observation refers to the process of assigning a precise meaning to sensory information collected about a performance: this process is closely related to perception and, in general, good observation involves all senses and not just visual inspection. Intervention refers to any feedback or correction that can help in improving performance. Performance refers to the effectiveness of movement aimed at achieving specific goals. Qualitative analysis is by its very nature a subjective process, in which a judgement is expressed on the quality of movement: to be more effective in-depth information, training and, above all, experience are required. It is therefore clear how this definition describes exactly the qualitative evaluation process adopted in clinical practice: the observation of how movement is performed during specific tasks is the basis for judging a performance and establishing an intervention (i.e. treatment) capable of improving it.

In reality, the analysis of human movement can take place along a sort of continuum, which goes from qualitative to quantitative with different intermediate levels depending on the complexity of the analysis: the whole qualitative part can be summarized as a non-numerical analysis of the movement; on the contrary, the quantitative part produces a numerical measure of some aspects of the movement[21]. If some characteristics of human movement can be objectively expressed as numbers, the analysis is quantitative: obviously, this does not automatically guarantee the validity and reliability of the measure, but if it were possible to guarantee it, objective data could support qualitative analysis with greater accuracy, consistency and precision[22]. There are many advantages of adopting a quantitative approach to human movement analysis: for example, the ability to "numerically" compare performance over time, quantify changes in performance, check whether a movement was performed correctly or how long has deviated from a reference.

1.3 Background and related work on quantitative analysis of human movement

The first attempts to characterize and quantify human body movement through instrumental measurements date back to several years ago, when, in many cases, dedicated systems or apparatuses were specifically designed to measure particular characteristics of movement. In Salter et al. (1953)[23], for example, a wrist-cuff mechanical arthrometer was designed to measure forearm rotation amplitude under elbow and shoulder flexion conditions.

In Thomas et al. (1959)[24], a first force platform was constructed and used to obtain a continuous record of the horizontal reaction forces and to estimate the centre of pressure of the foot, while in Murray et al. (1967)[25] the force platform was used to quantify the amplitude and orientation of the vertical supportive force during specific activities such as squats, jumping and in seated position. In Ramsey (1968)[26], a complex mechanical and electrical wearable structure was designed and used to quantify human effort and movement of the upper limbs: it can be considered a first example of an upper body exoskeleton, whose technological evolution produced those used today in many assisted rehabilitation treatments for upper limbs. Many other attempts can be cited with the aim of quantifying movement or physiological signals in different fields of interest can be cited: in Polo et al. (1968)[27], a sensitive bed was designed to measure obstructive sleep apnoea and sleep-related breathing disorders; in Angel et al. (1970)[28], a mechanical joystick with potentiometer was used to monitor hand movement and measure akinesia in Parkinson's disease; in Salzer (1972)[29], a three-dimensional accelerometer was used to determine the axis in which the tremor amplitudes were greatest; in Winter et al. (1972)[30], a television-computer technique was used to record and process images for kinematic analysis of human gait; in Lamoreux (1971)[31], an overview of tools for quantifying the human gait and differences in gait patterns was presented; in Velasco et al. (1973)[32], an attempt to quantify the positive effects of levodopa treatment on Parkinson's disease symptoms was tested by using mechanical and electrical equipment to analyse tremor and upper limb movements; in Morris (1973)[33], the potential of accelerometers for the analysis of leg movements and other parts of the body was explored; in Ackmann et al. (1977)[34], a transducer was designed to quantify the angular displacement of the wrist or metacarpophalangeal joints caused by flexion-extension tremor, with the aim of recording long-term data under conditions similar to everyday life; in Stern et al. (1983)[35], an instrumented walkway was used to study the gait and mobility of Parkinsonian patients through the analysis of videotapes.

In these first attempts to quantify human body movement, the role of the technical components is evident: in particular, the mechanical and electronic skills have allowed the design and development of instrumental systems for the capture of the physiological or pathological features of human movement. Already in those years, the synergy between technical and medical skills was fundamental, addressing the problem with a multidisciplinary approach to obtain good results. Other characteristics of these instrumental systems were the size, encumbrance and complexity due to the limited computational resources of those years, which made them usable only in dedicated research laboratories.

As mentioned above, it is important to note that the same efforts are still ongoing today due to the need to introduce new technologies and analytical techniques that can improve clinical practice. The technological progress of recent years is leading to less invasive and bulky but more usable and accurate solutions, finding the right compromise based on clinical needs. However, this process is still an open challenge and many factors need to be considered: cost, complexity, reliability, technical support, agreement between instrumental measures and clinical indicators.

Today, the most common solutions used for motion analysis fall into four categories: marker-based motion acquisition systems (MOCAP), marker-free vision-based systems, wearable sensors, and, most recently, applications for smartphone.

Marker-based motion capture systems involve the placement of special markers on the body according to specific biomechanical protocols and consist of a complex geometry of video-cameras capable of recognizing and tracking each individual marker during body movements[36]. Over the past few decades, marker vision-based systems have progressed to ever more accurate and automated systems, enabling their use in various fields including cinematography, sports, virtual gaming, rehabilitation, and clinical applications. In particular, the optoelectronic systems, the most famous MOCAP systems, are considered the gold-reference or gold-standard systems in the analysis of human movement in clinical applications, thanks to their precision in capturing and estimating body movements in several pathological and non-pathological conditions. To cite some examples, optoelectronic systems were used to analyze motor disability during gait in two genetic syndromes with the aim of producing data to establish common rehabilitation strategies[37]; evaluate the effects of transcranial direct current stimulation on gait patterns in children with cerebral palsy[38]; measure 3D scapula-humeral motion in children with hemiplegic cerebral palsy[39]; evaluate the effects of obesity on mechanical behavior and spinal morphology[40]; investigate the anatomical recovery of the function of the anterior cruciate ligament[41]. These few examples show how MOCAP can be used for quantitative analysis of movement in different pathological scenarios. Despite increased measurement accuracy, the use of these systems is generally limited to clinical and research environments due to the size, complexity, cost and oversight of technical personnel. These drawbacks and recent technological advances have pushed towards cheaper and more portable systems, capable of extending motion analysis to other environments but ensuring accuracy and consistency with the reference measurements obtained in the clinical setting.

Marker-free vision-based systems have always been considered an alternative to MOCAP systems. Among them, video motion analysis is a technique for describing movements from recorded videos. For many decades, video motion analysis has relied on cinematographic cameras, characterized by high image quality and high frame rates, and manual frame-by-frame localization of different points of interest (i.e. joint of body segments) which required long processing times[36]. The technological evolution and the availability of more performing computers have allowed to move to semi-automatic analysis supported by Computer Vision algorithms able to ensure great robustness and accuracy to vision-based systems without markers. However, the real revolution came ten years ago, when a new generation of commercial optical devices, called RGB-Depth sensors, first of all Microsoft Kinect©[42], was introduced to the gaming market. These devices were characterized by two innovative aspects compared to those previously available. The first was the ability to produce not only color images like any traditional camera, but also depth information (i.e. the distance from the sensor) allowing a three-dimensional reconstruction of the scene and measurements of physical quantities (such as length or height) as real dimensions. The second was the ability to capture full-body movements in a completely non-invasive way through automatic and real-time tracking algorithms of skeletal models. In a short time, these sensors were used in various applications as cost-effective solutions for the biomechanical analysis of movements[43]. Although the accuracy is lower than traditional MOCAP systems, it is still satisfactory as several studies have demonstrated, making these devices a good compromise between cost and performance[44,45]. To cite some examples of the first studies in clinical applications, RGB-Depth sensors were used to verify the feasibility of motion analysis in Parkinson's disease[46]; designing physical rehabilitation programs for young adults with motor disabilities[47]; measure the motor function of the upper limbs[48]; to quantify upper limb impairment due to stroke[49]. The widespread use of these systems as tools for motion analysis is also demonstrated by the numerous applications cited by Webster (2014)[50] related to elderly people and stroke rehabilitation; by Springer (2016)[51] on gait assessment; by Ibanez (2014)[52] on gesture recognition and human computer interaction; by Lun (2015)[53] on general applications of human motion recognition. Despite the innovative features and potential of these devices, the main drawbacks are related to occlusions, i.e. when part of the body is not visible; robustness of tracking, particularly when more general body movements are performed; small dimensions of the working volume that depend on the intrinsic characteristics (e.g. field of view, operating depth range) of the optical sensors. All of these topics will be covered in more detail in Chapter 3.

In recent times, wearable sensing technology has been successfully applied in many scientific fields that require the measurement of physiological and movement parameters of the human body, such as medicine, entertainment, safety and security in the workplace, sports and training[54]. This approach was widely used in monitoring of human activity, especially in the medical and rehabilitative sciences[55], when technological evolution made it possible to miniaturize wearable sensors making them more comfortable, flexible, less bulky and, above all, able to measure specific data from the human body[56]. It is particularly important that these sensors are lightweight so as not to hinder the natural movement of the body and not to be a burden if worn for long periods. In medical sciences, this sensing technology allows to monitor many physiological data such as body temperature, brain activity, hearth activity, muscle signals, sleep apnea[54]. Regarding motion analysis, wearable sensors are attached to body segments or parts to collect data during motor performance. Wearable sensors can be used in a "single sensor" configuration, as described by Long et al. (2009)[57] who proposed a single tri-axial accelerometer to classify sport activities; or "integration of multiple sensors" into a single device, as described for example by Nam et al. (2013)[58] where a tri-axial accelerometer and a video camera were embedded into the same wearable sensor to recognize nine human activities. Advances in wireless communication have led to complex multi-sensor wireless configurations[59], most notably Body Sensors Network (BSN), in which multiple synchronized wireless sensors are used to collect physiological data from the human body, allowing for the monitoring of human activities at affordable cost, for long periods, in a less-invasive way and in real time[60]. Despite the potential of wearable sensors in motion analysis applications, there are some issues that need to be addressed and that still represent an open challenge today. In particular, sensor calibration and pairing procedures that often require some technical skills; energy consumption for normal and communication activities which requires periodic recharging of the battery and limits the miniaturization of the sensors; the accuracy and completeness of the measurements that often require the use of more complex configurations with consequent higher costs.

Wearable technologies include all devices that can be worn, enabling the collection of data from the body and interaction with the surrounding environment. Without a doubt, nowadays, smartphones represent the most widespread and used object that we usually carry with us at any time of the day. Smartphones can be considered, to all intents and purposes, wearable devices that integrate different types of basic sensors suitable to recognize human activities[61]. Accelerometers and gyroscopes are the most popular choices for analyzing posture, movements and mobility, as they are easily worn on the body: the widespread use of

smartphones, equipped with accelerometers (available since 2007) and, more recently, gyroscopes is leading to consider smartphones as economical and alternative solutions to traditional wearable sensing technology in many motion analysis applications[62,63,64,65,66]. Certainly the advantages of using smartphones as wearable devices for motion and mobility analysis lie in the powerful on-board processing unit, in the long-lasting battery, in the ubiquitous connectivity through various wireless protocols, in the easy development of biomechanical applications and biofeedback using data from all integrated sensors. Despite this, there are some limiting factors in using smartphones as human motion sensors. In particular, due to the size and weight, they cannot be anchored to all parts of the body without interfering with natural movements. Another disadvantage concerns the inability to track complex movements that involve multiple parts of the body at the same time. The last drawback relates to some aspects that could influence the overall performance: the accuracy of the measurement, which often depends on the part of the body on which the smartphone is applied; inaccuracy in reading data from the integrated sensors; the dynamics of the movement that must fall within the dynamic range and the actual sampling rate of the sensor to be correctly detected[67].

1.4 Motivation and thesis outline

After exploring and analyzing possible technological solutions that can be used for the human motion analysis, this PhD thesis focused on vision-based systems without markers using RGB-Depth optical sensors. Although, at the time of the project proposal, these approaches were widely explored in clinical research, the state-of-the-art review revealed that their application was limited to specific parts of the body in most studies, without fully exploiting the potential of these technologies especially in pathologies characterized by a functional alteration on different body domains and, therefore, by the need for an overall view of motor impairment. In many cases, this problem is addressed using multi-sensor approaches, where different types of sensors are proposed to analyze specific areas of the body. Obviously, this introduces a greater difficulty of management and configuration which often makes these solutions unsuitable for autonomous use outside the clinical and research facilities.

Thanks to the low cost that could allow a large-scale diffusion; the practicality that could guarantee portability outside healthcare facilities; non-invasiveness through non-contact measurements; and for the versatility that makes them suitable for a wide spectrum of applications, RGB-Depth optical sensors have been the choice for the development of this

thesis in the context of Parkinson's disease, a pathology in which motor impairment affects different the areas of the body and differently in ways and times, thus requiring an overview for its evaluation and its treatment. This choice led to the development of innovative, economic and non-invasive solutions that could become a valid support to traditional clinical practice in the definition of new pathways and health services for the management of PD.

Specifically, the designed solutions aim at objectively and automatically quantifying body movements during the execution of some standard tasks used, in clinical practice, to assess the severity of motor impairment and establish the best treatment for motor symptoms. A combined approach of RGB-Depth optical sensors, Computer Vision techniques and Machine Learning methods was used to develop dedicated hand and body tracking algorithms, capable of accurately capturing body movements in motor tasks related to the upper limbs, the lower limbs and posture, characterizing them through appropriate kinematic and functional parameters that quantify the effects of typical symptoms on motor performance according to standard clinical assessments.

The main goal of the thesis was the development of these solutions for the accurate, quantitative and automatic evaluation of motor function in PD: in fact, it is not possible to introduce the concepts of comparison between motor performances, instrumental monitoring of disease progression, slight functional alterations not perceivable by the human eye, effectiveness of a treatment without the realization of tools capable of capturing and quantifying with precision, as far as possible, human movements as a whole. The secondary objectives are related to the following points: (1) the development of natural human-machine interfaces (HMI) using the same techniques to increase both usability and self-management by people with motor impairment and without specific technical skills; (2) the integration of these solutions in remote monitoring platforms, to collect and analyse motor performance more frequently and in home environments in order to follow patients outside of clinical facilities; (3) the feasibility of rehabilitation programs based on exergames to practice motor functions at home using virtual game scenarios; (4) the applicability of these solutions to other pathologies characterized by motor disabilities.

The remaining part of the thesis is structured as follows. Chapter 2 introduces the general characteristics of Parkinson's disease, in particular the origin of motor dysfunctions, epidemiology, typical motor symptoms, traditional clinical rating scales, pharmacological and non-pharmacological treatments available for motor impairment. Chapter 3 describes, in more detail, the vision-based systems currently used for quantitative analysis of motor function, with particular attention to RGB-Depth optical sensors and some promising and

innovative methods for body tracking that will surely find more and more applicability in the near future. Chapter 4 presents the solution developed and the results of the analysis of upper limb impairment in Parkinson's disease. The focus of this chapter is "A Self-Managed System for the Automated Assessment of UPDRS Upper Limb Tasks in Parkinson's Disease", published in Sensors in 2018. Chapter 5 focuses on the solution developed and the results of the analysis of lower limb impairment and postural instability, as described in "Feasibility of Home-Base Automated Assessment of Postural Instability and Lower Limb Impairments in Parkinson's Disease", published in Sensors in 2019. In Chapter 6, the preliminary results of a first experimental test on remote monitoring of upper limb impairment are presented: the focus is the "Home-based automated assessment of upper limb motor function in Parkinson's Disease", published in the Journal of Advances in Life Sciences in 2019. Finally, Chapter 7 deals with the conclusions on the results achieved and on the future developments of this line of research. To complete the chapter, the list of the main publications that summarize the research activity is shown in Table 1.

PUBLICATIONS	YEAR
Automated Assessment of Motor Impairments in Parkinson's Disease. The Clinical Neurologist International	2020
An Integrated Multi-Sensors Strategy for the Remote Monitoring in Parkinson's Disease. Sensors, 19 (21)	2019
Final results of the NINFA project: impact of new technologies in the daily life of elderly people. Aging Clinical and Experimental Research	2019
A vision-based approach for the at home assessment of postural stability in Parkinson's disease. FORITAAL 2019, Conference Proceedings	2019
Home-based automated assessment of upper limb motor function in Parkinson's Disease. Journal of Advances in Life Sciences, 11(1&2)	2019
Feasibility of home-based automated assessment of postural instability and lower limb impairments in Parkinson's Disease. Sensors, 19(5)	2019
A Self-managed System for Automated Assessment of UPDRS Upper Limb Tasks in Parkinson's Disease. Sensors, 18	2018
Assessment of Parkinson's disease at-home using a natural interface based system. FORITAAL 2018, Conference Proceedings	2018
Steps toward Automatic Assessment of Parkinson's Disease at Home. SPWID 2018, Conference Proceedings	2018

Table 1: List of the original articles published during the research activity

Chapter 2

Parkinson's Disease

This chapter presents a general overview of Parkinson's disease. The main pathophysiological and epidemiological aspects will be briefly discussed, focusing on the origin, characteristics and prevalence of the disease in the population. Particular attention will be paid to the description of the associated motor symptoms, to traditional clinical evaluation methods and to the main treatments available. Finally, the importance of supporting traditional clinical assessment with a quantitative analysis of motor impairment will be emphasized, as a possible support tool for better management of the disease and the patients. Although the goal was not to examine in detail all aspects related to the pathology, I believe that the content of this chapter may provide a greater understanding of some fundamental issues that motivated the development of this thesis.

2.1 History

In 1817, James Parkinson was the first scientist to provide the medical and systematic description of a new neurological syndrome. In his famous essay[68], he described the particular symptoms observed in six men and, due to the main characteristics, he referred to this disease as Shaking Palsy. Only about 60 years later, this syndrome was called Parkinson's disease. Parkinson described a clinical picture common to all six individuals: *"... Involuntary tremulous motion, with lessened muscular power, in parts not in action and even when supported; with a propensity to bend the trunk forward, and to pass from a walking to a running pace: the senses and intellects being uninjured..."*[69]. This sentence summarizes in a few words what are still considered to be among the main signs, symptoms and manifestations of the disease. In 1862, the French neurologist and professor Jean-Martin Charcot gave a more detailed description, recognizing bradykinesia as a different cardinal characteristic of the pathology[70]: "*...that their problem relates more to slowness in execution of movement than to real weakness. In spite of tremor, a patient is still able to do most things, but he performs them with remarkable slowness...*". With his studies, Charcot extended the clinical spectrum of the disease, defining two types of patients: those with signs of tremor and those with forms of stiffness/akinesia. This evidence led to the name of this syndrome being change from Shaking Palsy in Parkinson's Disease. Furthermore, Charcot's early studies on

tremor made an important contribution in differentiating Parkinson's Disease from other tremor disorders, in particular from multiple sclerosis in which action tremor was accompanied by weakness, spasticity, and visual disturbances. In contrast, he observed that patients with Parkinson's disease had resting tremor as well as stiffness, slowness, hunched posture, and soft speech. In addition, Charcot's studies helped in identifying other features in Parkinson's disease patients, including forms of postural alteration and bradykinesia of the facial muscles, the origin of the so-called "masked face" where the eyes remain wide-open and the forehead constantly wrinkled[69]. Subsequent studies have provided more details on the progression of disability[71] and on motor fluctuations[72]. Further pathological studies revealed the involvement of the midbrain[73] and the damage to the substantia nigra as the anatomical origin of Parkinson's disease[74]. The complete description of Parkinson's disease[75], including associated brainstem lesions, is the result of several subsequent studies; while clinical progression was analyzed in an important study, which led to the definition of the first internationally recognized clinical rating scale[76].

2.2 Epidemiology

The results of a systematic analysis of some epidemiological studies[10] show that in 2016 the number of individuals with Parkinson's disease was approximately 6.1 million worldwide, of which 47.5% were women and 52.5% were men, and that this number was 2.4 times higher than in 1990. Epidemiologic data on the prevalence and incidence of PD are particularly interesting for deepening the analysis of risk and protective factors, investigating the primary causes of the disease, providing information on population burden and planning national healthcare strategies[77]: the last point is crucial, considering that PD is a progressive and chronic disease in which, for example, the course of motor disability is associated with increasingly heavy rehabilitation needs over time.

In Italy, it is estimated that at least 230,000 people are affected by parkinsonism, and about two thirds by PD: by 2030, it is expected to be around half a million[78]. The onset of PD occurs on average in working age, around 55-60 years: about 5% are under the age of 50 years and about 70% are over 65. Parkinson's disease has an important impact on quality of life in the 10 years following onset: about 30-50% of subjects develop involuntary movements after 2-5 years of treatment; after 10 years, 65% of the subjects present postural instability and 48% dementia. About 46% of subjects stop working after 5 years; the 82% after 10 years, especially if the onset of disease occurs before the age of 65. Finally, PD appears to be slightly more frequent in men than in women (60% vs 40%). Parkinson's

disease has a high socio-economic impact: it is the second most frequent neurodegenerative disease after Alzheimer's and is highly disabling in its progression.

2.3 Pathophysiology

As mentioned in Chapter 1, the basal ganglia play an active role in motor control: since many clinical signs of damage to this area of the brain are various forms of motor impairments, they are considered to be motor structures. The basal ganglia are a set of subcortical structures, located in the brain, made up of several connected nuclei[79]: caudate nucleus, putamen, globus pallidus, sub-thalamic nucleus and substantia nigra [Figure 3]. The last two are connected to this system only functionally. The substantia nigra is made up of two parts: the pars compacta and the pars reticulata.

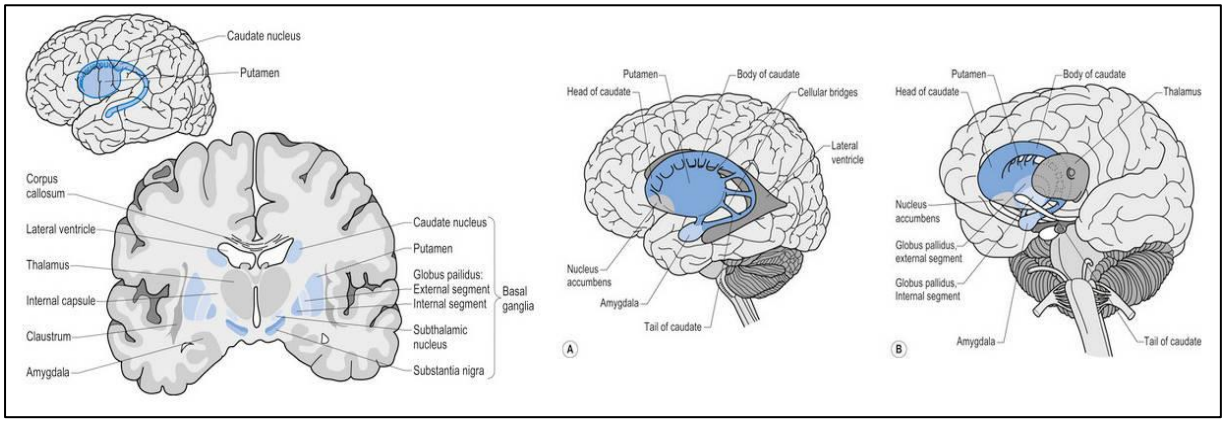

Figure 3: The anatomical structure of the basal ganglia and the related structures.
Anterior to posterior perspective (left); lateral perspective (center); 3D lateral perspective (right)
[Image source: 79]

Signal processing through the basal ganglia depends on two distinct pathways: the direct and the indirect pathway. They have opposite effects on the thalamic structures. The excitation of the direct pathway produces the excitation of thalamic neurons, which in turn create excitatory connections on the neurons of the motor cortex. On the contrary, excitation of the indirect pathway causes the inhibition of thalamic neurons, which will then be unable to excite the neurons of the motor cortex. The normal functioning of the basal ganglia involves a balance between these two pathways: an imbalance between the two pathways causes the motor dysfunctions that characterize various neurological diseases.

The direct pathway [Figure 4] starts from the striatum (caudate nucleus and putamen) whose neurons are excited by the cortex. The neurons of striatum send their axons to internal globus pallidus (GP_i) which send their axons to the thalamus. Other excitatory pathways go from the thalamus to the cortex (prefrontal, premotor and supplementary cortex) where they

influence the planning of movement. Neurons in the striatum and GP_i are inhibitory neurons so the striatum-GP_i and GP_i-thalamus pathways are inhibitory. In contrast, the cortex-striatum and thalamus-cortex pathways are excitatory. This system works on the principle of positive feedback: inhibitory neurons (synapses) are connected in series, so an inhibitory neuron of the striatum suppresses the activity of an inhibitory neuron of the GP. The consequence is a lower inhibitory influence of GP on the thalamus (disinhibition of the thalamus) which is equivalent to excitation of the cortex. Therefore, the direct pathway generates the excitation of the motor cortex, promoting movement[80]: any interruption or dysfunction of the direct pathway causes hypokinesia which is the generic term to indicate the lack or slowness of body movements.

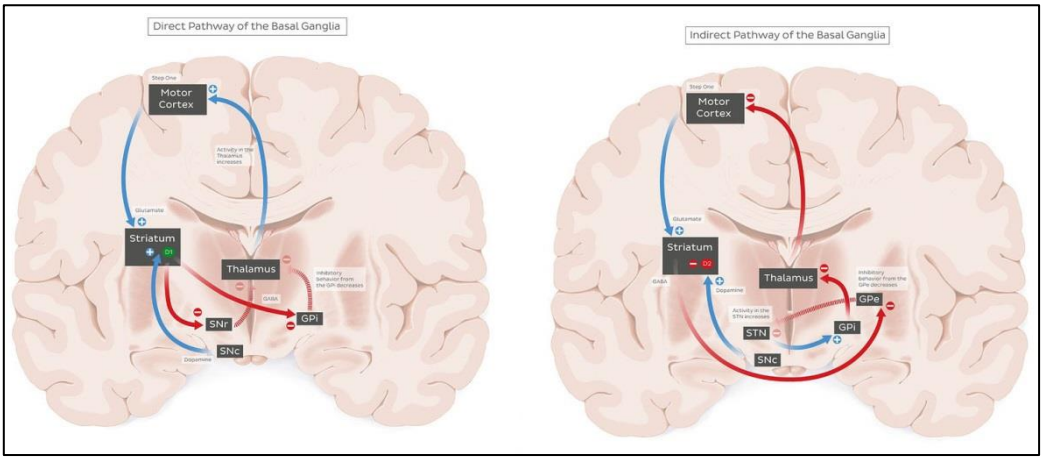

Figure 4: Direct (left) and indirect (right) pathways of basal ganglia from coronal view.
[Image source: 80]

The indirect pathway [Figure 4] also starts from the striatum, where other neurons create inhibitory connections with the external segment of globus pallidus (GP_e). GP_e neurons create inhibitory connections with the sub-thalamus which in turn sends excitatory projections to the GP_i. In practice, the striatum inhibits the GP_e causing a disinhibition of the sub-thalamus whose neurons become more active and able to excite GP_i. The consequence is a more inhibitory influence of GP_i on the thalamus (inhibition of the thalamus) which is equivalent to a decrease in the activity of the cortex. Therefore, the indirect pathway generates the inhibition of the motor cortex, reducing movement[80]: any interruption or dysfunction of the indirect pathway causes hyperkinesia or dyskinesia which are the terms for indicating the production of further involuntary movement of the body.

As a result of these activities (excitation, inhibition and disinhibition), when the cortex excites the direct pathway, further excitation of the cortex is obtained (positive feedback circuit); conversely, when the cortex excites the indirect pathway, there is a further inhibition

of the cortex (negative feedback circuit). The function of the basal ganglia is based on the right balance between the two pathways: the neurons of the motor cortex have to correctly excite the neurons of the direct pathways to further increase the excitatory effect and to excite the neurons of the indirect pathways to inhibit other unnecessary neurons for the required motor task.

The nigrostriatal pathway, from the substantia nigra pars compacta to the striatum, plays a crucial role in the modulation of direct and indirect pathways through the dopaminergic neurotransmitter. Dopamine has an excitatory effect on the direct pathway and an inhibitory effect on the indirect pathway. This dual effect is explained by the presence of two different dopamine receptors (D1 and D2) within the striatal neurons that respond differently to dopamine stimulation: stimulation of D1 receptors generates the excitation of neurons, stimulation of D2 receptors generates the inhibition of neurons. D1 receptors are found on striatal neurons whose axons form the direct pathway; on the other hand, D2 receptors are found on neurons whose axons form the indirect pathway.

The cause of PD is the loss of dopaminergic neurons in the substantia nigra pars compacta. Considering the function of the nigrostriatal pathway on direct and indirect pathways, it is therefore clear that this loss causes poverty of movement. Since the nigrostriatal pathway excites the direct pathway and inhibits the indirect pathway, nigrostriatal dysfunction alters the balance, favoring activity in the indirect pathway. Therefore, GPi neurons are abnormally active, leading to inhibition of thalamic neurons. Without thalamic function, neurons of the motor cortex are not excited and, consequently, the motor system is less able to perform voluntary motor planning.

2.4 Symptomatology and Clinical Diagnosis

The most debilitating symptoms in PD are related to motor dysfunction. In particular, four primary (or cardinal) symptoms are considered for the clinical diagnosis of PD: bradykinesia (or akinesia), tremor, stiffness and postural instability[81].

Bradykinesia is the most typical clinical feature of PD. It refers to excessive slowness of movement and is a common feature in basal ganglia disorders. The main effect includes considerable difficulty in planning, starting and executing movements and in carrying out sequential and simultaneous tasks. Motor symptoms are more correlated to dopamine deficiency.

Resting tremor is another common and recognizable symptom of PD: several studies indicate that about 69% of people with PD show tremor at rest at the onset of the disease. The

typical frequency of tremor is between 4 and 6 Hz. It almost always affects only one-side of the body and is most evident in the distal area of the extremities (in particular arms), but it may also affect the lips, chin, jaw and legs. One of the characteristics of resting tremor is its disappearance during action and sleep.

Stiffness is an involuntary increase in muscle tone that causes increased resistance to passive limb movements (i.e. flexion, extension or rotation around a joint), almost always accompanied by pain. It may occur in the proximal (e.g. neck, shoulders, hips) and distal (e.g. wrists, ankles) areas.

Postural instability is a manifestation of the most severe stages of PD, a consequence of the progressive loss of postural reflexes, and is one of the most common causes of falls. Many factors, even not directly related to PD, may influence postural instability: age-related changes; inability to integrate visual, vestibular and proprioceptive sensory inputs; but even the simple fear of falling may compromise the control of balance. Treatment of the disease (Section 2.5) generally improves axial abnormalities, but usually does not act effectively on postural instability.

Other common symptoms are related to abnormal axial postures, as a result of neck and trunk stiffness. Typical postural abnormalities are the flexed position of the neck and trunk (e.g. camptocormia, Pisa syndrome), or the flexion of elbows and knees during gait. Abnormal postures generally occur later, associated with the more severe stages of the disease: these conditions are generally aggravated by walking and recovered in a sitting or supine position, or by the extension of the trunk when, for example, the subject is against a wall. Deformities of the limbs (hands and feet) may also occur in some individuals.

Another highly disabling manifestation is freezing, or motor block, which is a form of akinesia (loss of movement) that is often associated to an increased risk of falls. Freezing occurs mainly in the legs during walking and presents as a sudden and transient inability to move: these episodes may occur when the person starts walking (called start hesitation) or in specific situations while walking, for example while turning or walking through narrow passages.

People with PD may also have other secondary motor symptoms, a consequence of bradykinesia and stiffness, which affect daily activities and may be even more disabling than primary features: speech disorders and hypophonia (i.e., softer voice), hypomimia (i.e., reduced expressiveness of face and eye-blinking called “poker face”), micrographia (i.e., smaller handwriting), respiratory and swallowing disorders. Parkinson’s disease is also characterized by non-motor symptoms that may generally occur years after the onset of the

disease: cognitive, behavioral and neuropsychiatry disorders; sensory dysfunctions; sleep disorders[82] are quite common symptoms as the disease progresses.

Due to its characteristics, PD can be confused with other pathologies such as vascular parkinsonism, drug-induced parkinsonism, tremor disorders, dementia with Lewy bodies, multisystem atrophy, progressive supra-nuclear palsy (PSP)[82]. To date, there is no test that can confirm the diagnosis during the life of the individual: only the presence of intra-neuronal Lewy bodies, verified post mortem, can provide the certainty and correctness of the diagnosis. The accuracy of the diagnosis improves with clinical experience in differential diagnosis, the purpose of which is to exclude that the observed symptoms may be due to other pathologies. The UK Parkinson's Disease Society Brain Bank (UPDSBB) diagnostic criteria[83] are used as a routine diagnostic tool in clinical practice: they consist of three main steps [Figure 5] that make the diagnostic process as accurate and objective as possible. *Step 1* refers to the primary symptoms necessary to hypothesize a diagnosis of PD (at least two of the four primary symptoms are required to be present); *Step 2* introduces the exclusion criteria, therefore other pathologies that have symptoms similar to PD and which must be excluded (i.e., differential diagnosis), also from the analysis of the subject clinical history; *Step 3* includes other positive features that might otherwise support a diagnosis of PD.

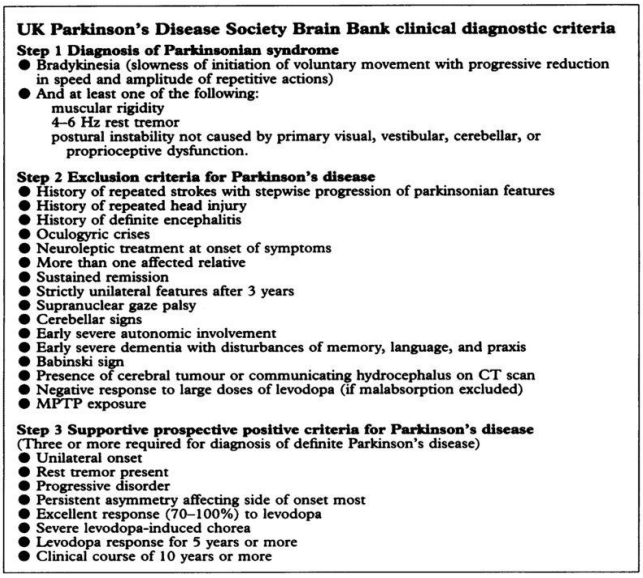

UK Parkinson's Disease Society Brain Bank clinical diagnostic criteria

Step 1 Diagnosis of Parkinsonian syndrome
- Bradykinesia (slowness of initiation of voluntary movement with progressive reduction in speed and amplitude of repetitive actions)
- And at least one of the following:
  - muscular rigidity
  - 4–6 Hz rest tremor
  - postural instability not caused by primary visual, vestibular, cerebellar, or proprioceptive dysfunction.

Step 2 Exclusion criteria for Parkinson's disease
- History of repeated strokes with stepwise progression of parkinsonian features
- History of repeated head injury
- History of definite encephalitis
- Oculogyric crises
- Neuroleptic treatment at onset of symptoms
- More than one affected relative
- Sustained remission
- Strictly unilateral features after 3 years
- Supranuclear gaze palsy
- Cerebellar signs
- Early severe autonomic involvement
- Early severe dementia with disturbances of memory, language, and praxis
- Babinski sign
- Presence of cerebral tumour or communicating hydrocephalus on CT scan
- Negative response to large doses of levodopa (if malabsorption excluded)
- MPTP exposure

Step 3 Supportive prospective positive criteria for Parkinson's disease
(Three or more required for diagnosis of definite Parkinson's disease)
- Unilateral onset
- Rest tremor present
- Progressive disorder
- Persistent asymmetry affecting side of onset most
- Excellent response (70–100%) to levodopa
- Severe levodopa-induced chorea
- Levodopa response for 5 years or more
- Clinical course of 10 years or more

Figure 5: The UPDSBB diagnostic criteria used in clinical practice.
[Image source: 83]

2.5 Disease Management

To date, unfortunately, there is no cure for Parkinson's disease: the only weapon to ensure a good quality of life despite the disease is the control of symptoms. This is done through

pharmacological, surgical and physical treatments that are much more effective than those for other neurological diseases.

Pharmacological Treatment

The pharmacological treatment is essentially based on three groups of drugs: Levodopa, dopamine agonists and MAO-B inhibitors. The stage and age of disease onset determine the most useful therapy[84]. At the onset of the disease, the goal is to find an optimal compromise between symptom control and drugs side-effects. Conversely, in the later stages, the goal is to manage the symptoms when the effect of the drugs is fluctuating, as a consequence of sudden changes in the response to the drugs or their overuse. The use of Levodopa is generally postponed to delay the onset of associated negative and long-term complications such as dyskinesia and fluctuations, initially preferring other drug treatments (e.g., dopamine agonists or MAO-B inhibitors) when possible. Despite this, Levodopa remains today the most effective treatment for the control of motor symptoms in PD and its use cannot be delayed in people with a low quality of life caused by motor disabilities[85].

Levodopa has been the most used drug treatment over the past 40 years to temporarily reduce the motor symptoms of PD. As mentioned above, the origin of the motor symptoms is the lowering of dopamine in the basal ganglia: the restoration of dopamine levels available in the brain is essential to partially recover motor function. But dopamine cannot be taken directly through drugs because it cannot cross the blood-brain barrier. On the other hand, levodopa (or L-dopa), which is a precursor of dopamine, is able to cross the barrier and reach the brain where it is rapidly converted into dopamine. Much of levodopa is transformed into dopamine in other parts of the body, causing various side effects, and only a small percentage (between 5% and 10%) passes through the blood-brain barrier. Other drugs are usually combined with levodopa to inhibit this transformation outside the brain, thereby increasing the availability of levodopa that can reach the brain[86]. The use of Levodopa induces two long-term side effects which are considered as serious complications: dyskinesia, i.e. involuntary and uncontrolled movements; and daily fluctuations in response to medications. In case of fluctuations, people alternate conditions of low motor symptoms (this phase is called *on state* associated with a good response to medications) and conditions with elevated motor symptoms that impair motor function (this phase is called *off state* associated with a poor response to drugs). Delay in initial use or, in any case, a lower dose of levodopa may contribute to postpone the onset of these complications. In the initial stage of PD, there is an immediate, prolonged and adequate response to Levodopa (*on state*) that allows for good

symptom control with a few daily doses of the drug [Figure 6]. However, as the disease progresses, an ever decreasing ability to convert levodopa into dopamine causes shorter, unpredictable and inadequate responses to levodopa that underlie the *wearing off* condition[87].

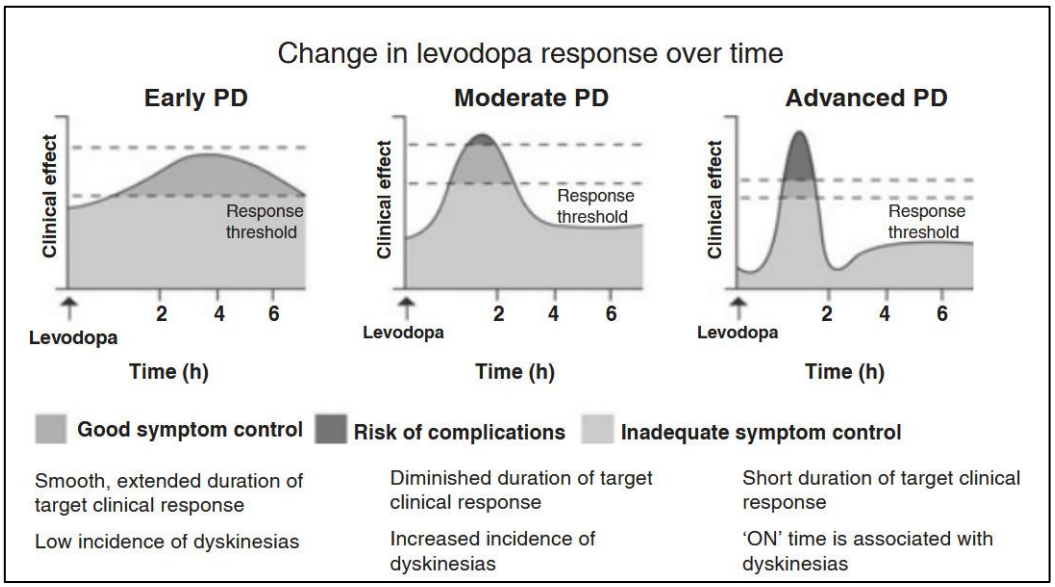

Figure 6: Evolution of the response to Levodopa with PD progression.
[Image source: 87]

Dopamine agonists are compounds that activate dopamine receptors. One way to treat PD is to supply extra dopamine by trying to restore availability levels in the brain (that is what levodopa is all about). Another way is to mimic the effects of dopamine as dopamine agonists do: they bind directly to dopamine receptors in the brain with similar effects to levodopa. For many years, dopamine agonists have been used as a complementary therapy to levodopa. In recent years, dopamine agonists have been used in the early stages of PD to delay the use of levodopa and the onset of induced complications, despite being less effective in controlling motor symptoms[88].

The purpose of MAO-B inhibitors is to increase dopamine levels in the basal ganglia by inhibiting the activity of the dopamine-breaking enzyme, the monoamine oxidase B (MAO-B). As dopamine agonists, MAO-B inhibitors are also used in early stages of PD to delay the levodopa therapy, although these drugs may cause side effects and are less effective in controlling motor symptoms[88].

Surgery Treatment

In the past, prior to the discovery of levodopa, surgical treatment of motor symptoms was a common practice in PD. The most common surgical treatment is deep brain stimulation (DBS), developed in the 1980s, a neuro-surgical procedure that consists in the placement of

neuro-stimulators (electrodes or leads), which deliver electrical impulses to specific brain areas[89]. The stimulation of the brain areas is controlled by an internal pulse generator (IPG) which is a programmable generator placed under the skin in the upper chest area. An extension cable, an insulated wire, connects IPG to the electrodes by passing under the skin of the head, neck and shoulder [Figure 7]. DBS is used, in particular, in people suffering from fluctuations and tremors, especially when pharmacological treatment is unable to control these conditions. The most common brain areas treated with neuro-stimulation are: the internal globus pallidus, with the aim of improving motor function; and the thalamus, with the aim of reducing tremor (although only minimal effects on bradykinesia and stiffness can be appreciated). DBS is associated with a 30–60% improvement the assessment of motor function assessment.

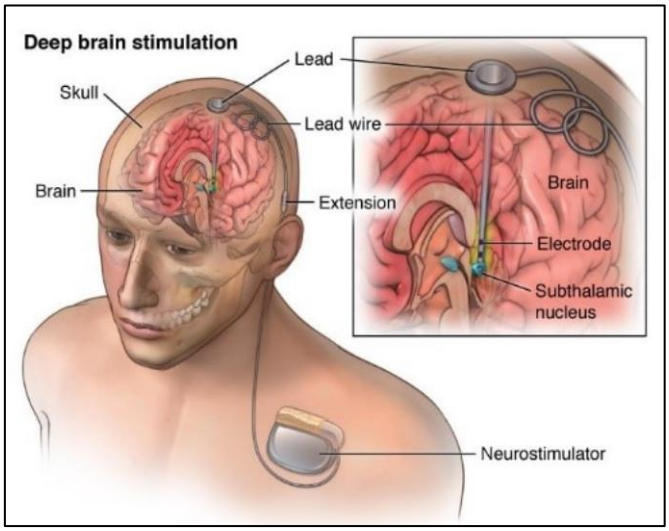

Figure 7: Deep Brain Stimulation: main components and brain areas treated.
[Image Source: https://www.aans.org/en/Patients/Neurosurgical-Conditions-and-Treatments/Deep-Brain-Stimulation]

Physical Treatment

The role of physical exercises, as a complementary strategy to pharmacological treatments of the motor symptoms, has been a hotly debated topic in recent years. In 2014, a new document[90], after a review of about 70 clinical studies that revealed the strong benefits of physical exercises, pointed to European guidelines for the use of physiotherapy in the treatment of specific motor symptoms of Parkinson's disease. As quoted in subtitle of Chapter 4[90]: *"Physiotherapy aims to maximize quality of movement, functional independence and general fitness, and minimize secondary complications whilst supporting self-management and participation, and optimizing the safety of people with Parkinson's disease".* To this end, the European guidelines suggest five core areas as the main focus of

physiotherapy: physical capacity, transfers, manual activities, balance and gait (including posture). Furthermore, the European guidelines emphasize the importance of a patient-centered approach, where treatment is linked to the current stage of disease progression for each patient. Recent literature agrees on the benefits of physical exercise in improving functional capacity, gait, balance, and strength and, consequently, the quality of life. When designing a rehabilitative program for PD, exercises should be *goal-based*, i.e. aimed at practicing specific impaired motor functions (for example, balance and gait control) and improving performance in activities of daily living. More recently, several studies have demonstrated the feasibility of using technologies and virtual environments to propose motor training exercises to PD subjects in the form of videogames. These exercise-based videogames (called *exergames*) are an emerging tool for the rehabilitation of individuals with PD, combining the fun of videogames with motor exercises that improve specific motor functions[91]. Although the clinical efficacy of exergames has not yet been much explored and demonstrated, they represent a new model for the physical treatment and management of PD in the near future.

2.6 Clinical Rating Scale

Impaired motor function is the most disabling effect in PD, so it is fundamental to assess the severity level in order to determine the most appropriate treatment to improve the individual's overall quality of life. At the same time, it is important to periodically check the effectiveness of therapies in controlling symptoms, adjusting them appropriately if necessary, based on any changes found in the response to treatments. The assessment of the severity of motor impairment in PD occurs through various standardized rating scales[92].

The Hoehn & Yahr (H&Y) rating scale is the oldest: it is the result of a study conducted in 1967 by Margaret Hoehn and Melvin Yahr on 856 patients[93]. The study made it possible to distinguish five stages of disability linked to progression of the disease: from stage I characterized by unilateral disability without serious motor disorders; to stage V, when the individual is confined to a wheelchair or bed. Subsequently, in 2004, following further studies, the scale was modified by adding two levels (levels 1.5 and 2.5) to better distinguish two intermediate conditions[94]. Furthermore, an interesting study on 695 subjects estimates the median time in months to pass from one stage to the next one[95]. The primary purpose of the H&Y scale is to provide immediate categorization of the severity of the impairment based on the main evidence associated to disease progression. Table 2 shows the original H&Y scale[93], the modified version[94] and the estimated time to move towards a more severe stage[95].

STAGE	H&Y[93]	MODIFIED H&Y[94]	TIME IN MONTHS[95]
1	Unilateral involvement, with minimal or no function disability	Only unilateral involvement	-
1.5	-	Unilateral and axial involvement	not considered
2	Bilateral or midline involvement, without impairment of balance	Bilateral involvement without impairment of balance	20
2.5	-	Mild bilateral disease with recovery on pull test	62
3	Bilateral disease: mild to moderate disability with impaired postural reflexes; physically independent	Mild to moderate bilateral disease; some postural instability; physically independent	25
4	Severely disabling disease; still able to walk or stand unassisted	Severe disability; still able to walk or stand unassisted	24
5	Confinement to bed or wheelchair unless aided	Wheelchair bound or bedridden unless aided	26

Table 2: The H&Y rating scale with description of the progressive forms of disabilities. The modified version with the two additional intermediate stages; the estimated time (in months) to transit to a more severe stage (stage 1.5 was not taken into consideration in the study)

The Unified Parkinson's Disease Rating Scale (UPDRS)[96] was defined in 1987: today, it is the most commonly used clinical rating scale. It consists of six sections according to which different aspects of the disease are evaluated: 1) Intellectual and Mood disorders; 2) Activities of Daily Living; 3) Motor Examination; 4) Complications; 5) Stages of the disease (by H&Y scale); 6) Self-assessment of independence in daily activities (by Schwab and England ADL scale). The first three sections and part of the fourth are rated on a five-point scale (from 0 to 4, using only integer values) that corresponds respectively to: 0- no involvement; 1- detectable disorders; 2- moderate disorders; 3- considerable disorders; 4- no function or severe disorders. Section III is dedicated to the motor examination, the purpose of which is to assess the severity of the impairment on specific domains related to movement such as upper and lower limbs, tremor at rest, posture and postural stability, gait, speech, facial expression.

In 2008, the Movement Disorder Society (MDS) proposed a revision of the UPDRS named MDS-UPDRS[97]. The MDS-UPDRS highlights the limitations of the original UPDRS: the lack of consistent anchoring between sections and poor attention to non-motor symptoms. MDS-UPDRS has a four-section structure: 1) non-motor experiences of daily living, consisting of 13 items; 2) motor experiences of daily living, consisting of 13 items; 3) motor examination, consisting of 18 items; 4) motor complications, consisting of 6 items. Each item is rated on a five-point scale (from 0 to 4, using integer values), as for the original UPDRS, but with a simpler meaning on the severity of the impairment: 0- normal, 1- slight, 2- mild, 3- moderate, 4- severe. A high correlation between MDS-UPDRS and the original UPDRS

($\rho = 0.96$) was demonstrated[97]. The MDS-UPDRS scale is the most common rating scale used in clinical practice.

During the clinical examination of subjects with PD, the examiner (a neurologist experienced in movement disorders) pays particular attention to Section III (i.e., motor examination) whose purpose is to evaluate the effects of symptoms on different motor functions by assigning a score severity, as established by each dedicated item (or motor task) of the rating scale. For example, the examination of tremor is checked in conditions of rest (resting tremor), with extension of the arms (postural tremor) and during movement (action tremor). Stiffness is assessed by passive movement of the major joints of the body. Bradykinesia is assessed by observing the subject's gait (i.e., short steps, festination) and gestures, spontaneous movements, tone of voice, facial expression, and by testing repetitive movements of the hands, arms, and legs.

The examiner must follow the guidelines provided in the introduction of the "motor examination" section for the correct administration of the planned motor tasks. For each item of the scale, the description indicates: what the patient should do; what the examiner should observe and how the examiner should evaluate the patient's performance during motor task.

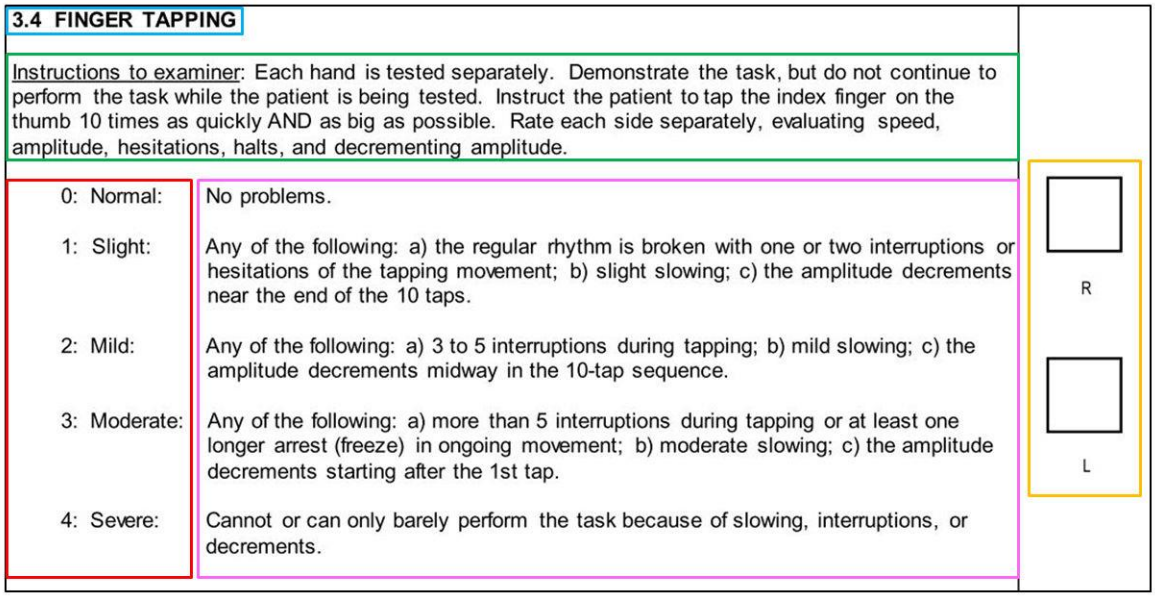

Figure 8: An example of MDS-UPDRS item (Finger-Tapping motor task)
[Image Source: 97]

In [Figure 8], the structure for the "Finger Tapping" item defined by MDS-UPDRS is shown. The different types of information provided to the examiner have been highlighted with the colored boxes: this information is used to evaluate the motor performance according to the criteria established by the MDS-UPDRS. The *light-blue box* contains the name of the motor task. The *green box* contains the instructions for the examiner: what the patient should

do and what the examiner should consider for evaluation. The *red box* contains the severity score to be assigned to the motor performance. The *magenta box* contains the criteria for assigning the severity score. The *yellow box* is the area where the scores, assigned separately to the left and right hand, are noted.

The assessment is based on the observation of how the motor task is carried out, according to qualitative and subjective evaluation criteria (as indicated in *magenta box*): the perception of a *slight* or *mild* slowdown; of decreasing amplitude and, whether this occurs, *near the end* or *in the middle* or *at the beginning*; of occurrence of anomalies during the performance (such as hesitations, freezing, interruption) and counting their number. All this elements may differ from one examiner to another, on the basis of personal experience or the ability to observe specific aspects of the movement.

The examiner is also required to take into account some physical quantities (such as speed, amplitude of movement, angular measurement, rhythm, variability), potentially measurable by some instrumentation but certainly not quantifiable simply by observing the performance. Furthermore, since the main requirement is that the task must to be done, for example, "as quickly and as big as possible" (as indicated in *green box*), the difficulty of considering all these features to assign a score in the short duration of the task is well understood.

At the moment, clinical rating scales represent the "gold standard" for assessing disease progression, although there are widely debated issues in particular regarding severity scores: the five-point scale, with no intermediate scores, is too coarse to detect slight changes in motor performance; and the qualitative evaluation does not allow easy comparison of performance over time.

But the most important issue depends on inter-rater reliability which is the degree of agreement of the different examiners and indicates how much homogeneity or consensus exists in the scores assigned by the various examiners. Two factors can influence the inter-rater reliability in MDS-UPDRS: examiner experience (there is difference between junior and senior examiner ratings) and greater difficulty in assessing some motor tasks than others[98]. To solve this last issue, a few years ago, several studies proposed the use of tapes to train examiners and ensure greater uniformity of assessment[99].

2.7 Contribution of the thesis on Parkinson's Disease

In the previous paragraphs, it was pointed out that the most debilitating aspects of PD are linked to a progressive reduction of motor functions caused by the death of dopaminergic

neurons. In addition, the importance of treating symptoms to ensure a good quality of life for people was highlighted. The treatment, both pharmacological and rehabilitative, is aimed at reducing disability, promoting functional recovery (at least partially) or, in any case, at optimizing residual motor function. In clinical practice, treatment is established on the basis of the evaluation of symptoms by observing their effects on different areas of the body through qualitative and subjective criteria, but without any measurement of those physical quantities that are implicitly taken into consideration as required by the rating scales.

Moving towards an objective and accurate assessment of motor symptoms, as required and in accordance with the clinical rating scales, is a key point in obtaining a complete indication of the patient's impairment status and disease progression. Quantitative measurements of specific characteristics would allow, for example, to detect any changes in motor function, to evaluate the effectiveness of specific treatments, to adapt the treatment according to the individual’s response, be it pharmacological or rehabilitative.

Specifically for PD, the goal is to develop dedicated vision systems to achieve an objective and automatic characterization of body movements as required by clinical rating scales, by observing and analyzing the motor performance captured by RGB-Depth cameras. This means:

- accurately quantify the motor performance
- when performing specific motor tasks as defined in clinical rating scales (for example MDS-UPDRS)
- provide an objective measurement of those physical quantities implicitly considered in the evaluation process (as required by the guidelines of the clinical rating scales)
- obtain an automatic assessment of motor performance according to standard clinical scores (therefore, automatic scores have the same meaning as clinical scores)

This is a rather complex technological challenge, but it would allow us to:

- support the clinical evaluation with objective measurements (facilitating the comparison between motor performance)
- increase the frequency of assessments (not only during periodic examinations)
- move the assessment at patient's home (through applications of remote monitoring and rehabilitation)

- quantify the effects of pharmacological and/or rehabilitative treatments (adapting the treatments to the patient's profile)

The work presented in this thesis project deals with some MDS-UPDRS items, as shown in [Table 3], whose feasibility has been verified and fully described in Chapters 4 and 5. The other items will be developed in the near future, with the aim of obtaining an increasingly complete "instrumental" evaluation of the neuro-motor status of subjects with PD.

MDS-UPDRS ITEM	NAME
3.4	Finger Tapping
3.5	Hand Movements
3.6	Pronation-supination movements of hands
3.8	Leg Agility
3.9	Arising from chair
3.12	Postural stability
3.13	Posture
3.10	Gait (only preliminary analysis and results)

Table 3: List of MDS-UPDRS items considered and analysed.

Chapter 3

Vision-based systems for motion analysis

Vision-based systems are among the leading tools for quantitative motion analysis using optical motion capture technologies. The analysis is based on the extraction of information from image sequences with the aim of describing movements with good accuracy. This process has evolved over the years, moving from manual digitization to automatic systems based on Computer Vision and Machine Learning approaches. This was possible thanks to the technological evolution, which led to the development of more sophisticated optical sensors and analysis systems with high processing power. After a brief description of the historical evolution of the vision-based systems, in this chapter both marker-based and marker-free systems will be described with particular focus on RGB-Depth devices, as they were the most used technology for motion capture during this project. Deep learning methods will also be briefly mentioned, as they are considered to be very promising and will certainly be widely used for motion analysis in the near future.

3.1 Historical evolution of vision-based systems

For many decades, manual digitization has been the most popular technique for motion analysis, and film cameras have been the "vision-based system" traditionally used for motion capture[36]. Although this solution was suitable for motion analysis due to high quality images and frame rates, the convenience was very low due to the long processing times for producing image sequences to be analyzed manually. Subsequently, film cameras were replaced by more modern video cameras (initially based on tapes and then based on digital technologies), certainly less expensive, able to guarantee higher resolutions and faster frame rates, but above all able to reduce the overall processing times to produce image sequences[22].

Regardless of the type of vision-based system, the digitization process consists of manually identifying some 2D points of interest (generally corresponding to specific joints of the human body) in each image of the sequence produced according to the viewing perspective of the camera. Through multi-camera systems and complex calibration procedures, it was also possible to transform the 2D points, identified on each image, into a 3D reconstruction of the body's joints in real space, thus allowing real measurements of body movement. An advantage of this approach is the non-invasiveness: it allows the motion

capture without having to apply markers on body segments. For this reason, manual digitization still persists today as a tool for the kinematic analysis of movement especially in sports biomechanics, as it allows analysis during training sessions without hindering the athletes' natural movements. However, this method has also some drawbacks: the difficulty of correlating 3D angular vectors, obtained from joints on 2D images, to anatomically relevant rotation axes in particular conditions (i.e., camera perspective, calibration problems); it is time-consuming; it can be influenced by human errors[36]. These drawbacks and the availability of more sophisticated technologies have favored the development of automatic, faster and more accurate solutions for motion analysis: among these, the *marker-based* solutions to which the optoelectronic systems belong. Manual digitization is still widely used today, especially in sports biomechanics, thanks to several dedicated software for motion analysis that help to speed up the process and make it more accurate and reliable: an example is Kinovea©, a free motion analysis software to estimate kinematics parameters from sequence of 2D images.

3.2 Marker-based motion capture: the optoelectronic systems

In recent years, many developments have been done in automatic optoelectronic systems and, today, numerous commercial solutions are available for the study and analysis of human movement. These systems are based on stereo-photogrammetry, that is the reconstruction of three-dimensional coordinates of points on an object framed by two or more cameras in a fixed and known position with respect to each other. In particular, optoelectronic systems that use multiple cameras operating in the visible or near infrared range, together with special markers placed on the subject's body, represent the most widespread technological solution for estimating human movement. Although these systems have different operating requirements, they use the same basic principles. Each camera is able to emit *pulsed light* and capture images of the *reflected light* through special sensors aligned with the emitters: this information is used to triangulate the 3D position of multiple markers in the field of view of two or more calibrated cameras, to obtain the 3D coordinates of the points in the real space of the working volume. The system cameras are arranged according to specific configurations: the number, features and geometry of the cameras determine the size of the working volume, that is the space in which the precision of the motion capture is guaranteed. The expansion of the working volume is obtained by increasing the number of system cameras: this entails some practical difficulties related to the complexity of calibration and synchronization procedures, the overall cost of the system, the space required by the geometry of the system.

A configuration example is shown in [Figure 9]. The cameras can be mounted on mobile supports (such as tripods) or on fixed structures (such as walls or ceilings): the first solution is certainly more flexible and adaptable to different needs, but requires repeating the calibration procedure every time the geometry of the system is modified (for example even when cameras are moved unintentionally); in the second case, the geometry is fixed during installation and safer from involuntary shifts: this is certainly a more suitable solution when a dedicated area is available for the installation of the system.

Figure 9: Example of environment dedicated to motion analysis with an optoelectronic system. In this configuration, the system cameras are mounted on tripods and the "grey circular area" represents the working volume in which accuracy of motion capture is guaranteed.
[Image source: www.btsbioengineering.com]

Optoelectronic systems are divided into two categories[100]: those that use active markers and those that use passive markers. The passive markers are covered with retroreflective material capable of reflecting the light emitted by the cameras: the features of the cameras can be calibrated to capture only the brightest elements of the scene (as is case of passive markers) and ignore skin and fabrics. The position of each marker is estimated from the sequence of 2D images captured by each camera: knowing the geometry of the system (i.e. the position of each camera with respect to the others) and if at least two calibrated cameras are able to see the same marker, it is possible to triangulate the 2D positions and estimate the 3D position of each marker in real space [Figure 10]. In general, passive markers are placed directly on the body or on special suits, without requiring additional cables or electronic equipment. The diameter of the passive markers varies from 5 to 20/25 mm: the appropriate size is established based on the size of the body segments to be analyzed. Optoelectronic systems with passive markers are mainly used in clinical research to analyze human movement in normal and pathological conditions.

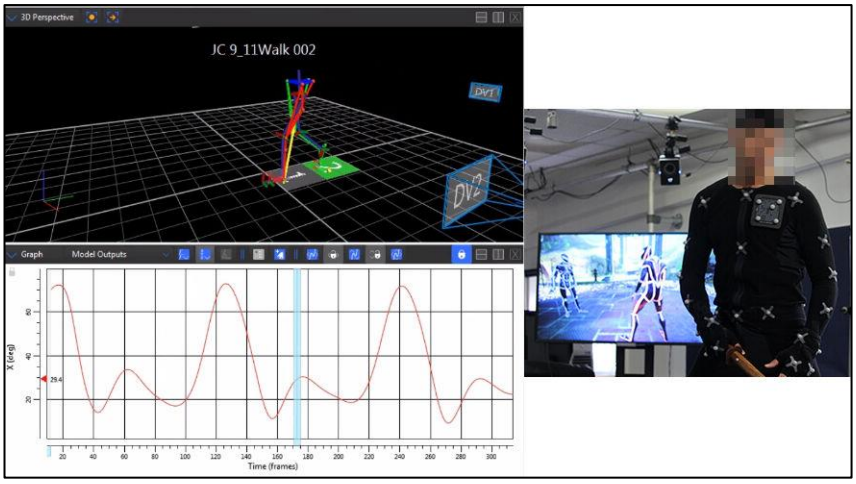

Figure 10: Optoelectronic system with passive markers
[Image source: https://www.vicon.com/about-us/what-is-motion-capture/]

Rather than reflecting light as passive markers, active markers are real light sources: in fact, this type of markers emits its own light, often in the infrared spectrum, which is captured by the system's IR sensors [Figure 11]. Active markers allow for even more robust measurements and greater safety in terms of light interference than passive markers, but require additional wires and batteries that can limit the natural movement of the body. When using complex marker configurations, the maximum sampling rate is reduced so that the signal of each marker has a distinguishable frequency from the others. Due to their features and performance, optoelectronic systems with active markers are mainly used in cinematography and 3D character animations.

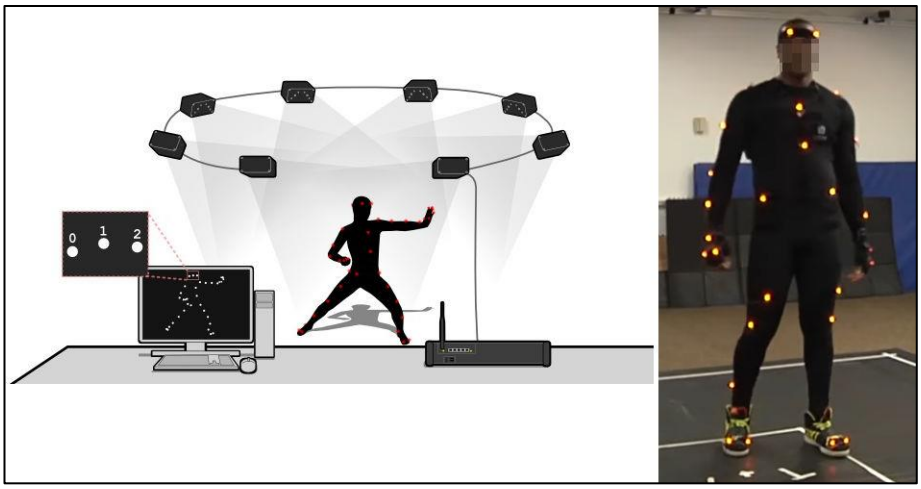

Figure 11: Optoelectronic system with active markers
[Image source: https://www.phasespace.com/applications/3dcharactercreation/]

Regardless of the type of marker, occlusions and markers swap are the most common problems when these systems are used for human motion acquisition. Occlusion occurs when a marker is hidden by a moving part of the body, preventing it from being seen by the

cameras and, consequently, identified and tracked. The swap instead takes place when two or more markers are very close: this can cause crossings during the body movement that make their exact identification difficult. Both of these issues need to be addressed to get an accurate measurement of movement. This is addressed through the placement of markers on body segments according to specific biomechanical protocols. Over the years, several biomechanical protocols have been developed to obtain reliable measurements of human movement: the aim was to ensure maximum visibility of each marker and to limit the number of markers needed to accurately capture the movement of interest. An example is the Davis-Helen Hayes protocol[101] which is one of the most common for gait analysis. This protocol is based on the anthropometric measurements of the subject (including weight, height, tibia length) to identify the anatomical references on which to apply the marker set. This configuration, consisting of 22 markers, is optimal because the markers are positioned outside the body segments, thus making them highly visible [Figure 12]. The first phase of the protocol consists of a static acquisition, with the subject in upright position for few seconds (calibration phase): the centers of rotation of the joints are estimated with the aid of anthropometric measurements. Once the calibration is complete, it is possible to reconstruct the movement of joints and segments even in dynamic conditions, evaluating the trajectories, speeds and accelerations of markers, extracted from the estimated joint rotation centers.

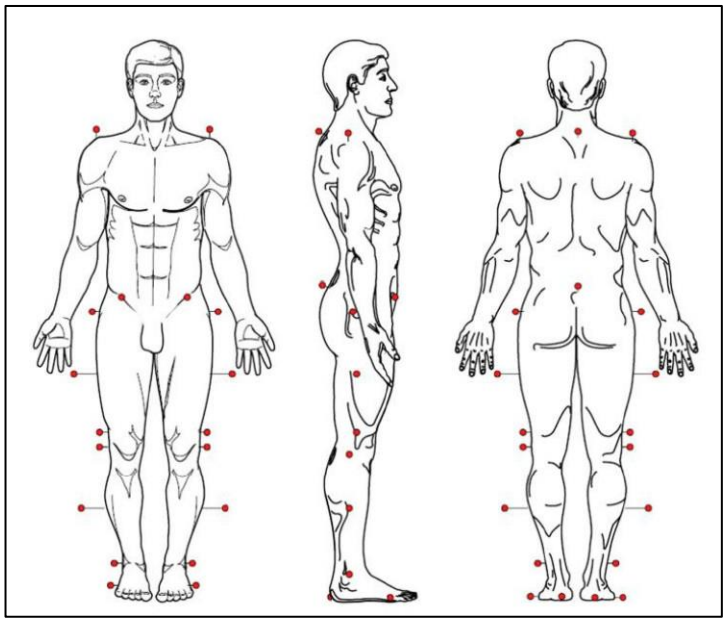

Figure 12: Helen-Hayes marker set or Davis protocol
[Image source: 101]

Traditional biomechanical protocols can be modify by adding further markers to standard configurations or by combining different protocols to better adapt to the characteristics of specific movements to be analyzed[102].

In the last decades, the use of well-designed international protocols and the improvement of anatomical calibration procedures have made it possible to obtain increasingly accurate measurements of movement analysis with marker-based systems, making significant advances in biomechanics. In addition, technological development has made it possible to increase the reliability of motion capture thanks to optical sensors characterized by high resolutions (up to 2048x2048 pixels) and high acquisition frequencies (up to 240 fps); solve part of the problems related to artifacts, thanks to high precision calibration procedures; to automate and speed up the overall analysis process, thanks to dedicated software capable of continuously monitoring and tracking the 3D positions of the joints with reduced drift and delay (i.e., processing in real time).

Despite these strengths, some constraints must be considered: the long preparation times, due to the "manual" positioning of the markers on body; possible incorrect "manual" positioning or detachment of markers during movement; usability only in controlled environments, due to sensitivity to atmospheric factors, the interference of external light sources and the presence of obstacles that can generate occlusions; usability only in dedicated environments, large enough to cover the working volume suitable for motion capture; and, finally, the high cost determined by the complexity and technical characteristics of the system (i.e., the number of cameras and their technical specifications)[36,100].

In clinical setting, the use of optoelectronic systems is limited to clinical and research facilities, where the analysis of human movement takes place in controlled and dedicated environments, under the supervision of qualified technical personnel and according to well-defined biomechanical protocols. Optoelectronic systems are considered the *reference systems* (or *gold standard*, or *gold reference*) for the analysis of movement in clinical practice thanks to their precision and accuracy.

Recent technological advances have pushed towards the development of cost-effective and more portable *marker-free systems*, with the aim of spreading the movement analysis to other environments but, at the same time, guaranteeing measurement accuracy comparable to the reference systems. In fact, before being used as a tool for the acquisition and analysis of movements, any technology or methodology used in this field should be validated and compared with an optoelectronic system to verify its performance and measurement accuracy.

In the context of this thesis, optoelectronic systems have been used only as "gold reference" with the aim of validating the algorithms developed for the acquisition and analysis of UPDRS motor tasks described in the previous chapter. In particular, a motion capture system (with passive markers) produced by BTS Bioengineering (Milan, Italy) was used. BTS Bioengineering supports various types of optoelectronic systems, with different configurations and technical specifications to better meet the customer needs. As indicated in [Figure 13], each solution can support a different number and type of cameras (TVC), which determine the accuracy, the working volume, the quality (sensor resolution), the minimum and maximum acquisition frequencies (expressed as fps or frame per second) and, of course, the price of the entire system that can vary between 10,000 € up to 150,000 €.

TVC	DX 100	DX 400	DX 700	DX 6000	DX 7000
Infrared digital cameras per datastation	up to 4	up to 16	up to 16	up to 16	up to 16
Sensor Resolution	0,3 Mpixel	1 Mpixel	1,5 Mpixel	2,2 Mpixel	4 Mpixel
Acquisition frequency at maximum resolution	140fps	100fps	250fps	340fps	500fps
Maximum acquisition frequency	280fps	300fps	1000fps	2000fps	2000fps
Accuracy/Volume	<0,2mm on 2x2x2m	<0,3mm on 4x3x3m	<0,1mm on 4x3x3m	<0,1mm on 4x3x3m	<0,1mm on 6x6x3m

Figure 13: Types of BTS optoelectronic systems with technical specifications
[Image Source: www.btsbioengineering.com]

The optoelectronic system used for the validation was a BTS SMART DX400©, consisting of 8 fixed and synchronized cameras operating at 100Hz (acquisition frequency): this system is installed in the *Laboratorio di analisi della Postura e del Movimento "Luigi Divieti"*, at the Department of Electronics, Information and Bioengineering (DEIB) of the *Polytechnic in Milan (Italy)*. More details on the validation procedure and the biomechanical protocols will be provided in Chapter 4 (validation of hand tracking algorithms) and Chapter 5 (validation of body tracking algorithms).

3.3 Marker-free motion capture: the 2D camera-based systems

Typical 2D camera-based systems used for marker-free motion capture consist of optical devices capable of generating a single flow of data (specifically color stream) and algorithms that attempt to estimate the third dimension (or depth), thus obtaining a realistic 3D reconstructions of body movements.

These solutions allow only two-dimensional (2D) approaches to motion analysis, for example using the color stream (i.e., a sequence of images in RGB format) and tracking

algorithms based on Computer Vision and Image Processing methods. For many years, this has been the only way to analyze body movement without markers, used both for tracking and recognition of specific body parts[103,104]. Many methodological approaches were based on the extraction of specific features (or descriptors) from single images (i.e., contours, silhouettes, edges, colors, textures); others more complex methods have tried to approximate the kinematic properties, shape and appearance of the body through human 3D models consisting of spheres and cylinders[105].

The main difficulties were encountered in designing two-dimensional approaches to marker-free motion capture:

- Reliability of motion tracking: complex models and algorithms based on multiple descriptors were used to provide more robust and reliable body tracking, with a growing demand for computing resources (real-time issue);
- Self-occlusions and depth ambiguities: multi-camera systems were usually preferred to solve the typical issues of single view solutions, but this has led to an increasing complexity of the systems and of the calibration procedures;
- Uncontrolled environments: dynamic backgrounds, lighting conditions, shadows, reflective surfaces in the scene are common challenging situations that affect the results of motion capture and movement analysis;
- High-dimensional problems: some parts of the body, such as hands, are characterized by high degrees of freedom (DOF) and interdependence constraints between the individual elements (as fingers and phalanges) which make it impossible to reliably recognize and track only through shape, appearance and color.

Generally, constraints on movements and environments are adopted to partially solve or simplify the problems. However, the same constraints are not acceptable or practicable in all contexts and must therefore be considered on a case-by-case basis.

3.4 Marker-free motion capture: the 3D camera-based systems

The real revolution for motion capture and movement analysis was marked by Microsoft Kinect© which, as we will see, allowed for the true 3D reconstruction of body movement[106]. Microsoft Kinect© was launched in November 2010 as low-cost accessory for the Xbox 360, a very popular game console in those years. Since the announcement of its release on the market, this device has raised great expectations in Computer Graphics and Computer Vision, as it proposed a totally innovative and natural way to interact with videogames based on

gestures, movements and voice. In a short time, Microsoft Kinect© ([Figure 14]) has become a widely used device in industry and research: at the beginning of 2012, over 18 million units had already been sold; in February 2012, a new version of the device was released, which can be used in Windows environment, in order to speed up the diffusion in new sectors and the development of applications not strictly related to XBOX 360 and video games. Microsoft Kinect© technology enabled a new way of processing images to obtain 3D reconstructions, a complex process when only the color information of 2D systems was available. The potential of this technology was so high that it paved the way for new opportunities, including the real-time 3D motion capture that was arguably the most innovative[107].

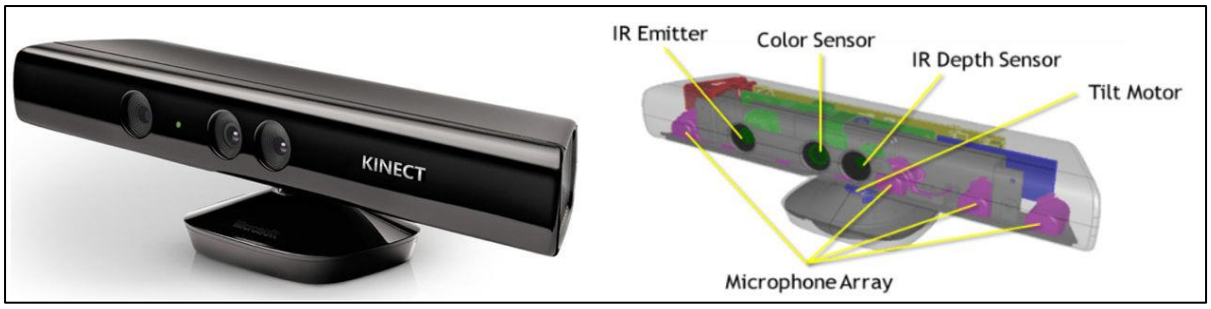

Figure 14: The Microsoft Kinect© (on the left) and its main inside elements
[Image Source: Research Gate]

Unlike previous optical devices, able to generate almost exclusively *color images* (so called RGB cameras), Microsoft Kinect© was also able to produce *depth information*: this new structure of data is called RGB-D or RGB-Depth and Microsoft Kinect© was the first RGB-Depth camera. Inside the device, there are the following components:

- Color Sensor: generates the color stream, which is the sequence of color images with a resolution of 640x480 pixels for three channels (RGB) at 30 FPS. It works like a webcam.
- Depth Sensing System: consists of an infrared (IR) emitter that produces structured light patterns and an IR camera (IR Depth Sensor) that captures the reflected light patterns and their deformation allowing for the depth estimation. The IR camera operates at 30 FPS with a resolution of 1200x960 pixels which is downsampled to 640x480 pixels with 11-bits, providing 2048 levels of depth sensitivity.
- Tilt Motor: allows to tilt the device head up and down to set the viewing angle appropriately
- Microphones array: consists of four directional microphones

Considering the two main components, it is like having a multi-camera system inside a single physical device, making it much more compact, easy to use and characterized by high portability. The problems related to the calibration procedure, typical of systems with multiple cameras, were solved directly by the manufacturer, as the two cameras are in fixed and known positions with respect to each other and at a well-defined distance on the baseline.

This device generates synchronized color and depth images (also called depth maps) which are two-dimensional images made of pixels. When the images are aligned, there is a 1:1 correspondence between pixels of the color and depth images [Figure 15]. Using standard projection procedures, based on the known focal length and center, it is possible to obtain the three-dimensional reconstruction of the scene (called point cloud) in real space.

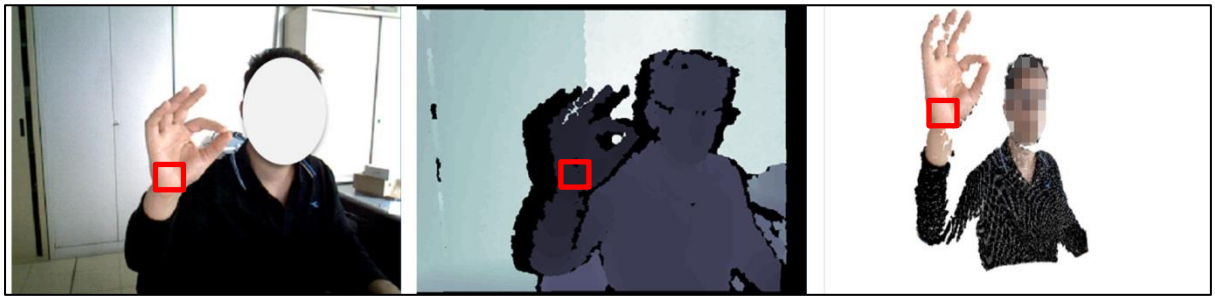

Figure 15: Images generated by the RGB-Depth camera.
Left: the color image where each pixel (red square) is a three-channel color (Red, Green, Blue); Center: the depth image where the corresponding pixel (red square) is a distance measure (in mm); Right: the point cloud (the 3D reconstruction of the scene) where the corresponding point (red square) refers to the real space (X,Y,Z)

But the most innovative feature proposed for the first time by this device was *skeletal tracking*, an algorithm capable of recognizing people (up to 6 person) in the sensor's field of view and following their actions[108]. Furthermore, up to two people could be tracked in more detail through an algorithm that identified points (joints) on the person's body and tracked their movements [Figure 16]. The *joints* are 3D points of a skeleton model that approximately correspond to real anatomical points of the human body: the matching takes place by applying a Machine Learning approach and classifiers trained on depth images. Skeletal tracking is optimized to recognize people in front of the camera, whether standing or sitting, making sure the camera sees their head and upper body. In the *default range mode*, the operating range is between 80 cm and 10 m, but for skeletal tracking, the suggested practical range is between 1.2 m and 4.0 m. In the *near range mode*, the minimum operating distance is between 50 cm and 3 m.

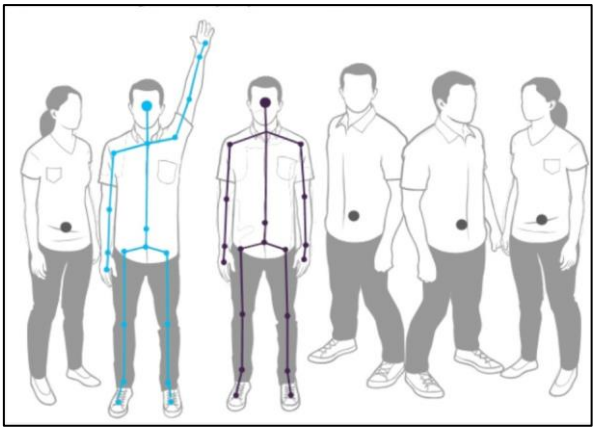

Figure 16: The skeletal tracking algorithm.
Up to 6 people recognized and tracked. Up 2 people tracked with skeleton model and joints

The skeletal tracking or *body tracking* algorithm has allowed to overcome many of the limitations of systems based on 2D cameras, in particular by solving and simplifying the issues related to the 3D reconstruction of the human body. This has led to the use of optical devices in many applications not strictly related to the videogames, for example in medical/clinical applications where today they represent an alternative to optoelectronic systems (more expensive) and wearable sensors (more invasive).

The next generation of the device, Microsoft Kinect v.2, was launched in October 2014 with the aim of further improving the performance of the previous model. This new model has several changes both in hardware and software [Figure 17].

First of all, it has a different design than the previous model. The hardware components are essentially the same but with improvements in terms of functionality and performance: color sensor, depth sensing system (IR emitter and IR camera), array of microphones. The tilt motor has been replaced by a manual adjustment because it was too delicate and subjected to damage.

Hence, the depth sensing system uses *time-of-flight* (ToF) technology, a new method for calculating the depth map that is very different from the structured light of the predecessor. ToF technology is based on pulsed light, generated by the IR emitter at a specific frequency, and on the estimation of the time that the light pulses take to travel the camera-object-camera distance. The light pulses are reflected by obstacles (objects) that are in the camera's field of view. As a consequence of the camera-object distance and the speed of light, a temporal shift is generated between the emitted and reflected signals that is equivalent to the phase shift between light pulses (with known frequency). This shift is detected by the IR camera for each pixel of the scene, thus allowing to calculate the camera-object distance through the formula $d = c * \varphi / 4\pi$, where c is the speed of light and φ is the temporal shift, considering that the

distance must be covered twice (round trip). This innovative technology allow for greater reliability and accuracy in estimating depth. The technical differences between the hardware components of the two models are summarized in [Table 4]. A new version of SDK was released to have access to the potentiality of the new Kinect model[109].

Figure 17: The Microsoft Kinect v.2 (left) and 3D reconstruction of the scene (right)
[Image source: https://developer.microsoft.com/en-us/windows/kinect/]

HW COMPONENT	KINECT V.1	KINECT V.2
Color Sensor	640x480 (30 FPS)	1920x1080 (30 FPS)
Depth Sensor	320x240 (30 FPS) (extended to 640x480)	512x424 (30 FPS)
Depth Technology	Structured Light	Time-of-Flight
Operative Range	0.8-4.0 m (0.4 in near mode)	0.5-4.5m
FOV Angle (horizontal)	57 degrees	70 degrees
FOV Angle (vertical)	43 degrees	60 degrees
Tilt Motor	yes	no
Microphones	yes	yes
USB standard	2.0	3.0
Supported OS	Windows 7, 8	Windows 8, 8.1, 10
Price (at launch)	$ 150-250	$ 200

Table 4: Comparison between Kinect v.1 and Kinect v.2: hardware components

The skeletal tracking algorithm has also been significantly improved and optimized in terms of recognition and stability of the model thanks to greater reliability and accuracy in estimating depth. The number of joints of the skeletal model has increased from 20 to 25: of particular importance are the points added on the hands. The 3D position of the joints has also been slightly modified, especially for the trunk-shoulder-hip areas, to be more faithful to the position of the corresponding anatomical points. These improvements have allowed further diffusion in research and applications such as gesture and pose recognition, body tracking and movement analysis. The technical differences between the hardware components of the two models are summarized in [Table 5]. In addition, an improved face model has been released for face tracking, face recognition and expression analysis. Only the

hand tracking remained unexplored from both devices. This is probably due to the fact that the producers' resources have focused mainly on the greater possibilities offered by body tracking (let's not forget that Kinect was born to support video gaming consoles). Another aspect concerns the operating features of the devices which, precisely for this reason, have been optimized for longer distances, even if the near range mode has tried to overcome this limit. To overcome this lack, the only way is to develop ad-hoc algorithms, based on Computer Vision and Machine Learning techniques, which work on the raw images (RGB and DEPTH) generated by these devices. This is the approach used, for example, in the analysis of the motor function of the upper limbs explained in the next chapter.

SW COMPONENT	KINECT V.1	KINECT V.2
Body Segmentation	up 6 bodies	up 6 bodies
Body Skeleton	up 2 bodies	up 6 bodies
Number of Joints	20 per body	25 per body
Hand State	open/close	open/close/lasso
Gesture	no	yes
Face	yes	yes (improved)
Hand	no	no
Speech	yes	yes

Table 5: Comparison between Kinect v.1 and Kinect v.2: software components

In late 2014, Kinect v.1 was declared discontinued, perhaps to promote Kinect v.2 which was just launched to replace the predecessor. However, the applications and scientific studies based on Kinect v.1 continued for several years. The transition to Kinect v.2 was not possible for all previously developed applications (with the exception of those related to body tracking) for which it was preferred to continue with the use of the old device model while waiting for new alternatives. In 2018, Kinect v.2 was also declared discontinued, following a change in Microsoft's business strategy. Again, the device continued to be used after this announcement and is still the most popular device used today for body monitoring, as evidenced by the numerous scientific studies published in 2019-2020: by doing an advanced Google Scholar search in this period and using the keywords "Kinect v2" OR "Kinect" OR "depth" in the title, you get an availability of over 500 papers. But, in this case, the reason is the lack of other body tracking algorithms as powerful as the one made available by Kinect v.1 (first) and Kinect v.2 (later). The large databases used by Kinect (v.1 and v.2) for skeletal tracking and the optimization work to ensure the real-time tracking did not allowed for

similar results with any of the new devices and/or tracking algorithms that have recently been proposed as possible alternatives for body tracking.

Among the most recent optical devices that have been presented as an alternative to Microsoft Kinect there are: the Intel RealSense D400 series (specifically, D415[110] and D435[111]) and the Orbbec series (specifically, Astra and Astra Pro[112]). These are RGB-Depth cameras that have many similarities with Microsoft products, but their performance, at the moment, is not so good in terms of accuracy and reliability, especially in the estimation of the depth map with an obvious impact on body tracking algorithms [Figure 18].

Figure 18: The alternatives to Microsoft Kinect: Astra Pro (left), D415 (centre), D435 (right)
[Image source: manufacturer web pages]

Astra sensors are closest to Kinect v.1 in both image resolution and use of structured light technology. However, the firmware does not allow the control of the internal device parameters (such as gain, exposure, color balance), making them very sensitive to changes in ambient light conditions. The manufacturer provides a proprietary body tracking algorithm based on a very similar skeletal model to Kinect v.1, although it is not comparable in terms of tracking stability.

RealSense sensors offer more options both in terms of both resolution and frame rate, being suitable for tracking in dynamic scenes and 3D reconstruction of static scenes. These are ToF cameras such as Kinect v.2, which allow the control of various internal parameters in order to optimize the functionality according to the needs of the application. However, they are characterized by a rather noisy depth map, unless special filters are used to improve the quality of the depth at the expense of the frame rate. In this case, the manufacturer does not provide a proprietary body detection and tracking algorithm. This functionality is even more delegated to third-party companies that develop cross-platform tracking algorithms, compatible with the main RGB-Depth cameras available on the market. In general, they allow the use of their algorithms through free licenses (limited in time or functionalities) or through the payment of monthly/annual subscriptions. This is the case, for example, of Nuitrack SDK[113] developed by 3DiVi Inc.: this is a middleware for body tracking with depth cameras that generates a skeleton model based on 19 joints [Figure 19]. It is compatible both

with Astra and RealSense cameras and runs in Windows, Linux and Android environments. Nuitrack is currently one of the most used alternatives to Microsoft Kinect's body tracking algorithm, but it has not achieved the same reliability. The main problems concern the stability of the joints in the extremities of the body (i.e., hands and feet) and the tracking performance in sitting position.

Figure 19: The Nuitrack skeletal model
[Image source: Nuitrack web page]

As for the hand tracking, currently the only device that produces a proprietary algorithm capable of capturing the hand (in all its parts) and forearm movements is Leap Motion[114]. It is not quite an RGB-Depth sensor like the previous ones as it provides neither color nor depth streaming. It works on IR emitters and cameras to reconstruct a hand skeleton model, that is complex enough to capture fine hand movement [Figure 20]. It is used in dedicated applications, mainly as a human-machine interaction device due to the limited working volume and performance degradation with high dynamic movements.

Figure 20: The Leap Motion (left) and the hand skeletal model (right)
[Image source: Leap Motion web page]

In 2019, Microsoft announced Kinect Azure, the next generation RGB-Depth sensor[115]. Unlike previous models, born as accessories of video game consoles, Kinect Azure is an independent device that Microsoft has developed to allow the use of its services based on Artificial Intelligence (AI). Expectations were immediately very high worldwide, although initially this sensor was only distributed on the US and Asian markets. Kinect Azure uses ToF technology to estimate depth. It has the same sensors as the Kinect v.2 (color sensor, depth sensing system, microphone array) plus the Inertial Management Unit (IMU) sensor. All sensors have been improved over previous models. The color sensor is a 4K RGB camera that can be used as a standard USB device. Several resolutions and operating modes are available to meet the needs of developers. The depth sensing system relies on an IR emitter and 1MP camera to take more accurate depth values. The microphone array consists of 7 high quality microphones. The IMU sensor allows to detect movements on the three reference axes [Figure 21].

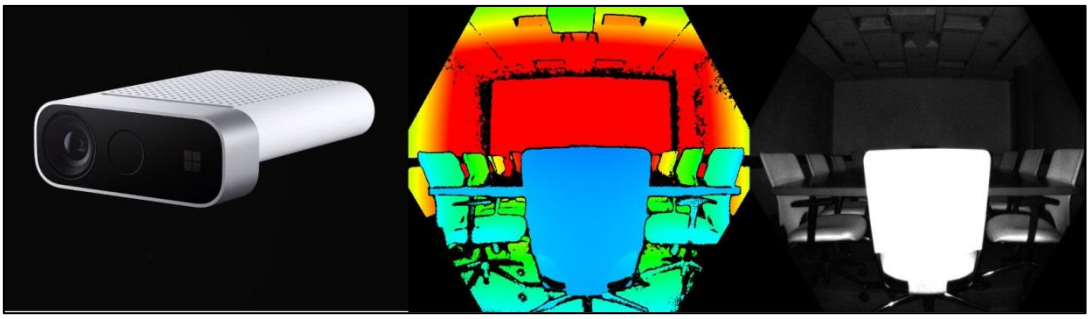

Figure 21: The Kinect Azure (left), the depth image (centre) and the IR image (right)

One of the most promising features is the body detection and tracking algorithm which has been further improved over that of Kinect v.2. The skeletal model consists of 32 joints organized in a hierarchy ranging from the center of the body to the extremities [Figure 22]. The current body tracking algorithm of Kinect Azure uses a machine learning model trained on a large database to estimate poses and to reconstruct the skeletal model. This entails a fairly high computing power compared to Kinect v.2 in order to guarantee real-time performance: at the moment, this represents the greatest limitation in the use of the new device.

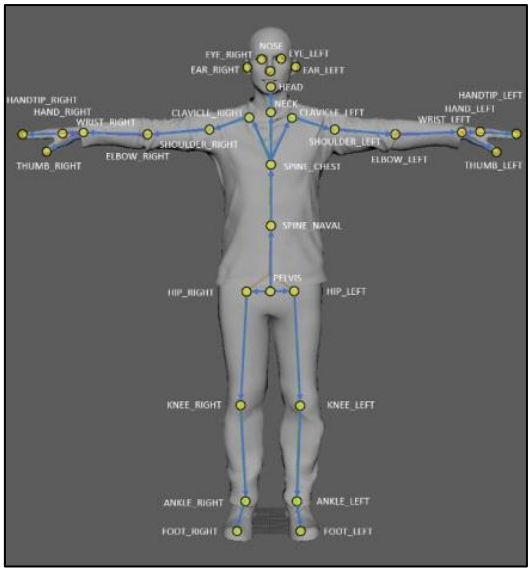

Figure 22: The skeletal model of Kinect Azure
[Image Source: https://docs.microsoft.com/en-us/azure/kinect-dk/body-joints]

3.5 The future: Deep Learning approaches (OpenPose)

In the future, the body detection and tracking algorithms will increasingly be based on artificial intelligence and deep learning, with an ever larger training dataset in order to obtain most reliable and general algorithms as possible.

Some frameworks developed according to this new methodology are already available today. Among these, the most promising seems to be OpenPose[116]: it is a framework to detect some key points in the scene that are part of the same human body, using only color images (2D approach) and Convolutional Neural Network (CNN) models. CNN generates confidence and affinity maps for each pair of key points to recognize multiple skeletons in the same scene [Figure 23].

The performance of OpenPose needs to be verified for biomechanical applications in terms of reliability and accuracy in movement analysis[117]. The actual limitation is related to real-time processing: at the moment, the required computing resources are very high (in fact, real-time processing is impossible without high-performance GPU) and it is often preferred to process recorded video sequences rather than the real-time streaming. However, the improvement of technologies and power processing suggests that this will no longer be a problem in few years, allowing for greater tracking accuracy by combining the potential of 3D vision systems.

Figure 23: Multi-persons tracking with OpenPose
[Image Source: 116]

3.6 Thesis Motivation on RGB-Depth cameras

As we have seen, many vision-based systems are available for motion analysis, each with their strengths and weaknesses. In this thesis, I have chosen to focus my attention of 3D camera-based systems using RGB-Depth optical devices.

In order to identify new therapeutic and rehabilitation pathways suitable for home environment, RGB-Depth cameras certainly offer greater opportunities than optoelectronic systems (constrained by cost and size to the clinical and research setting) and wearable sensors (widely used for the movement analysis but certainly more invasive, less practical to manage and capable of capturing the movement of only some parts of the body at the same time). Solutions based on RGB-Depth cameras are certainly cost-effective compared to other options; they work in real-time; allow contactless measurements; they are portable and easy-to-use; they are not bulky; they are very versatile and can be used in different applications. As for body tracking, they allow both to use tracking algorithms provided by manufacturers or third-parties; or to create dedicated algorithms from the raw information provided by the optical device in the case of suboptimal performance or algorithms not suitable for the specific applications.

The typical problems of these solutions concern the possibility of occlusions (i.e., when the movement is partially hidden by other objects or parts of the body itself); the operating requirements (i.e., minimum and maximum operating distances, the size of the field of view and the working volume, and ambient light condition that may interfere with the IR camera); the definition of the appropriate setup, identifying the optimal point-of-view to capture the movement of interest (for example, choose between a front view, side view, top view, and a specific distance).

These strength and weakness are common to all the RGB-Depth cameras previously described, although some of them (such as Kinect Azure) also require computational resources that are still quite high and therefore unlikely in home environments.

For the purposes of the thesis, Kinect v.1 and Intel RealSense SR300 (a predecessor of D400 series) were used for the analysis of the movement of upper limbs. A dedicated algorithm, based on color and depth images has been developed for hand tracking (more details will be provided in Chapter 4 and Chapter 6). Instead, Kinect v.2 was used for the analysis of movement of lower limb and posture. In this case, the skeletal tracking algorithm, provided by the manufacturer via the SDK, was used for body tracking (more details will be provided in Chapter 5).

The choice of Kinect v.1 and Kinect v.2 was determined by the fact that, when this project started, there were no other alternatives so good and efficient that they could be used successfully. Obviously the future work, on which we are already working[118], will be to evaluate other more good, efficient cost-effective solutions (for example based on Astra and Nuitrack) or more performing (for example based on Kinect Azure and its SDK Skeletal tracking); but also the new approaches based on Deep Learning, given the continuous development of powerful graphic cards that will also allow to use this methodology for the analysis of movements in real-time.

Chapter 4

Quantitative assessment of hand motor function using vision-based systems

After describing the general context in which the project was developed, now the technological solutions that have been implemented and the results achieved will be presented in greater detail.

This chapter will deal in particular with the approach for the quantitative evaluation of the hand movement and the motor function of the upper limb through a 3D vision-based system and RGB-Depth optical devices. It will also describe the hand tracking algorithm, developed specifically for this purpose, as other frameworks and libraries were released only after the start of this project. This was the first study undertaken and completed within the PhD project.

The implemented solution, described in this chapter, led to the paper "*A Self-Managed System for Automated Assessment of UPDRS Upper Limb Tasks in Parkinson's Disease*", which will be referred as Paper 1 in this chapter, which was published in 2018 on the special issue "Sensors for Gait, Posture and Health Monitoring", part of the Sensors journals (MDPI).

4.1 Schema of the proposed approach

The main goal of this study was the analysis and characterization of the motor function of the upper limbs, with particular interest in the movement of the hand. As previously indicated, motion analysis is based on standard motor tasks used in the clinical setting to assess the severity of hand motor impairment. Various solutions are available in the literature for the analysis of the motor function of the upper limbs. Some are based on wearable sensors[119-123] which are more invasive for people with motor disabilities and can affect the motor performance compared to optical devices; others rely on video processing[124], reflective markers[125] or bare-hand tracking[126-128], but they are limited to single task or have limited robustness. The aim of the proposed approach is to overcome these limitations and obtain an accurate and complete evaluation of the motor function of upper limbs.

The proposed approach can be summarized by the following schema [Figure 24]. The first block relates to the *"Data Acquisition"*, that is the acquisition of motor performance to be

analyzed. This involves the development of the *acquisition system*, that is the 3D vision-system based on RGB-Depth optical devices; the *validation phase*, an experimental campaign to verify the accuracy and robustness of both the acquisition system and the tracking algorithms with respect to the reference systems for motion analysis; and finally the definition of the *experimental protocol*, i.e. the set of motor tasks and participants included in the study. The second block concerns the *Performance Analysis* that is the characterization of the motor performance through kinematic parameters. This involves the *parameter selection* procedure to identify the most relevant parameters in the initially defined set; *statistical analysis* to identify the most significant parameters with respect to standard clinical evaluation; and the *graphical representation* to give an intuitive and immediate indication of a performance compared to a reference one. This block led to the objective evaluation of motor performance through physical measures in accordance with standard clinical scales. The last block concerns the *Classification*, that is the automatic assessment of motor performance through Machine Learning approaches starting from the kinematic parameters selected. This involves the training of multiple *supervised classifiers* and the selection of the one with the best classification performance; the analysis of various *classification problems* such as the "diagnostic problem" that is the classification as healthy or pathological subject, and the "severity problem" that is the classification of motor performance according to the UPDRS severity scores; the *accuracy and correlation* analysis that refers to the classification performance of supervised classifiers.

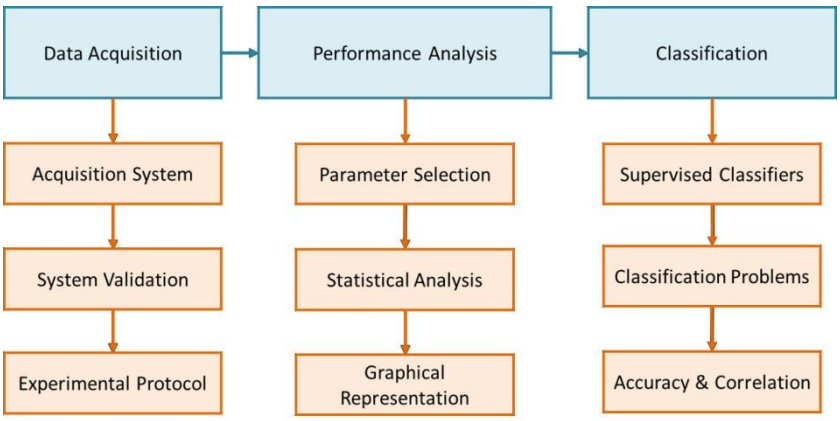

Figure 24: Schema of the proposed approach for upper limb assessment

4.2 Data Acquisition

4.2.1. The Acquisition System

The implemented acquisition system is a 3D vision-based system consisting of both hardware and software components that are not only related to acquisition, but also to image and video processing.

As for the *hardware component*, the system uses an RGB-Depth camera: initially the Microsoft Kinect v.1 was used, then the Intel RealSense SR300. Both of these devices provide synchronized RGB (color) and DEPTH streams, with a minimum frame rate of 30 FPS which is sufficient for hand movement capture event at high speed. The operational function is optimized for *near mode* motion capture, i.e. less than 2.0 m. The RGB-Depth camera is connected, via an USB port, to a processing unit, which can be a laptop, desktop or a mini-pc such as the Intel NUC i7. The processing unit can be connected, depending on the type, to a monitor or a TV screen via VGA or HDMI connections to provide the visual feedback of the hand movement [Figure 25].

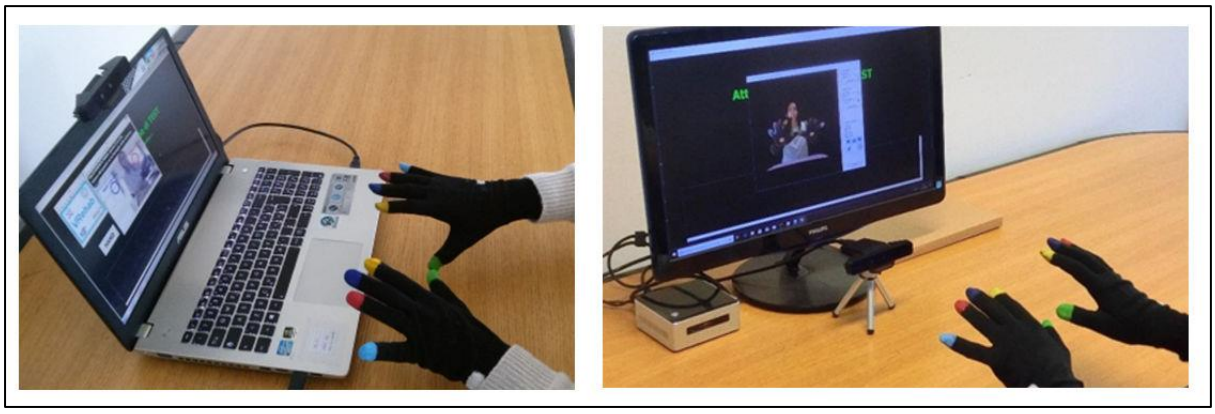

Figure 25: The acquisition system: configurations with notebook (left) and mini-pc (right)
[Image source: Paper 1]

An important element of the system are the gloves with color markers visible in [Figure 25]: these are passive gloves in black silk, with color markers imprinted in specific parts of the hands, in particular on the fingertips, on the wrist and on the palm. The purpose of this equipment is to simplify the hand tracking algorithm, so reducing the complexity of the problem in terms of model and computational resources: the 3D tracking of color blobs using Computer Vision techniques is sufficient to capture movements of interest defined by the experimental protocol.

As for the *software component*, it consists of custom C++ and MATLAB scripts that run on the processing unit. Several functionalities are implemented by the software component: the hand tracking algorithms based on raw video streams provided by the RGB-Depth

sensor; the analysis and characterization of movement through the processing of the trajectories of the 3D color blobs; the automated evaluation of motor performance through supervised classifiers.

Hand tracking using Gloves with color markers

The use of gloves allows to follow in real time the movement of specific parts of the hand (palm, wrist) and fingers (fingertip) corresponding to the colored areas. The hand tracking algorithms implemented and based on Computer Vision techniques are able to recognize and follow the movement of the colored areas. The tracking algorithms integrate streams of color and depth provided by the RGB-Depth sensor to ensure greater robustness with respect to individual information: the color information allows the identification of specific areas on the depth map which, otherwise, could be confused with others. This approach represents a simplification of the problem as the hand points corresponding to the color markers are sufficient for the motor tasks of interest: a complete capture of the hand movement would require more complex algorithms and models, with higher computational requirements. The idea of these gloves comes from the following needs: to have a uniform color of the hand (which is impossible considering the color of the skin); ensure rapid identification of points of interest by increasing the contrast between colors; make sure that the position of the markers is maintained during rapid movements (for this reason markers have been imprinted on the gloves); allow natural hand movements without cables or heavy structures; ensure minimal invasiveness and comfort when wearing them (for this reason the gloves are made of light material as silk or cotton). Some markers have different in shape in addition to color: this is because they are used for special needs.

The hand tracking algorithm consists of two phases: the first relates to the *"initialization phase*", the second is the *"tracking phase"* of hand and fingers.

The *"initialization phase"* is a procedure that is automatically activated when the system software is started: in this phase, which lasts only a few seconds, the hand has to be held open in front of the RGB-Depth device. The initialization phase consists of several algorithms dedicated to *system calibration activities* with the aim of setting the optimal operating condition of the system.

The first activity of the initialization phase is the *global brightness adjustment* of the RGB stream: according to the brightness of the environment, some internal parameters of the RGB-Depth sensor are automatically modified to avoid exposure conditions associated with too low or too high light.

The second activity of the initialization phase is the *hand segmentation* that is the procedure to identify the hand in the environment: for this operation, the depth stream is acquired and processed with Computer Vision methods to recover the centroid of the 3D points of the depth map closer to the RGB-Depth sensor. The hand centroid is used to segment the hand from the background and to define the hand bounding box both on color and depth images.

Finally, a *color constancy algorithm* is applied to compensate for different ambient light conditions, such as the intensity of ambient light or the predominance of a chromatic component. For this purpose, the white circular marker placed on the palm is detected by its shape to evaluate the average luminance in this area. The average levels of the color components are also evaluated to compensate for the predominance of one of them. Based on the estimated type of light conditions detected on the glove (low, normal or high intensity), a set of color thresholds (one for each color on the glove) is set to correctly recognize and track each color blob. At the end of the *initialization phase,* the system is calibrated according to the ambient light conditions which are supposed not to change during the use of the acquisition system.

During the *tracking phase,* the segmentation of the hand is continuously performed on the depth stream and the 3D position of the hand centroid is consequently updated as well as the 2D and 3D bounding boxes. The color thresholds, selected during the initialization phase, are used to detect and track the color blobs of markers within the 3D bounding box. Detection and tracking of color blobs is based on the CamShift algorithm. Cumulative histograms for black glove and color markers are used to define the hand area and each marker more accurately. The 2D pixels of every area of interest on the RGB image are re-projected into the corresponding 3D points using the associated depth information and the 3D centroid of each marker is then evaluated, as an estimate of the 3D position of the corresponding area of interest on the hand (i.e., fingertip positions, palm position, wrist position).

The hand tracking algorithm produces the 3D trajectory of each color marker which corresponds to the 3D trajectory of that part of the hand performing the required movement [Figure 26].

Figure 26: Hand Tracking algorithm: static open hand (left); dynamic semi-closed hand
Hand segmentation, detection of color markers, bounding box and centroids of hand with glove and color blobs
[Image source: Paper 1]

4.2.2. System Validation

The acquisition system and the hand tracking algorithm were subjected to a *validation procedure* with the aim of evaluating the performance of the proposed solution (in terms of tracking accuracy and robustness) compared to a gold-reference system. In particular, a BTS SMART DX400 optoelectronic system (BTS Bioengineering, Milan, Italy) with 8 TVC and acquisition rate of 100 fps was used as gold-reference system for the validation procedure. An experimental setup was defined to allow the two systems to simultaneously acquire hand movements while performing specific motor tasks. UPDRS tasks of the upper limbs (i.e., Finger Tapping, Hand Movements, Pronation Supination) ,used for the experimental protocol (see section 4.2.3), were considered also for the validation procedure. To allow the optoelectronic system to capture the movements performed with the gloved hand, small reflective markers were applied to the glove at the points of interest on the hand, as shown in [Figure 27].

Figure 27: Glove with reflective markers for the optoelectronic system
[Image source: Paper 1]

Several tests of the three motor tasks were carried out, to cover different speeds and different positions in the working volume common to the two systems. The 3D trajectories of the color markers were acquired simultaneously. In the post-processing phase, the trajectories were aligned both in time and in space to be correctly compared: this is because the two systems have different time bases, acquisition rates and reference systems. For each motor tasks, the relative distance between the reference markers was defined, based on the required hand movement. For each test performed, the difference between the estimated distance from the two systems (D) was evaluated. As a measure of tracking accuracy, three parameters were considered: the mean of the distances (D_{MEAN}), the standard deviation (SD) and the maximum absolute difference (MAD). The tracking accuracy is shown in [Table 6]. The results show that the tracking accuracy is very good. In particular, the maximum difference between the two systems is less than 1 cm on all the tasks and all the tests analyzed, and the residual error is mainly due to the different position of the centroids of color blobs, estimated by the tracking algorithm, and the position of the reflective markers on the hand.

ACCURACY PARAMETERS	FINGER TAPPING	HAND MOVEMENTS	PRONATION SUPINATION
D_{MEAN} (mm)	2.5	3.1	4.1
SD (mm)	3.0	3.5	4.0
MAD (mm)	5.2	6.0	7.0

Table 6: Accuracy of the tracking algorithm for the three tasks

This result indicates that the hand tracking algorithm is accurate for capturing the hand movements, showing a performance comparable to the gold-reference system for all the motor tasks considered. Furthermore, the robustness of the algorithm is verifiable by comparing the 3D trajectories of distance and speed after the data alignment procedure, as shown in [Figure 28] where the trajectories correctly overlap.

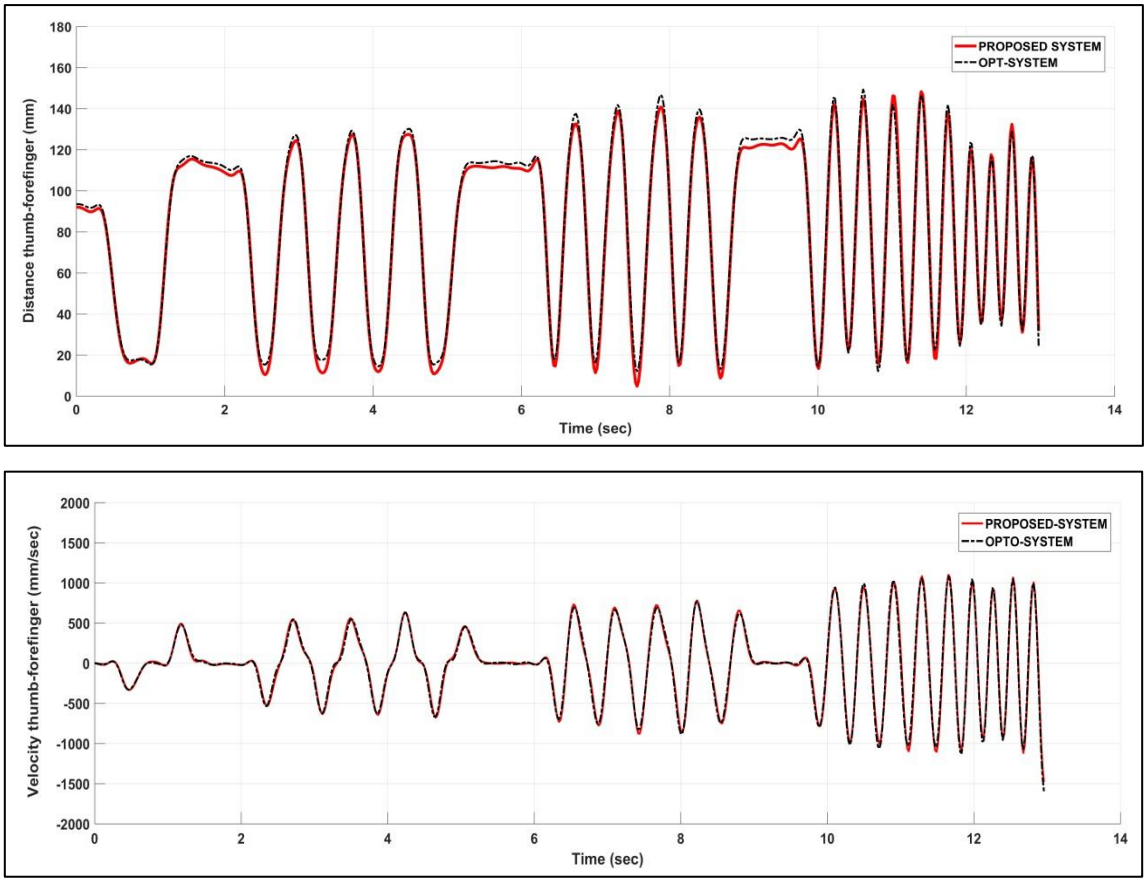

Figure 28: Example of FT task: 3D trajectory (top) and speed (bottom) captured by the two systems [Image source: Paper 1]

A second experiment was conducted to compare the performance of the proposed solution and the Leap Motion hand tracking algorithm that was released after the start of the project. In this case, the experimental setup involved a configuration to capture hand movements from the three systems simultaneously. Leap Motion provides a model of the hand consisting of 3D joints as explained in Chapter 3: for each motor task, the joints corresponding to the position of the reflective markers were considered. Also in this case, the results of the proposed solution are substantially in line with those reported in Table 6. On the contrary, Leap Motion has obtained worse results in terms of precision, as shown in [Table 7], which indicates higher tracking errors for the three motor tasks, in particular for Pronation-Supination task which is the most challenging for a tracking algorithm.

ACCURACY PARAMETERS	FINGER TAPPING	HAND MOVEMENTS	PRONATION SUPINATION
D_{MEAN} (mm)	11.7	13.8	20.1
SD (mm)	13.3	22.8	26.6
MAD (mm)	32.1	35.2	45.1

Table 7: Accuracy of the Leap Motion tracking algorithm for the three tasks

These tests highlighted some limitations of the Leap Motion hand tracking algorithm, especially in high dynamic conditions. [Figure 29] shows some of the tracking errors that emerged during testing. The higher error in Pronation-Supination task is due to the unexpected inversion of the X and Z components of the hand model, with the consequence that the right hand was considered as if it were the left [Figure 30].

The *validation procedure* has therefore demonstrated the accuracy and robustness of the acquisition system and the proposed hand tracking algorithm, not only compared to a gold-reference system but also compared to a more recent commercial system.

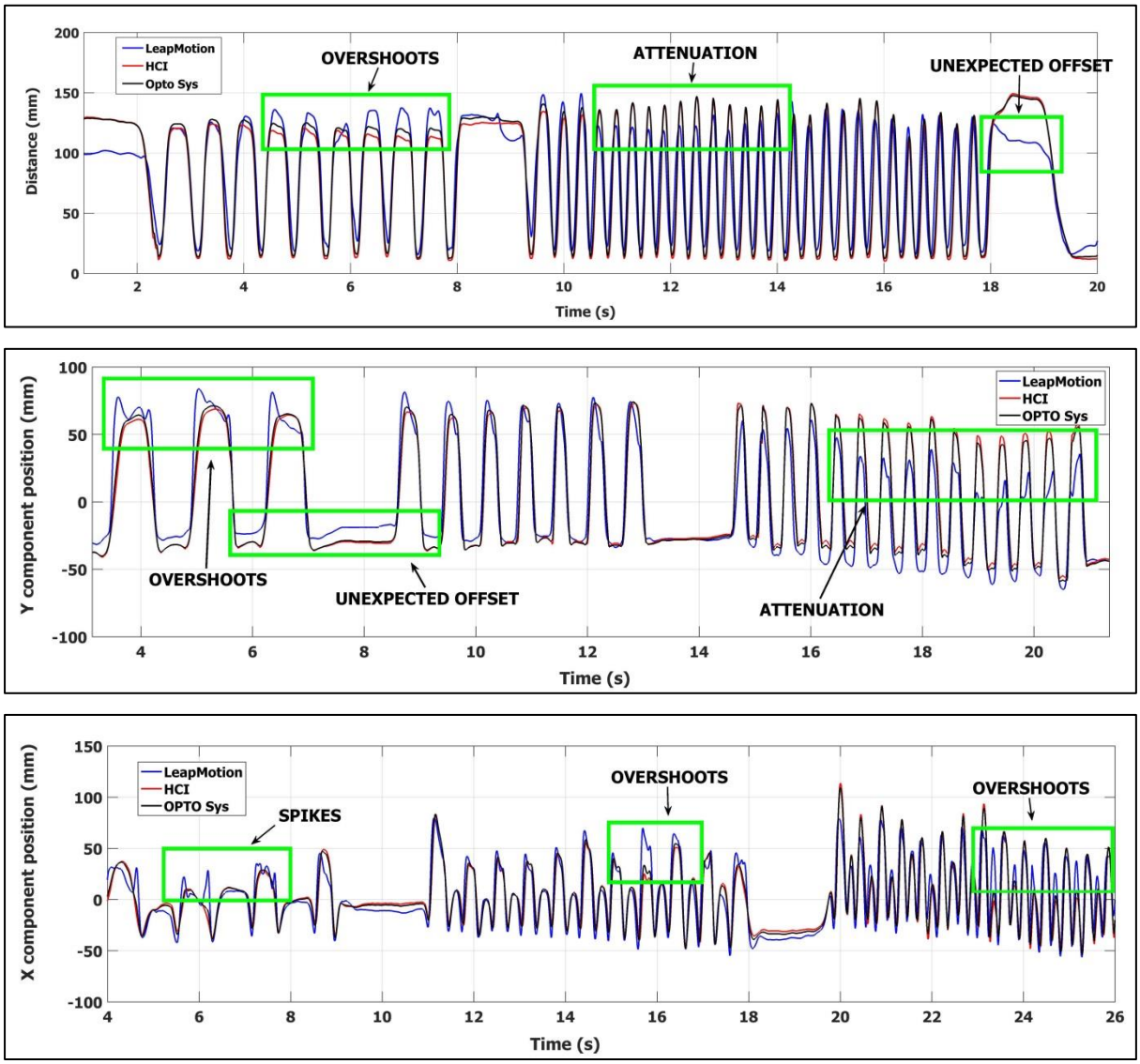

Figure 29: Tracking errors of Leap Motion tracker (blue line)
versus optoelectronic system (OPTO Sys: black line) and the proposed hand tracking algorithm (HCI: red line)
[Image source: Paper 1]

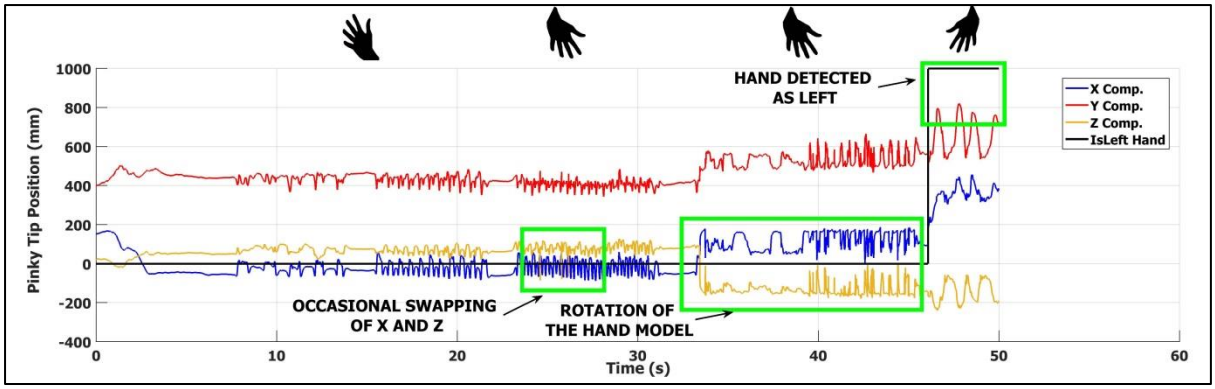

Figure 30: Example of the Leap Motion failures in little-finger trajectory during the Pronation-Supination [Image source: Paper 1]

4.2.3. Experimental Protocol

The experimental protocol involved two group of subjects. The first group consisted of 57 subjects with Parkinson's disease (referred as PD group) whose main personal and pathological characteristics are listed in [Table 8]. The following inclusion criteria were met: no previous neurosurgical procedure, tremor severity < 1 (according to UPDRS assessment), no cognitive impairment (Mini-Mental State Examination > 27/30). All subjects with PD took the medication routinely. The other group consisted of 25 healthy controls (referred as HC group) with no history of neurological, motor or cognitive disorders.

	PD GROUP	HC GROUP
Number (M/F)	57 (37/20)	25 (10/15)
Age (years) range	45-80	55-75
Mean Hohen & Yahr Score (min, max)	2.1 (1,4)	-
Disease duration (years) range	2-29	-

Table 8: Characteristics of PD and HC groups

The experimental protocol consists of the three motor tasks for the upper limb defined in MDS-UPDRS. The Finger Tapping (FT) task (item 3.4) consists in repeating the tapping movements with the thumb and forefinger, at the maximum speed and amplitude possible. The Hand Movements (OC) task (item 3.5) consists in repeating the opening-closing movements of the hand, at the maximum speed and amplitude possible. The Pronation-Supination (PS) task (item 3.6) consists in repeating the pronation-supination movements of the hand, at the maximum possible speed and rotation. These tasks stress motor coordination, repetition and alternation of movements, activities that are increasingly difficult with the increase in motor disability.

All the PD and HC subjects performed motor tasks with both hands. For PD subjects, the experimental protocol required starting with the least compromised hand, in order to correctly complete the calibration procedure of the acquisition system. Subjects were seated in front of the system, wearing gloves with color markers. The movement of the hand was acquired during the execution of motor tasks and then analyzed by the acquisition system: for PD subjects, each motor performance was also evaluated by a neurologist expert in movement disorders at the same time according to the UPDRS evaluation criteria.

The neurologist assessed all motor performance of the PD group in four UPDRS levels of motor impairment: 0 (normal performance), 1 (performance with slight impairment), 2 (performance with mild impairment), 3 (performance with moderate impairment) on the basis of the perception of speed, amplitude, rhythm, hesitations, halts, onset of fatigue, and so on as required by the UPDRS evaluation criteria. No performance was rated as 4 (performance with severe impairment) likely due to the initial subject selection.

The acquisition system automatically estimated and recorded the 3D trajectories and videos of each motor performance for the next phase of movement analysis.

All the subjects interacted with the acquisition system through the graphical user interface (GUI) that allows the self-management of the entire test session.

Human Computer Interaction and Graphical User Interface

In the perspective of using the acquisition system for home monitoring of upper limb motor function in subjects with PD, the ability to track the hands was used also to provide the system with a natural interface based on gestures and visual feedback, realizing a Human Computer Interaction (HCI) suitable for people with limited computer skills and with forms of motor impairment. This makes the system easy-to-use and self-managed through the graphical user interfaces (GUIs) that guide the user through the test session. The GUIs was designed to support the user with video and textual suggestions, both to make choices by selecting interactive objects displayed using Augmented Reality (AR) and to manage some critical system operations such as the initial system calibration, as shown in [Figure 31].

Figure 31: Example of GUIs for the gestural human-interaction with the acquisition system
Input of information about perceived health status condition (top-left), task selection menu (top-right), starting hand selection (bottom-centre) [Image source: Paper 1]

In this way, the user can control and interact with the system through simple gestures such as closing the hands or pointing the finger at interactive objects. With the same mechanism, the user can introduce information relating to the perceived health status that will be recorded with trajectories and videos. This simple real-time interaction is enabled by the same hand tracking algorithm used for motor performance evaluation. Important features have been considered in the design of the GUI: visibility of interactive object and textual suggestions; planning of rest periods between motor tasks to avoid the onset of anxiety; position of interactive objects to be easily accessible without stressful movements.

4.3 Performance Analysis

Clinical assessment of the severity of motor impairment is based on observing how UPDRS task is performed (see Chapter 2, Figure 8), taking into account certain physical quantities (i.e., kinematic features), as required by the UPDRS assessment criteria, which certainly cannot be “measured” by the human eye.

Underlying these evaluation criteria is a consolidated evidence: the strong correlation between the kinematic features of motor performance and the severity of the assigned clinical UPDRS scores (from class 0 to class 4).

The objective and automatic evaluation of UPDRS tasks aims to quantify the physical features of motor performance through a set of kinematic parameters, which characterize the movements of the hand and which are closely related to those quantities implicitly considered by clinicians to evaluate motor performance. Using the proposed acquisition system, the kinematic parameters are estimated from the 3D trajectories of the hand and finger movement, captured by the hand tracking algorithm.

The correlation between kinematic features and assigned clinical UPDRS scores is evident by observing the 3D trajectories of the hand motor performance in subjects characterized by increasing motor deficit. The performance of healthy subjects are generally characterized by greater amplitude, velocity and regularity [Figure 32]. The performance of PD subjects assessed as UPDRS 0 (normal performance) could be characterized by good amplitude and speed, however the regularity may be slightly lower, as in the case of [Figure 33, first figure]. The performance of PD subjects assessed as UPDRS 1 (slight impairment) could be characterized by irregular amplitude and lower speed, as in the case of [Figure 33, second image]. The performance of PD subjects assessed as UPDRS 2 (mild impairment) could be characterized by irregular and lower amplitude and speed, as in the case of [Figure 33, third figure]. The performance of PD subjects assessed as UPDRS 3 (moderate impairment) could be characterized by irregularity, reduced amplitude and speed, as in the case of [Figure 33, fourth figure]. The performance of PD subjects assessed as UPDRS 4 (severe impairment) could be characterized by very low amplitude and speed, or difficulty in performing the required movement, as in the case of [Figure 33, fifth figure]. It is clear that such different 3D trajectories will generate different kinematic features.

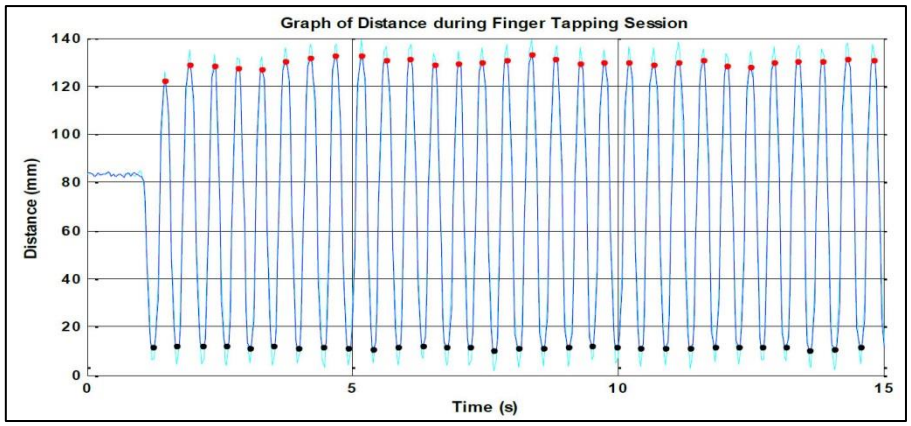

Figure 32: Example of 3D trajectory of an healthy subject (FT task)

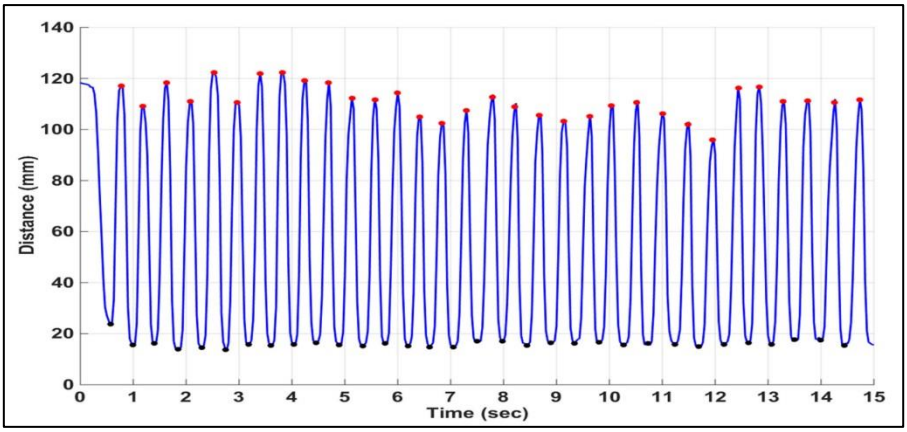
Distance (mm)
Time (sec)

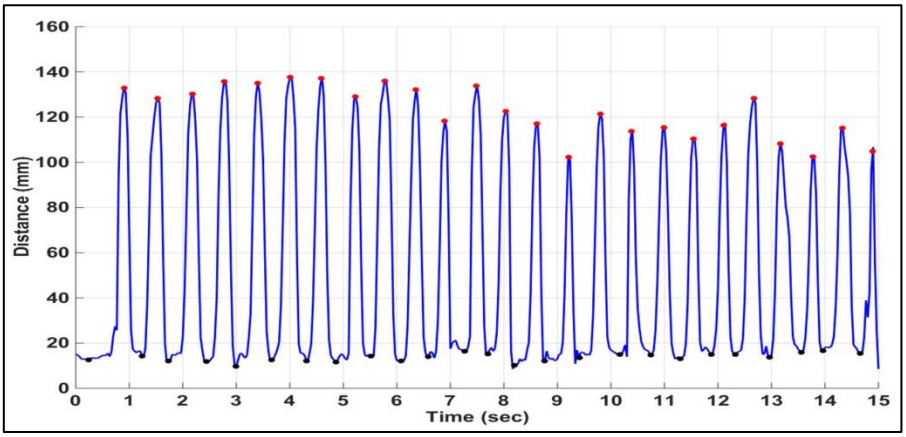
Distance (mm)
Time (sec)

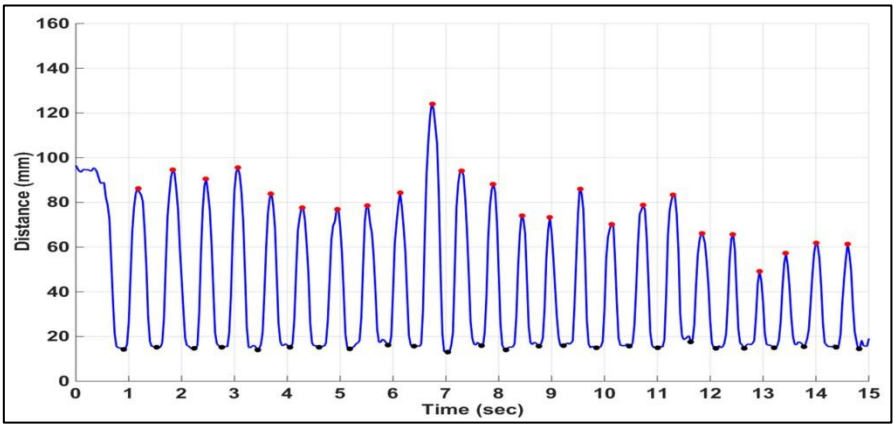
Distance (mm)
Time (sec)

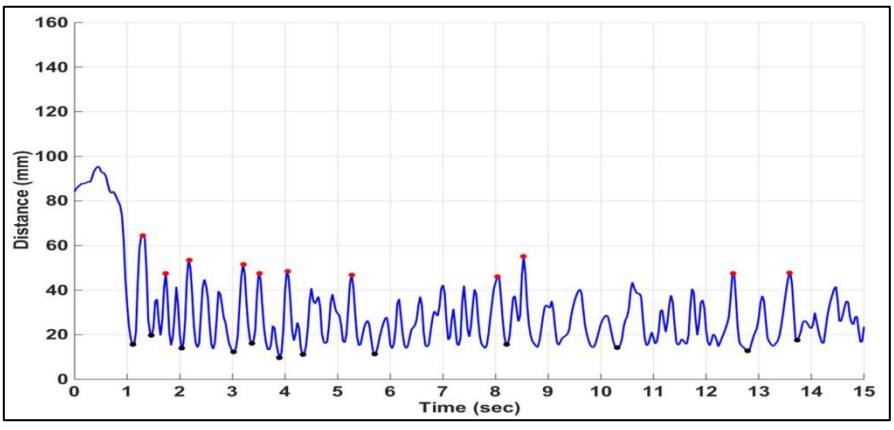
Distance (mm)
Time (sec)

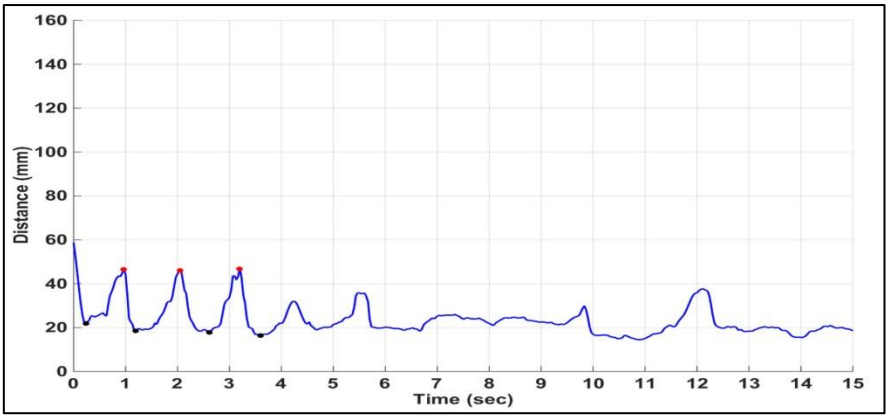

Figure 33: Example of 3D trajectories (FT task) for different level of impairment. From UPDRS 0: normal (top) to UPDRS 4: severe (bottom)

Characterization of movement from 3D trajectories

During the data preprocessing phase, the 3D marker trajectories are resampled (to generate a fixed time step) and filtered by applying a Butterworth low-pass filter (4^{th} order, 10 Hz cut-off) to remove artifact noise due to higher frequencies. The characterization of motor performance is based on the 3D distance between two 3D reference points during the execution of each individual exercise [Figure 34]. In case of FT task, the distance between the marker on thumb and forefinger has been considered; for the OC task, the distance between the little finger and the wrist has been considered; for the PS task, the distance between little finger and a reference point of the hand envelope, that moves solidly with it, has been considered. The 3D distance between the reference points is calculated over the duration of the task, using the traditional Euclidean distance formula between the 3D points. From the distance thus calculated, all the physical quantities representing the features of the movement performed will be extracted.

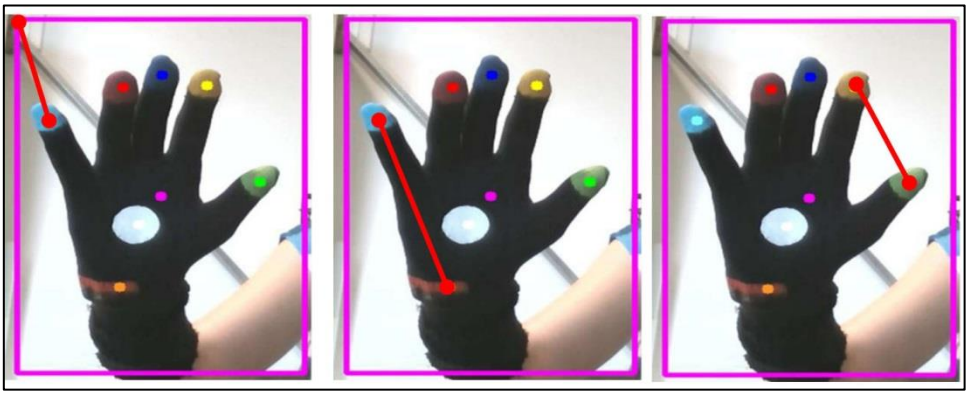

Figure 34: 2D representation of the 3D reference points used for PS (left), OC (centre) and FT (right) tasks

To obtain a complete analysis of the motor function, it is necessary to detect some motor characteristics typical in subjects with PD, relating to kinematic aspects, anomalies and

fatigue. To achieve this, the analysis includes: global measurements over the entire duration of the task, detection of typical anomalies (such as hesitations, freezing, partial movements), and trend lines on task sub-periods. Each task consists in the repetition of a sequence of elementary movements, the detection of which represents the basis for the subsequent characterization of motor performance. For example, according to the Hand Movements (OC) task, the analysis is based on the detection of a sequence of maximum (open hand) and minimum (close hand) points over the time. The period between two consecutive minima is called *movement*, as shown in [Figure 35]. A single movement is characterized by elementary spatial and temporal features such as *amplitude* (that, in the case of OC task, represents the maximum opening of the hand); *excursion* (that is the difference between the maximum and the previous minimum points within a movement); *duration* (that is time difference between the start and end points of a movement); *speed* (that is the velocity of execution of the movement); *rate* (that is the number of movements performed per unit of time). The detection of all movements allows the global and local characterization of the kinematic aspects of motor performance.

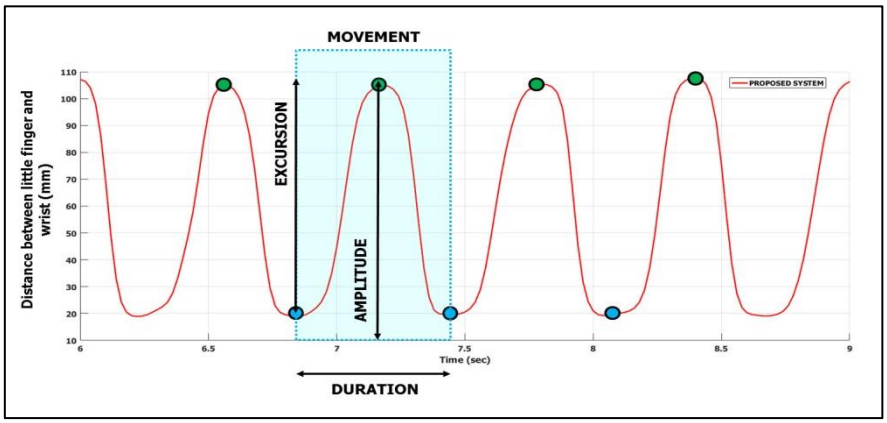

Figure 35: Detection of elementary movements (OC tasks)

As estimators of global measurements were considered: the *mean*, defined as in (1) and the *coefficient of variation* (CV) defined as in (2). The mean of a measure is calculated considering the values of that quantity on all detected movements and represents the magnitude of that measure. The coefficient of variation is calculated considering the values of that quantity on all the detected movements and represents an index of irregularity (in practice, lower values of the coefficient of variation correspond to more regular performances relative to the measure considered).

$$\mu_{measure} = \frac{\sum_{i=1}^{n} measure_i}{n} \qquad (1)$$

$$CV_{measure} = \frac{\mu_{measure}}{\sigma_{measure}} \qquad (2)$$

where *n* is the number of movements detected in the 3D trajectories.

In addition to being evaluated over the entire duration of the task, the kinematic features are also evaluated over three sub-periods, to detect if and when the onset of fatigue occurs. The sub-periods are defined as *initial*, *central* and *final* and each of them corresponds approximately to one third of the total duration. The analysis of movements in the three sub-periods allows to obtain *trend lines* of motor performance and therefore establish how motor performance changes in the three sub-periods: for example, a decreasing trend in speed means that motor performance is slowing down, as shown in [Figure 36]. Also in this case, the same estimators indicated in (1) and (2) were used for the characterization of motor performance: the estimators were calculated for each periods considering the movements detected in each single period.

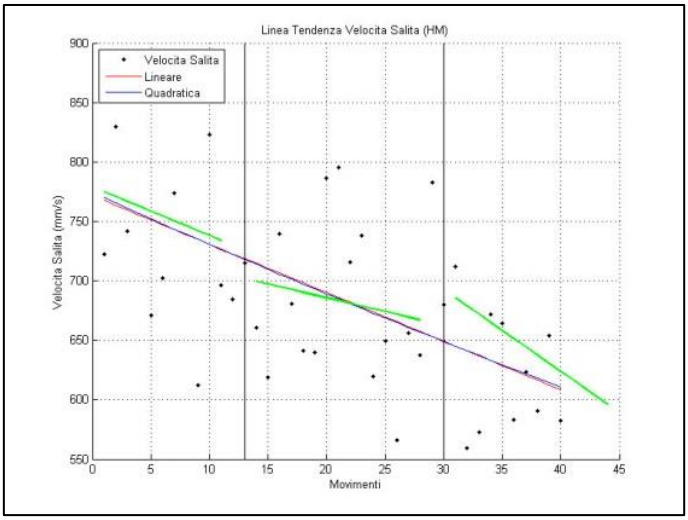

Figure 36: Example of descending speed in central and final periods

In the characterization of motor performance, it is also important to detect *typical anomalies* in subjects with PD: *freezing*, or blocks of movement, detected as outliers in movement duration ([Figure 37]); *partial movements*, detected as anomalous values in the opening or closing phases ([Figure 38]); *hesitations*, detected as changes in the movement direction ([Figure 39]). The number of anomalies detected influences the clinical score assigned to motor performance, so the automatic analysis must also do the same.

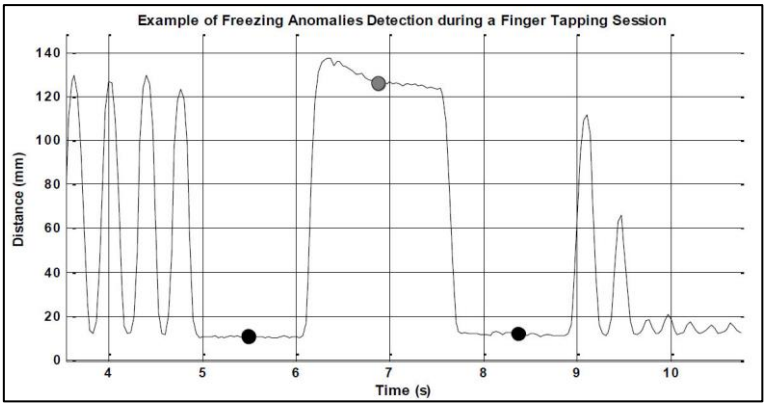

Figure 37: Example of "freezing" detection

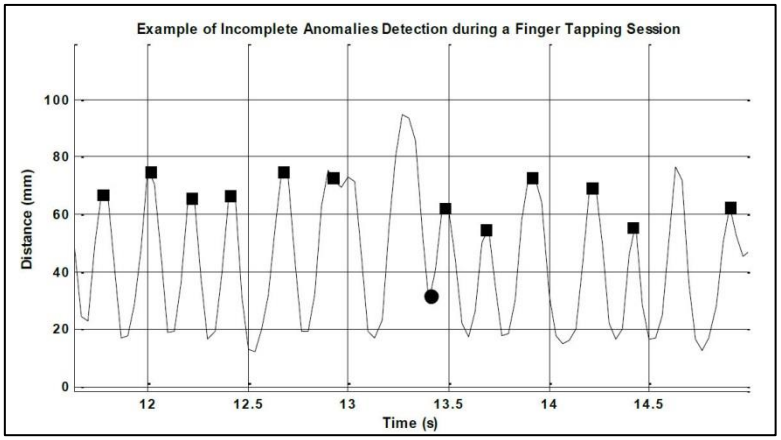

Figure 38: Example of "partial movement" detection (incomplete hand closure)

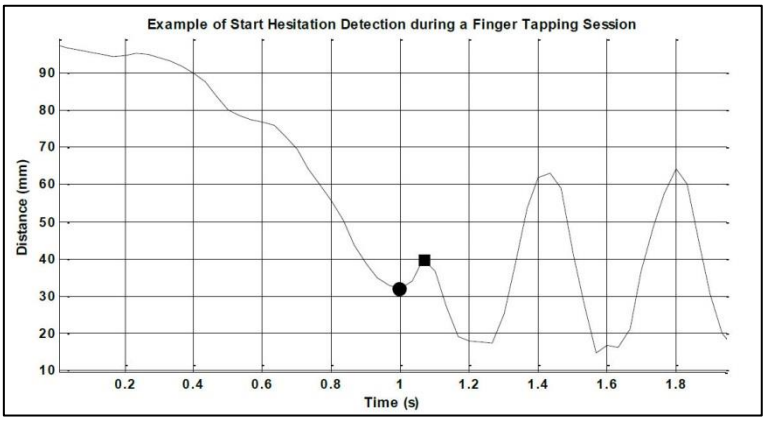

Figure 39: Example of "hesitation" detection

Another important feature of motor performance is related to *rhythm* or *rhythm variation* over time. It is quite difficult to characterize this feature. Frequency analysis could be a valid support in this sense: observing the shape of the trajectory, it is plausible to hypothesize that it consists of a series of sinusoidal waveforms with specific frequencies. To detect the frequencies that make up the signal, the Fast Fourier Transform is used by transforming the trajectory from the time domain to that of the frequency. A signal consisting of many

different and significant frequency components could be considered belonging to a motor performance with many rhythm variations.

In particular, attention has been focused on the *frequency range of voluntary movement* (range 0-3.5 Hz), although higher frequencies have been also considered in the transformation. By examining the signal power spectrum, it is possible to note that, in the case of motor performance without rhythm variations, the number of "significant frequencies" is limited and distributed over a narrow sub-range, as shown in [Figure 40 (Top)]; on the contrary, in case of performance with several rhythm variations, the number of "significant frequencies" will be higher and distributed over a wider sub-range [Figure 40 (Bottom)].

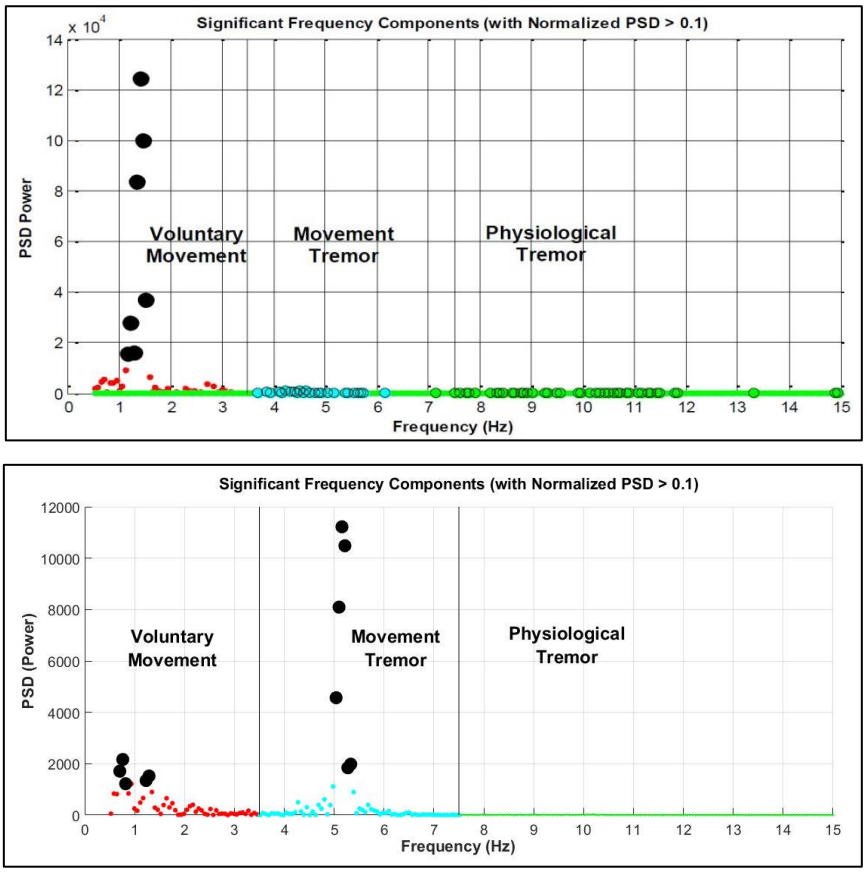

Figure 40: Frequency Analysis to detect rhythm variations in the motor performance
Top: Example of performance with less "significant frequencies", Bottom: Performance with more "significant frequencies"

4.3.1. Parameter Selection and Statistical Analysis

Based on previous considerations, three groups of kinematic parameters were initially defined for the characterization of hand movements and anomalies for the three tasks. These parameters were closely related to the physical quantities implicitly considered by neurologists to evaluate the hand motor performance as indicated by the UPDRS guidelines:

the aim was to ensure that the objective parameters had clinical relevance. Initially, the groups of parameters consisted of about twenty parameters per task, deriving from the analysis described above but some of them proved irrelevant, redundant or simply less important from a clinical point of view. In fact, one of the most interesting and challenging aspects of kinematic analysis in Parkinson's disease is to identify the most significant parameters, that is, the parameters most related to the standard UPDRS assessment. With the aim of determining the most significant parameters, various techniques were considered that produced congruent results: the starting point for this analysis was the experimental database of motor performance of PD subjects and healthy controls, with the UPDRS scores assigned by the reference neurologist.

First, the mean value of each parameter was calculated by grouping the subjects into the classes indicated as *CTRL* (for healthy subjects) and $UPDRS_0..UPDRS_3$ for PD subjects based on the severity score assigned to motor performance. This analysis showed that some parameters have a *direct relationship* with the UPDRS score (i.e., the value of the parameter increases as the assigned UPDRS score increases and, therefore, with the severity of the motor disability); other parameters have an *inverse relationship* (i.e., the value of the parameter decreases as the assigned UPDRS score increases and, therefore, with the severity of the motor disability). Example of parameters with a *direct relationship* are those relating to the regularity of the movement (more impairment = greater irregularity in movement). Examples of parameters with *inverse relationship* are those relating to the amplitude and speed of the movement (more impairment = less amplitude or/and less speed). Figure 41 shows the relationship graph for the 19 initial parameters of Finger Tapping task: the average values of the parameters by classes have been normalized in the range 0..1 to be better represented graphically. Parameters with an inverse relationship are those in which the CTRL class (healthy subjects) corresponds to 1; parameters with a direct relationship are those in which the CTRL class (healthy subjects) corresponds to 0.

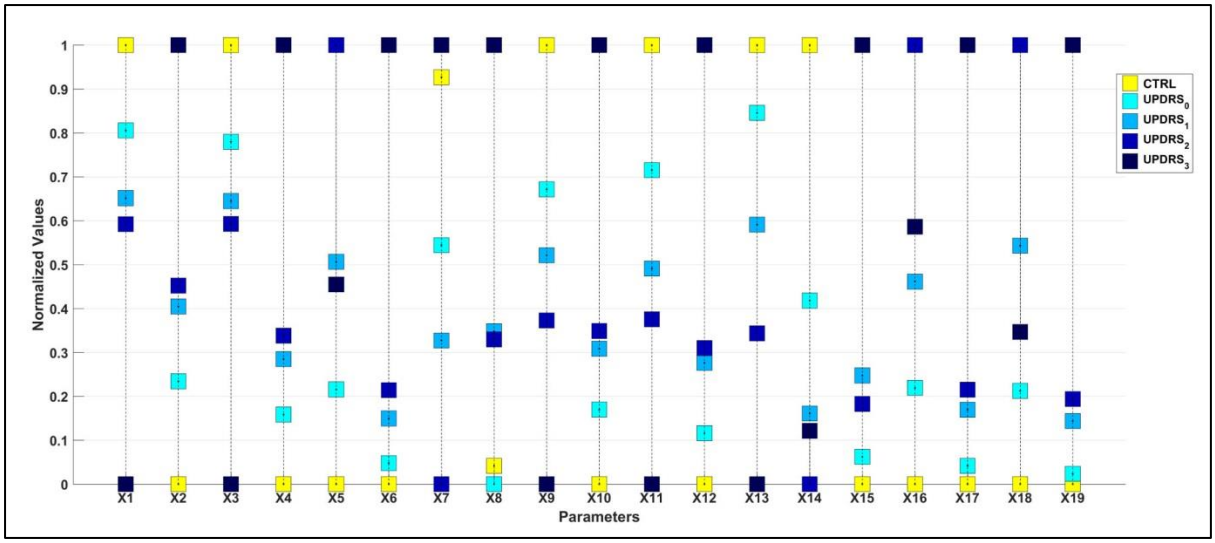

Figure 41: Relationship of parameters for Finger Tapping task

Furthermore, the *best parameters* are expected to be associated with the performance of healthy subjects (CTRL); while the *worst parameters* are expected to be associated with the performance of the most compromised subjects (in this case belonging to $UPDRS_3$): the CTRL and $UPDRS_3$ classes should therefore correspond to the minimum or maximum points. Based on this consideration, the parameters X5, X7, X8, X14, X16 do not seem to be significant with respect to the clinical evaluation, although they provide important information to characterize the motor performance of the individual subject. It should also be noted that only some parameters clearly separate the UPDRS classes respecting the order of increasing severity; while for other parameters there are partial overlaps or the order of increasing severity is not respected. According to these further considerations, only the parameters X1, X2, X3, X4, X6, X9, X10, X11, X12, X13, X17 and X19 could be considered as significant parameters.

For a quantitative measurement of the previous qualitative hypotheses[124], the Guttman Coefficient of Monotonicity (μ_2)[129] was used to verify both the correlation between pairs of parameters (Equation 3) and the correlation with the UPDRS clinical evaluation (Equation 4). The Guttman scale fits the ranked nature of the dataset in which an expert rates several performance (i.e., parameters) according to severity levels, as it can provide a hierarchical rank-order structure to a set of parameters that are associated with a severity level.

$$\mu_2 = \frac{\sum_{i=1}^{n}\sum_{h=1}^{n}(x_h - x_i)(y_h - y_i)}{\sum_{i=1}^{n}\sum_{h=1}^{n}|(x_h - x_i)||(y_h - y_i)|} \qquad (3)$$

where (x_h, y_h) denote the pairs of parameters being correlated by μ_2

$$\mu_2 = \frac{\sum_{i=1}^{n}\sum_{h=1}^{m}(x_h - x_i)(y_h - y_i)}{\sum_{i=1}^{n}\sum_{h=1}^{m}|(x_h - x_i)||(y_h - y_i)|} \qquad (4)$$

where, in this case (x_h, y_h), denote the pairs "parameter, m-value clinical score" of parameters being correlated by μ_2.

The coefficient μ_2 indicates the measure to which a variable increases in one direction as the other variable increases, without assuming that this happens exactly along a straight line. The coefficient varies between −1 and 1, reflecting a perfect monotonic trend in the negative (-1) or positive (1) direction.

	X1	X2	X3	X4	X5	X6	X7	X8	X9	X10	X11	X12	X13	X14	X15	X16	X17	X18	X19
X1	1.00																		
X2	-0.78	1.00																	
X3	1.00	-0.78	1.00																
X4	-0.90	0.99	-0.90	1.00															
X5	0.51	-0.56	0.54	-0.57	1.00														
X6	-0.83	0.84	-0.83	0.92	-0.19	1.00													
X7	-0.62	0.67	-0.63	0.68	-0.99	0.43	1.00												
X8	-0.63	0.40	-0.64	0.52	-0.25	0.52	0.09	1.00											
X9	0.94	-0.49	0.94	-0.71	-0.27	-0.75	0.06	-0.43	1.00										
X10	-0.76	0.93	-0.77	0.96	-0.34	0.88	0.48	0.34	-0.66	1.00									
X11	0.89	-0.50	0.89	-0.71	-0.42	-0.76	0.17	-0.39	0.97	-0.66	1.00								
X12	-0.84	0.95	-0.85	0.98	-0.29	0.91	0.41	0.52	-0.71	0.94	-0.77	1.00							
X13	0.19	-0.10	0.17	-0.29	-0.80	-0.65	0.48	0.09	0.63	-0.48	0.74	-0.47	1.00						
X14	-0.10	-0.09	-0.12	0.05	-0.43	0.06	0.32	0.12	0.08	-0.09	0.19	-0.09	0.45	1.00					
X15	-0.87	0.79	-0.88	0.88	-0.74	0.89	0.62	0.57	-0.69	0.77	-0.67	0.83	0.02	0.21	1.00				
X16	0.43	-0.57	0.45	-0.57	1.00	-0.14	-0.99	-0.19	-0.34	-0.35	-0.40	-0.27	-0.78	-0.39	-0.68	1.00			
X17	-0.78	0.80	-0.78	0.91	0.08	0.99	0.23	0.38	-0.73	0.84	-0.76	0.88	-0.70	0.02	0.82	0.12	1.00		
X18	0.57	-0.53	0.60	-0.55	1.00	-0.23	-1.00	-0.30	-0.20	-0.32	-0.42	-0.30	-0.81	-0.46	-0.77	0.99	0.03	1.00	
X19	-0.84	0.79	-0.85	0.91	-0.08	0.99	0.28	0.52	-0.83	0.90	-0.86	0.93	-0.80	0.05	0.88	-0.02	0.96	-0.13	1.00

Figure 42: Guttman Monotonicity Coefficients between pairs of parameters

X1	X2	X3	X4	X5	X6	X7	X8	X9	X10	X11	X12	X13	X14	X15	X16	X17	X18	X19
-0.75	**0.61**	**-0.73**	**0.74**	0.27	**0.84**	0.05	0.37	**-0.80**	**0.70**	**-0.83**	**0.76**	**-0.68**	-0.18	**0.61**	0.30	**0.84**	0.23	**0.86**

Figure 43: Guttman Monotonicity Coefficients between parameters and UPDRS severity scores

Figure 42 provides a quantitative measure of the monotone relationship existing between pairs of parameters (Equation 3), thus allowing to identify the possible "redundant" parameters: values close to 1 (or -1) indicate a perfect monotone correlation between the pair of parameters; values $\mu_2 > 0.5$ or $\mu_2 < -0.5$ indicate a strong correlation; smaller values indicate weak correlation. Figure 43 provides a quantitative measure of the monotone relationship existing between each parameter and UPDRS clinical scores (Equation 4), thus allowing to identify the possible "most significant" parameters: values close to 1 (or -1) indicate a perfect monotone correlation between parameter and UPDRS clinical scores; values $\mu_2 > 0.5$ or $\mu_2 < -0.5$ indicate a strong correlation; smaller values indicate weak correlation.

It is interesting to note that the *quantitative* measurement obtained in this way confirms the previous *qualitative* indication, both as regards the type of relationship between parameter and clinical evaluation (positive μ_2 values indicate a direct relationship while negative μ_2 values an indirect relationship), both as regards the significance of the parameters. The analysis of μ_2 coefficients confirms that the parameters qualitatively indicated as significant (X1, X2, X3, X4, X6, X9, X10, X11, X12, X13, X17 and X19) are actually quantitatively significant. The only exception seems to be X15 that was initially discarded due to the wrong order between $UPDRS_1$ and $UPDRS_2$ classes, while the μ_2 coefficient still indicates a strong correlation: this discrepancy could depend on the fact that, for this parameter, there seems to be anyway a clear separation between pairs of severity classes (CTRL and $UPDRS_0$, $UPDRS_1$ and $UPDRS_2$, $UPDRS_3$).

Another approach analyzed to select the most significant parameters was the Principal Component Analysis (PCA), commonly used for dimensionality reduction by projecting the original dataset of parameters into a new space in order to preserve as much data variation as possible: the information content of the original dataset is concentrated only on the first major components. The PCA applied to the reference dataset showed that 96% of the information content is concentrated in the first 4 components (1st component: 82%; 1st and 2nd components: 89%; 1st to 3rd components: 93%; 1st to 4th components: 96%). Analyzing the components, it is highlighted that the most significant parameters contribute with greater weights to the four components selected, while the less significant parameters do not appear or contribute with minimum weights. [Table 9] shows the highest percentage contributions associated with specific parameters.

1ST PCA COMPONENT		**2ND PCA COMPONENT**		**3RD PCA COMPONENT**		**4TH PCA COMPONENT**	
X1	14%	X1	8%	X1	17%	X1	7%
X3	30%	X3	7%	X2	6%	X3	11%
X9	15%	X9	19%	X3	30%	X6	16%
X11	24%	X11	22%	X4	7%	X13	14%
		X13	14%	X6	6%	X17	18%
		X19	7%	X9	8%	X19	13%
				X10	8%		
				X12	7%		
Tot:	**83%**	**Tot:**	**77%**	**Tot:**	**89%**	**Tot:**	**79%**

Table 9: Contribution (%) of parameters to the major PCA components

It is interesting to note that heavier parameters contribute over 75% of the overall weight of the components: this is another indication of the significance of the selected parameters. Finally, as a further confirmation, the Spearman Correlation Coefficient was evaluated for each individual parameter with respect to clinical evaluations: parameters showing an absolute correlation coefficient greater than 0.3 ($\rho < 0.01$) were considered as significant parameters: also in this case, the results confirm the previous analysis.

The selection of significant parameters and the statistical analysis are presented only for the Finger Tapping task, but the same procedure was also performed for the other upper limb UPDRS tasks: the result of this procedure was the definition of three groups of significant parameters that show good correlation with standard clinical assessments. The list of selected parameters is shown in Table 10, Table 11 and Table 12.

PARAMETER NAME	MEANING	SPEARMAN CORRELATION COEFFICIENT P
MO_m (X1)	Mean of Maximum Opening	-0.45
MO_v (X2)	Variability [1] of Maximum Opening	0.32
MOS_m (X9)	Mean of Maximum Speed (opening phase)	-0.57
MOS_v (X10)	Variability [1] of Maximum Speed (opening phase)	0.36
MCS_m (X11)	Mean of Maximum Speed (closing phase)	-0.58
MCS_v (X12)	Variability [1] of Maximum Speed (closing phase)	0.40
MA_m (X3)	Mean of Movement Amplitude	-0.44
MA_v (X4)	Variability [1] of Movement Amplitude	0.38
Freq (X13)	Principal Frequency of voluntary movement	-0.46
D_v (X6)	Variability [1] of Movement Duration	0.44

Table 10: Significant Parameters for Finger Tapping task (FT)

[1] Variability is the coefficient of variation CV, i.e. ratio of standard deviation (σ) and mean (μ), CV = σ /μ

PARAMETER NAME	MEANING	SPEARMAN CORRELATION COEFFICIENT P
MOS_m	Mean of Maximum Speed (opening phase)	-0.61
MOS_v	Variability [1] of Maximum Speed (opening phase)	0.42
MCS_m	Mean of Maximum Speed (closing phase)	-0.58
MCS_v	Variability [1] of Maximum Speed (closing phase)	0.56
MA_m	Mean of Movement Amplitude	-0.57
MA_v	Variability [1] of Movement Amplitude	0.34
D_v	Variability [1] of Movement Duration	0.55

Table 11: Significant Parameters for Hand Movements task (OC)

[1] Variability is the coefficient of variation CV, i.e. ratio of standard deviation (σ) and mean (μ), CV = σ /μ

PARAMETER NAME	MEANING	SPEARMAN CORRELATION COEFFICIENT P
MR_m	Mean of Movement Rotation	-0.30
MR_v	Variability [1] of Movement Rotation	0.31
MSS_m	Mean of Maximum Speed (supination phase)	-0.48
MSS_v	Variability [1] of Maximum Speed (supination phase)	0.36
MPS_m	Mean of Maximum Speed (pronation phase)	-0.44
MPS_v	Variability [1] of Maximum Speed (pronation phase)	0.43
Freq	Principal Frequency of voluntary movement	-0.43
DS_v	Variability [1] of Supination Duration	0.34
DP_v	Variability [1] of Pronation Duration	0.35

Table 12: Significant Parameters for Pronation-Supination task (PS)

[1] Variability is the coefficient of variation CV, i.e. ratio of standard deviation (σ) and mean (μ), CV = σ /μ

4.3.2. Graphical Representation

A *radar chart* representation was used to provide an immediate indication of the trend of motor performance. Radar chart[130] (also known as spider chart or Kiviat diagram) is a graphical representation of multivariate data, in the form of a two-dimensional chart of three or more variables. The variables are represented on uniformly spaced axes, all starting from the central point. The value of each variable is represented by a point along the corresponding axis: its position is proportional to the maximum value of the variable on all available observations. A line is drawn connecting all the points, obtaining the typical radar shape: each radar corresponds to an observation of the set of variables. This representation is frequently used for quality control, program metrics or player strengths and weakness.

Radar charts are mainly suitable for showing outliers and commonality or when all the variables that make up a chart are greater than those of another: it is in fact commonly used for ordinal measures, that is, when the value of a variable can be defined as "best", from a certain point of view, compared to other values on a measurement scale. Conversely, radar charts are poorly suited for making decisions when one chart is greater than another on some variables, but less on others.

This graphical representation was adopted for the selected significant parameters. Each parameter (or variable) corresponds to an axis, while its value as a point on it. Considering that some parameters have a direct relationship to the clinical evaluation while others an indirect relationship, the radar chart would not be the most suitable representation as overlapping radar graphs could be generated. To avoid this phenomenon, the indirectly

related parameters have been inverted before the graphical representation, so that all parameters had the same trend with respect to the clinical evaluation.

Furthermore, to avoid biases due to the different scaling of the parameters (which represent quantities with different magnitude order), the average values of the parameters relating to the PD subjects were normalized by the average values of the parameters relating to the HC subjects (Equation 5). In fact, it is expected that, on average, the parameters of HC subjects are always better than those of PD subjects and moreover, as seen in Figure 42, the parameters have an ordinal nature, i.e. they assume, on average, values distributed according to an ordinal measurement scale.

$$\overline{pPD_i} = \frac{pPD_i}{pHC_i} \qquad (5)$$

In this way, the normalized parameters highlight the increasing severity of motor impairment, which corresponds to higher clinical evaluation scores, as their values increase. This is confirmed by the radar graphs in [Figure 44], [Figure 45] and [Figure 46], which represent the normalized mean values of the selected parameters with respect to the severity of the impairment, i.e. UPDRS clinical assessment scores.

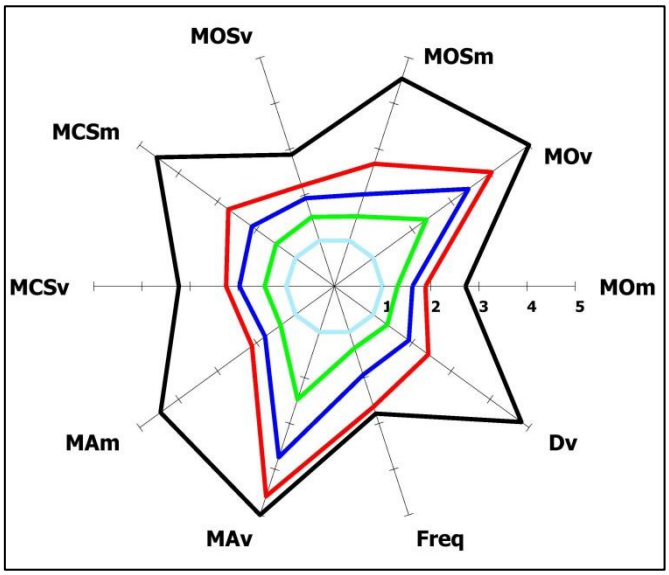

Figure 44: Radar chart of significant selected parameters versus UPDRS (Finger Tapping task)
[Image source: Paper 1]

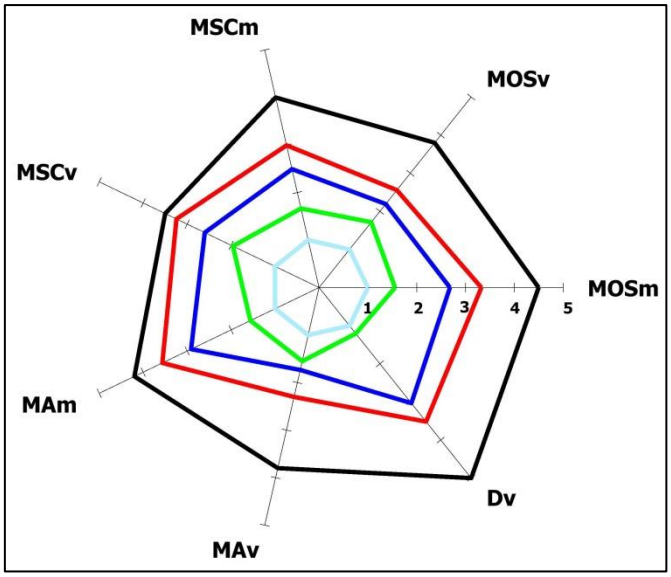

Figure 45: Radar chart of significant selected parameters versus UPDRS (Hand Movements task)
[Image source: Paper 1]

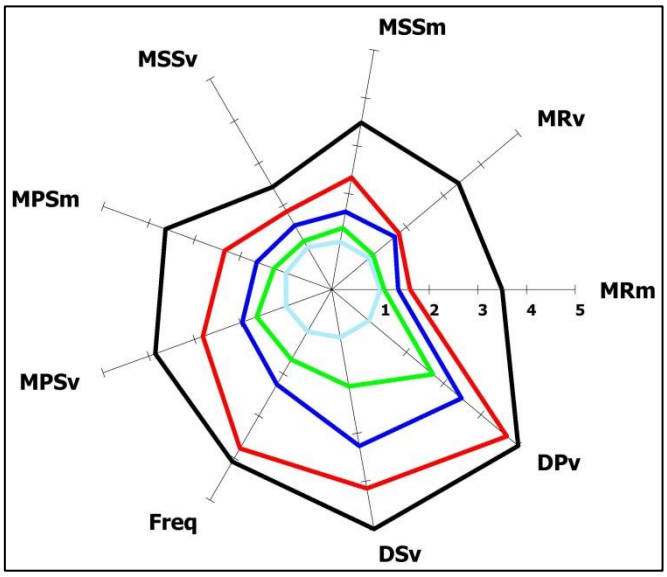

Figure 46: Radar chart of significant selected parameters versus UPDRS (Pronation-Supination task)
[Image source: Paper 1]

The radar charts of HC subjects are represented by cyan lines; the radar charts of PD subjects (class $UPDRS_0$) are represented by green lines; the radar charts of PD subjects (class $UPDRS_1$) are represented by blue lines; the radar charts of PD subjects (class $UPDRS_2$) are represented by red lines and, finally, the radar charts of PD subjects (class $UPDRS_3$) are represented by black lines.

From these charts, it is evident that the selected parameters are able to discriminate between UPDRS severity classes, denoting a strong correlation with the standard clinical evaluation. Radar charts are encapsulated and do not overlap, which clearly indicates a

monotone increase in parameters as clinical assessment increases due to deterioration of motor performance. According to this trend, it can be assumed that, on average, wider radar charts are associated with poorer performance, while narrower radar charts are associated with good performance.

Finally, another aspect to note is the shape of the radar charts: for each task, there is a certain similarity between the shapes of the radar charts associated with the severity classes. This cloud suggests that all selected parameters tend to increase with a well-defined worsening factor as motor impairment increases, but this hypothesis can only be verified through further experiments, thus increasing the number of subjects observed.

4.4 Classification

4.4.1. Supervised Classifiers

Everything described up to now has made it possible to achieve an objective characterization of motor performance through sets of parameters that are well correlated with the standard clinical evaluation and that allow quantitative comparisons between motor performance. The objective parameters certainly provide a lot of information on motor performance, but to obtain an automatic evaluation it is necessary to find a tool capable of "synthesizing" all the selected parameters in a *summary score* directly comparable with the assigned UPDRS score. A Machine Learning approach that uses supervised classifiers could be used with this aim.

Supervised Classifiers are special objects that can learn from a set of known experiences, essentially mapping a given input to a well-defined output on the basis of known reference samples made up of input-output pairs. Based on a labeled reference data set (called training set), supervised classifiers are able to create predictive models, thus learning how to associate new unknown inputs with known outputs. This is the *training* or *learning phase*, whose schema is clarified in [Figure 47].

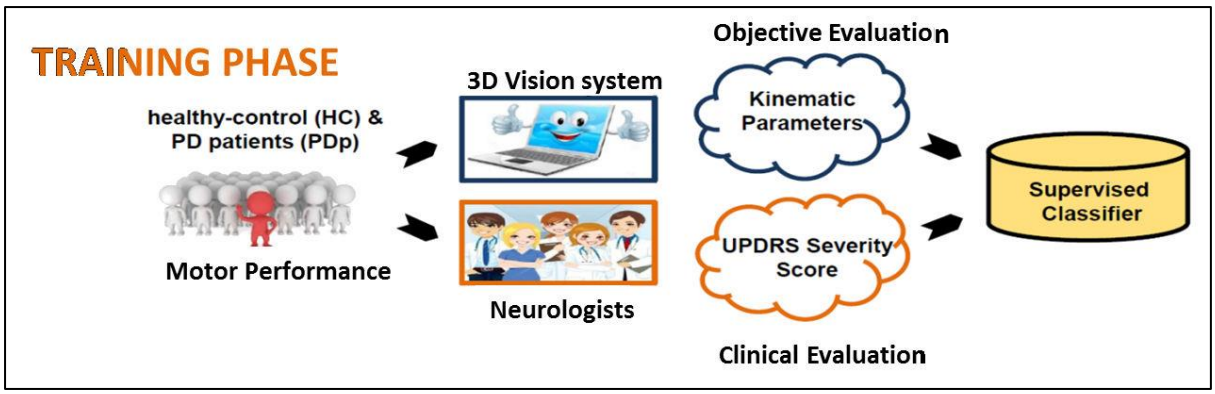

Figure 47: Schema of the training phase for supervised classifiers

The dataset of motor performance of HC and PD subjects was used as a training set for supervised classifiers. Each motor performance was assessed both clinically by a neurologist, who assigned a UPDRS severity score, and instrumentally by the system implemented through the estimation of significant parameters. The "significant parameters – clinical evaluation" pairs were used for the training phase of the supervised classifiers.

Once trained, the supervised classifiers are able to assign a probabilistic score to a new motor performance expressed only by the significant parameters provided as input: the schema and the result of the *prediction phase* are shown in [Figure 48] and [Figure 49].

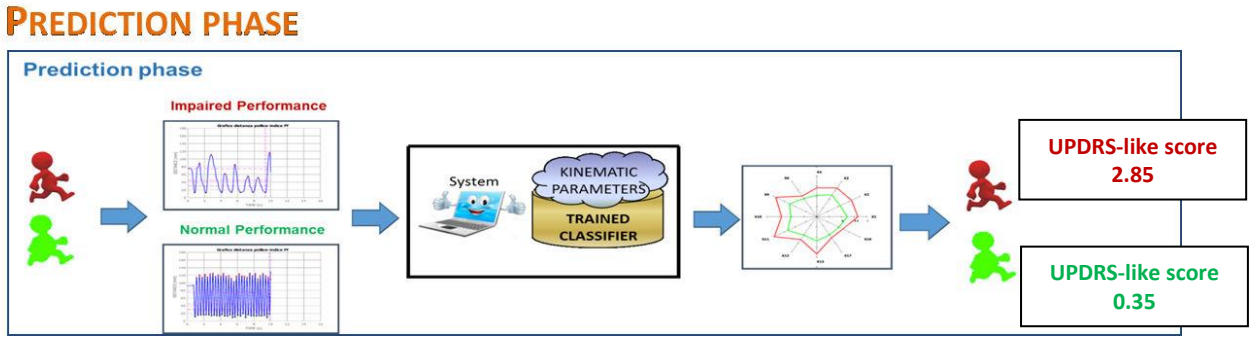

Figure 48: Schema of the prediction phase of supervised classifiers

	GOOD	BAD
SYSTEM ESTIMATED SEVERITY SCORE	0 (79.9%)	3 (86.7%)
NEUROLOGISTS UPDRS SEVERITY SCORE	0	3

Figure 49: Example of classifiers prediction for the GOOD and BAD performance of Figure 48

The output of the supervised classifiers consists of the *predictive score or predictive class* (which in this case is the estimated UPDRS severity score) and the *output probability* which indicates the probability that input parameters refer to a performance belonging to the predicted class (first line of [Figure 49]). The predicted class generally corresponds to the class with the highest associated probability: the supervised classifiers are therefore able to output an array of probabilities, whose elements are the probabilities associated with each of

the classes considered in the training phase. Taking this information into account, it was possible to define a *UPDRS-like score* (W) as the linear combination of the probability array (Equation 6).

$$UPDRS - like\ score\ (W) = \sum_{i=1}^{n} i * prob_i \qquad n = classes\ of\ training\ phase \quad (6)$$

In this way, an automatic score was obtained not only in line with the standard clinical UPDRS score, but which is expressed on a continuous scale, allowing even slight variations in motor performance to be appreciated. Examples of automatic evaluation of motor performance through UPDRS-like scores are shown in [Figure 48] that corresponds to predictive scores of [Figure 49].

4.4.2. Classification problems

There are several types of supervised classifiers: they differ substantially in the way the predictive model is built based on the training dataset.

Different supervised learning methods were evaluated for automatic assessment of the three upper limb tasks: Naïve-Bayes (NB)[131], Linear Discriminant Analysis (LDA)[132], Multinomial Logistic Regression (MLR)[133], K-Nearest Neighbors (KNN)[134] and Support Vector Machine (SVM)[135]. Three dedicated supervised classifiers, one for each task, were trained for each method using the "significant parameters – clinical evaluation" set of pairs as input. The Leave One Out Cross Validation (LOOCV) and the K-fold Cross Validation (with K=10) methods were used to evaluate the performance in terms of both accuracy and generalization ability.

LOOCV is an exhaustive method in which, at each iteration, 1 observation of the original dataset is considered as *testing set*, while the other N-1 observations are considered as *training set*: the algorithm considers all observations both as testing and training element. This is the best way to evaluate the generalization ability of classifiers. Also, several executions of this method will always generate the same output results.

The 10-fold Cross Validation is a special case of the K-fold method (with K=10) and belongs to the non-exhaustive category. The original dataset is randomly partitioned into K (i.e., 10) subsamples of approximately equal sized: one of them is used as *testing set*, the other K-1 subsamples as training set. The cross-validation process is then repeated K times, with each of the K subsamples used exactly once as *testing set*. This method is faster than LOOCV, but it is not deterministic in the sense that successive runs will generate different

results: this depends on the random generation of the K subsamples. Furthermore, by changing the value of K generally different results are obtained. LOOCV can be considered more conservative than 10-fold in terms of classification performance: precisely because of its completeness and determinism, it generally obtains more conservative accuracies.

Supervised classifiers were used in two distinct classification problems: *binary classification* problem, used to distinguish HC from PD subjects regardless of the severity score assigned; *multiclass classification* problem (five classes: HC and four PD severity classes) used to distinguish HC from PD subjects by considering the assigned severity score.

In the *binary classification* problem, only two labels (or classes) were matched to the significant parameters and used for the training phase: label "0" for HC subjects; label "1" for PD subjects.

In the *multiclass classification* problem, five labels were matched to the significant parameters and used for the training phase: label "0" for HC subjects; label "1" for PD subjects belong to the $UPDRS_0$ class; label "2" for PD subjects belong to the $UPDRS_1$ class; label "3" for PD subjects belong to the $UPDRS_2$ class; label "4" for PD subjects belong to the $UPDRS_3$ class.

Several metrics are commonly used to evaluate the performance of classifiers[136]. Among these is accuracy, that is, the ability to correctly classify (i.e. predict) an observation. For *binary classification*, it is simple to evaluate accuracy according to the following rules and the formula indicated in Equation 7. Given an observation:

- If observation is True and prediction is True: this is a *True Positive*
- If observation is True and prediction is False: this is a *False Negative*
- If observation is False and prediction is False: this is a *True Negative*
- If observation is False and prediction is True: this is a *False Positive*

		OBSERVATION	
		T	**F**
PREDICTION	**T**	TRUE POSITIVE	FALSE POSITIVE
	F	FALSE NEGATIVE	TRUE NEGATIVE

$$Accuracy = \frac{(True\ Positive + True\ Negative)}{(True\ Positive + True\ Negative + False\ Positive + False\ Negative)} \quad (7)$$

In *multiclass classification*, it is preferable to estimate a *per-class average accuracy* by reducing the problem to a binary classification: for each class, a 2x2 matrix is created

considering the logic "one class against all the others", in order to calculate the accuracy according to Equation 7.

The main problem in using accuracy as a metric for evaluating the performance of classifiers is related to datasets with unbalanced classes for which probably very high classification results are obtained, but the condition in which these were obtained is not certainly correct. Accuracy is a good and reliable evaluation metric only in case of balanced or roughly balanced classes: in this study, the considered reference dataset consists of roughly balanced classes, so accuracy was used as an estimator of the classification performance.

4.4.3. Accuracy and correlation: results

Table 13 shows the results of classification on the reference dataset consisting of the motor performance of HC and PD subjects in the three UPDRS tasks: Finger Tapping (FT), Hand Movements (OC), and Pronation Supination (PS). The same type of classifiers have been trained and tested using LOOCV and 10-Fold Cross Validation methods: in the latter case, the accuracy reported is the average of 500 executions due to the intrinsic nondeterminism of this approach.

		HC vs PD		HC vs UPDRS	
Task	**Classifier**	**LOOCV**	**10-Fold CV**	**LOOCV**	**10-Fold CV**
FT	NB	91.19	91.70	59.94	59.45
	LDA	93.71	93.71	66.31	66.63
	MLR	95.60	95.60	73.35	73.06
	SVM	**98.23**	**98.44**	**76.06**	**76.71**
	KNN	93.71	94.10	69.69	69.22
OC	NB	86.67	86.16	58.19	58.84
	LDA	88.57	88.57	61.05	61.56
	MLR	90.48	**91.44**	**65.95**	**66.21**
	SVM	**90.48**	90.06	65.14	65.24
	KNN	89.52	90.34	59.14	59.17
PS	NB	**98.97**	**98.97**	56.67	56.79
	LDA	91.75	91.75	55.67	57.10
	MLR	**98.97**	98.70	56.79	56.51
	SVM	**98.97**	**98.97**	**58.73**	**58.87**
	KNN	**98.97**	97.94	57.82	58.25

Table 13: Accuracies for binary (Healthy vs PD) and multiclass (Healthy vs UPDRS) classifications

The accuracy of binary classification is higher for all three tasks than for multiclass classification. This is not strange in classification problems: in fact, it is more difficult to make a correct prediction when the number of classes to be recognized increases. Also, the accuracy for FT task is higher than for OC and PS tasks. This depends on two factors: the size of the reference dataset for FT which includes more observations than the OC and PS

datasets; and the most demanding evaluation of the PS task, both clinically and instrumentally.

As can be seen in Table 13, the SVM classifier achieves the best results for all tasks in both the binary classification (HC vs PD) and the most difficult classification across multiple classes (HC vs UPDRS): the only exception is the classification of OC task in which MNR achieves slightly higher performance, in particular for multiclass classification.

Since the goal of automatic classification is to obtain an evaluation in line with the clinical one, another important element that characterizes the performance of the classifiers is the classification error. The absolute classification error was defined as (Equation 8):

$$ec = |C - C'| \qquad (8)$$

that is the difference between clinical scores (classes of severity) *C* and the predicted classes *C'*. The absolute value is used because classifiers may predict a lower or higher class (*C'*) than the clinical class *C*. For the SVM classifiers, the classification errors are always less than 1 UPDRS class: this means that SVM prediction is incorrect by one UPDRS class at most. Conversely, the MLR prediction sometimes is incorrect also by two UPDRS classes. For this important reason, the SVM classifiers were preferred for the automatic assessment of motor performance of upper limb tasks.

4.5 Example of automatic assessment

Considering that the symptoms of Parkinson's disease can affect the right and left sides of the body differently, objective and automatic assessment can be useful to quantitatively compare this condition. As an example, one of the cases analyzed is reported: it was characterized by a rather similar motor performance of the two upper limbs, however the system was able to detect minimal differences, even compared to a previous reference performance.

Finger Tapping task:

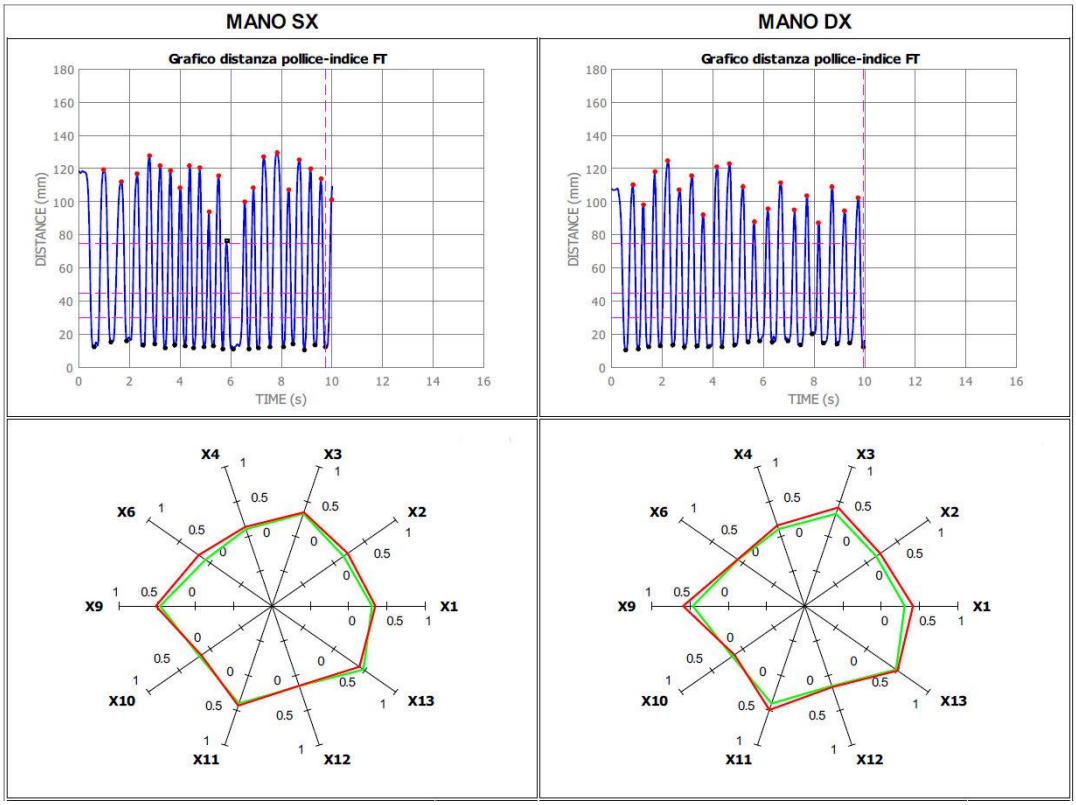

Figure 50: Example of performance with LEFT and RIGHT hand (Finger Tapping)

Both performances are characterized by a fairly good speed but a limited and very irregular amplitude. An anomaly (poor amplitude) was detected by the system in the performance of LEFT hand followed by a delay in the next tapping movement. It is interesting to note that the shape of the radar charts (red lines) is also similar compared to a previous reference performance (green lines), almost as if there was some kind of movement signature. But this point needs further investigation to be confirmed. The table below shows the automatic evaluation of the motor performance, where slight differences were highlighted by the system.

	LEFT	RIGHT
CLINICAL EVALUATION (UPDRS SCORE)	1	1
SYSTEM EVALUATION (PREDICTED SCORE)	1 (58.5%)	1 (53.2%)
AUTOMATIC SCORE (UPDRS-LIKE SCORE)	1.09	1.05

Hand Movement task:

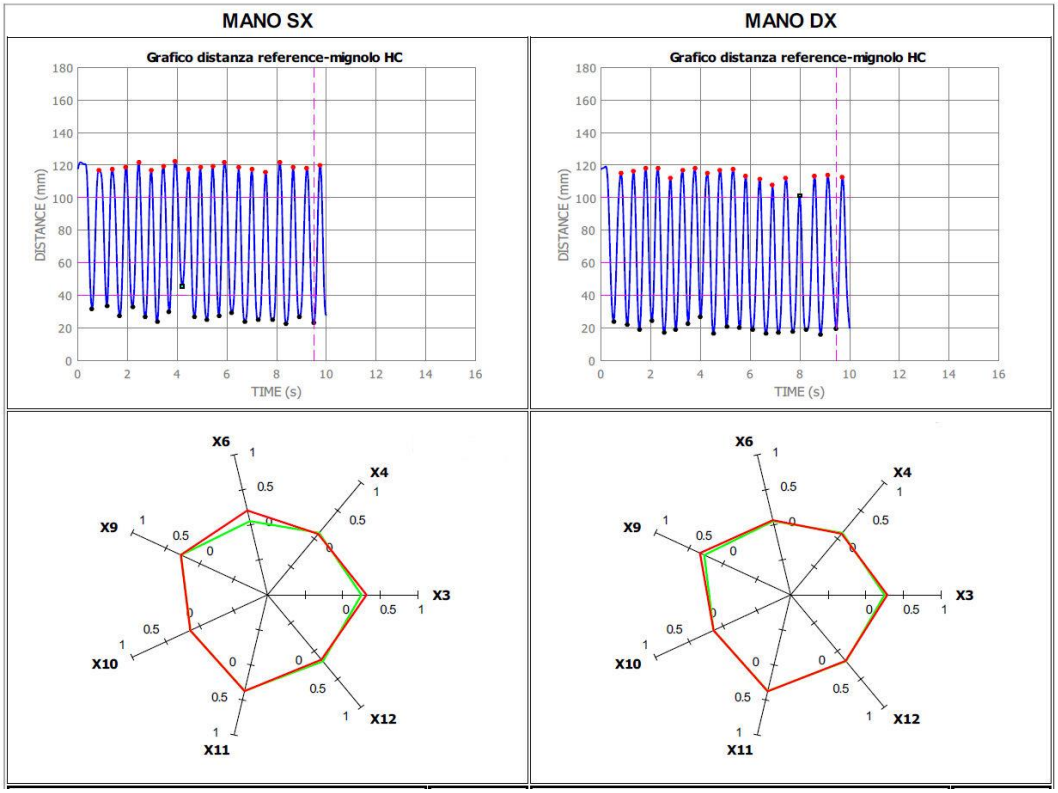

Figure 51: Example of performance with LEFT and RIGHT hand (Hand Movements)

Both performances are characterized by a fairly good speed but imperfect closures of the hand, in particular for the LEFT hand. An anomaly (very poor closure) was detected by the system in the performance of the LEFT hand, while a reduced opening was detected for the RIGHT hand. Once again, it is interesting to note that the shape of the radar charts (red lines) is also similar compared to the previous reference performance (green lines). The table below shows the evaluation of the motor performance, where slight differences are highlighted by the system.

	LEFT	RIGHT
CLINICAL EVALUATION (UPDRS SCORE)	2	1
SYSTEM EVALUATION (PREDICTED SCORE)	2 (52.6%)	2 (36.9%)
AUTOMATIC SCORE (UPDRS-LIKE SCORE)	1.57	1.38

Pronation Supination task:

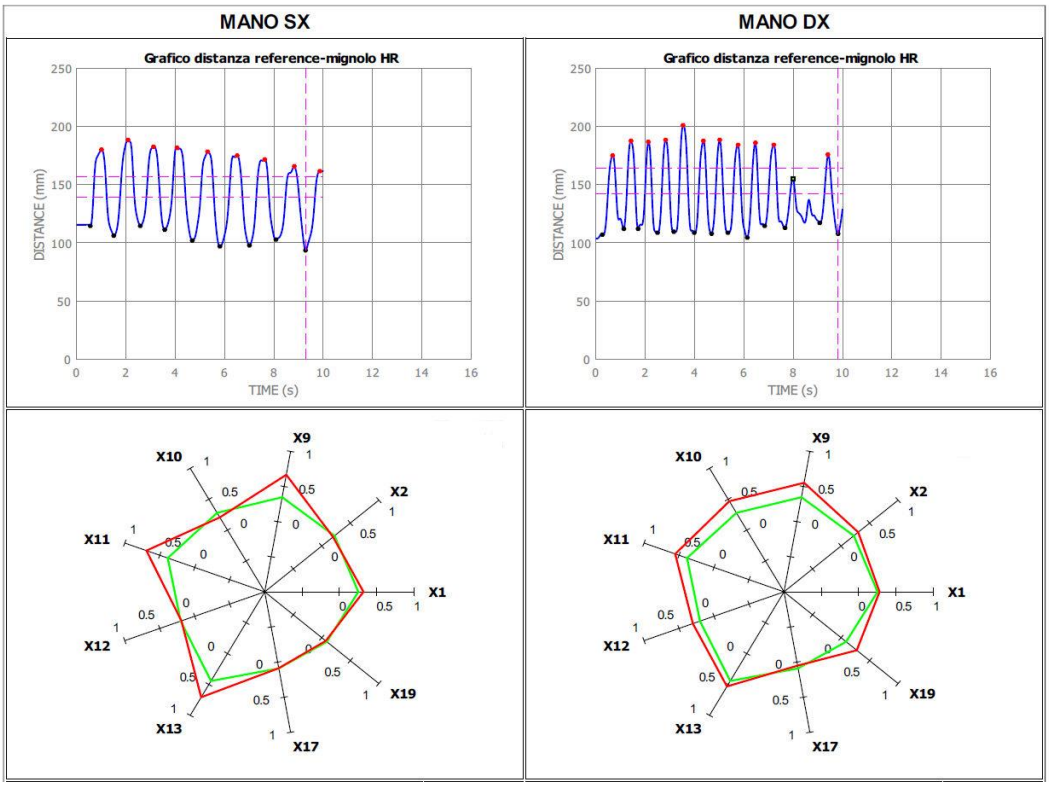

Figure 52: Example of performance with LEFT and RIGHT hand (Pronation Supination)

LEFT hand performance is characterized by smooth but slow speed. On the contrary, the performance of the RIGHT hand is characterized by a greater speed but an anomaly was detected in the final period which affected the evaluation. In this case, the two performance are different and this is evidenced by a different shape of the radar charts (red lines). Furthermore, the shapes differ also from the previous reference performance, especially for the LEFT hand, denoting an alteration of motor behavior. The following table shows the evaluation of the two performances.

	LEFT	RIGHT
CLINICAL EVALUATION (UPDRS SCORE)	2	2
SYSTEM EVALUATION (PREDICTED SCORE)	2 (53.1%)	2 (51.4%)
AUTOMATIC SCORE (UPDRS-LIKE SCORE)	1.95	1.73

It is important to underline that, in this way, it is possible to obtain a complete analysis of the motor function of the hand, identifying not only the side with the greatest impairment but also the type of movement most difficult to be performed, thus highlighting the greatest impact of symptoms and where to intervene with a possible personalized treatment.

4.6 Issues and Limitations

As already mentioned in Chapter 3, the RGB-Depth devices used for this solution are characterized by low cost (designed for large retailers), low invasiveness (contactless measurements), high usability (no complex calibrations or maintenance procedures are required), high portability (small size, easy to move, simple USB connection), great versatility (suitable for very different applications, from monitoring, rehabilitation and human-machine interaction). Despite this, the design of such a system requires paying particular attention to some issues, typical of vision-based systems:

- Operative requirements: in the case of "near-mode" devices, as for this solution, it is important to consider the minimum and maximum operating distance as well as the horizontal and vertical field of view to establish a working volume in which hand and finger movements are captured with the necessary accuracy
- Environmental light: since the tracking algorithms use RGB video stream as raw information to implement color recognition, it is important that the lighting conditions are favorable. Extreme conditions, such as too dark or too much light, will generate an underexposed or overexposed video stream, unusable for color detection and recognition: in "too dark" conditions, colors will be invisible; in conditions of "too much light", the colors will be indistinguishable. Furthermore, a direct light entering the device makes it blind, interfering with the correct estimate of the DEPTH map, essential for the 3D reconstruction of movements
- Occlusions: it is a typical problem of object tracking algorithms that occurs when the object to be tracked is partially or totally hidden during its movement, for example by another object. In case of hand tracking, it is possible that, during complex movements, some parts of the hand are occluded, i.e. hidden, preventing them from tracking

To overcome these problems, some precautions were taken for clinical setting: the system was set up so that the patients were seated in a favorable position and at the right distance from the optical device; adequate ambient light conditions have been used to avoid interference between light sources; the colors on the gloves have been applied to the entire first phalanx in order to maximize visibility and reduce occlusions, especially in the case of more impaired patients. Obviously, these issues could turn into limitations and weaknesses of the system, especially in an unsupervised home environment: if the system is used incorrectly, this could compromise the entire remote monitoring experiment. It is therefore

important that each patient is adequately and previously trained in the use of the system, but also that the system itself or a remote supervision may promptly correct the patient in case of improper use. This is one of the main challenges of home monitoring, as described in Chapter 6.

4.7 Summary and Discussion

The aim of this study was the development of a 3D vision system for the objective and automatic assessment of the motor tasks for the upper limb (Finger Tapping, Hand Movements, Pronation Supination) defined in the UPDRS standard clinical assessment scale. The core of the system is a low-cost RGB-Depth camera and a dedicated hand tracking algorithm with the aid of gloves with color markers that allow the acquisition of the 3D trajectories of hand points involved in the movements required by the UPDRS tasks. The accuracy and robustness of the system were verified in an experimental test against an optoelectronic system, considered the "gold standard" in motion analysis. Motor performances of healthy and subjects affected by Parkinson's disease were assessed by a neurologist according to UPDRS guidelines. At the same time, the motor performances were objectively characterized by groups of kinematic parameters extracted from the 3D trajectories of hand and fingers. The three initial sets of parameters, one for each task, were reduced by selecting the most significant parameters, that is the parameters more related to standard clinical assessments. Different approaches have been adopted for the parameter selection procedure, all of which resulted in the same choice of significant parameters. To give an immediate and intuitive indication about the motor performance, a graphical representation of the selected parameters has been adopted, in the form of radar charts in which the worst motor performance are associated with radar charts characterized by larger areas. The selected parameters were the used to train supervised classifiers by applying a machine learning approach to obtain an automatic evaluation of motor performance correlated to the standard clinical evaluation. Different classifiers were compared on the basis of the reference datasets of motor performance available for the three tasks: considering the overall performance, in terms of classification accuracy and classification errors, the SVM classifiers have been considered the best classifiers for automated assessment of motor performance. The 3D vision system has been also equipped with a natural human machine interface, designed to make the system easy to use in the perspective of the remote monitoring application at patients' home.

The results obtained are very promising, but must be consolidated from two points of view: by increasing the size of the reference datasets for the three tasks and by increasing the number of neurologists who perform the clinical evaluation, in order to overcome any inter-rater reliability issue. From a more technical point of view, however, the 3D vision system and the hand tracking algorithm developed will have to be adapted to the most recent RGB-Depth devices such as Microsoft Kinect Azure.

Chapter 5

Quantitative assessment of body motor function using vision-based systems

In this chapter, the second study of the doctoral project is presented. The goal is the quantitative assessment of body movement and motor function related to the lower limbs and postural tasks defined in the UPDRS clinical rating scale. Once again, a 3D vision system, based on RGB-Depth optical device, has been developed for this purpose. Unlike the upper limb solution where a custom hand tracking algorithm has been developed, in this case the body tracking algorithm used is the one provided by the device manufacturer that is accessible through dedicated ad-hoc programs developed in C ++ and MATLAB.

The implemented solution, described in this chapter, led to the paper "*Feasibility of Home-Based Automated Assessment of Postural Instability and Lower Limb Impairments in Parkinson's Disease*", which will be referred as Paper 2 in this chapter, which was published in 2019 on the special issue "Sensors for Gait, Posture and Health Monitoring", part of the Sensors journals (MDPI).

5.1 Schema of the proposed approach

The main goal of this study was the analysis and characterization of the motor function of the lower limbs, postural attitude and postural instability that typically arise in the mid-advanced stages of Parkinson's disease. As previously indicated, the movement analysis is based on standard motor tasks used in the clinical setting to assess the severity of motor impairment: as we shall see, the postural stability analysis was performed by defining a non-standard task, since the standard UPDRS task cannot be proposed in a domestic setting. Several technological solutions are described in the literature for the analysis of lower limbs and posture. Many of them are based on wearable sensors[137,138,139] including wearable sensor networks for the assessment of lower limbs UPDRS tasks[140]; accelerometers to monitor motor fluctuations in PD[141]; multisensory approaches (accelerometer and electromyography) to assess the severity of symptoms[142]; inertial units to quantify gait[143], freezing of gait[144], axial rigidity and postural instability[145]. More recently, smartphones have also been widely used in this context[146], thanks to the widespread diffusion of this technology that we practically all "wear" all day. In particular, smartphone-based approaches were used to

quantify disease severity[147], freezing of gait [148] and gait [149]. In general, wearable technologies are more widespread but also more invasive since they must applied and held in place on the body by means of adjustable strips or bulky structures; require greater management efforts (e.g., periodic battery recharges) and allow to capture only the movements of those areas of the body on which they are applied, preventing an overview of motor behavior when this could be important. A typical case is movement of the arms during gait, which cannot be captured unless a sensor is applied on each arm. From this follows another important point, namely the cost which is, in general, directly proportional to the number of sensors employed: in order to contain costs, the number of sensors is often limited, but consequently also the possibility of a complete capture of the body movement.

In recent years, various optical body tracking systems have been proposed as an alternative to wearable sensors. These solutions have been employed successfully for the analysis of balance and postural control[150], gait[151,153], postural sway[152], lower limbs and time-up-and-go test[154], neurological rehabilitation[155], postural stability and risk of fall[156,157]. In general, these solutions are focused on the analysis of single task or feature in neurological disease or their use is limited to clinical facilities. The aim of the proposed approach is to overcome these limitations and obtain an accurate and comprehensive assessment of body motor function.

The proposed approach can be summarized by the following schema [Figure 53]. The first block relates to the *"Data Acquisition"*, that is the acquisition of motor performance to be analyzed. This involves the development of the *acquisition system*, that is the 3D vision system based on an RGB-Depth optical device; the *validation phase*, an experimental campaign to verify the accuracy and the robustness of both the acquisition system and body tracking algorithm with respect to the reference systems for movement analysis; and finally the definition of the *experimental protocol* i.e. the set of motor tasks and participants included in the study. The second block concerns the *Performance Analysis* that is the characterization of motor performance through functional parameters (for this study, parameters are both kinematic and postural). This involves the *parameter selection* procedure to identify the most relevant parameters in the initial set; the *statistical analysis* to identify the most significant parameters with respect to standard clinical assessment; and the *graphical representation* to give an intuitive and immediate indication of a performance compared to a reference one. This block led to the objective assessment of motor performance through physical measures in accordance with the UPDRS clinical scale. The last block concerns the *Classification*, that is the automatic assessment of motor performance from the selected functional parameters

through Machine Learning approaches. This involves training of multiple *supervised classifiers* and selecting the one with the best performance; the analysis of various *classification problems* such as the "diagnostic problem" (i.e. the classification as healthy or pathological subject) and the "severity problem" (i.e. the classification of motor performance according to the UPDRS severity scores); the *accuracy and correlation* analysis that refers to the analysis of the performance of supervised classifiers.

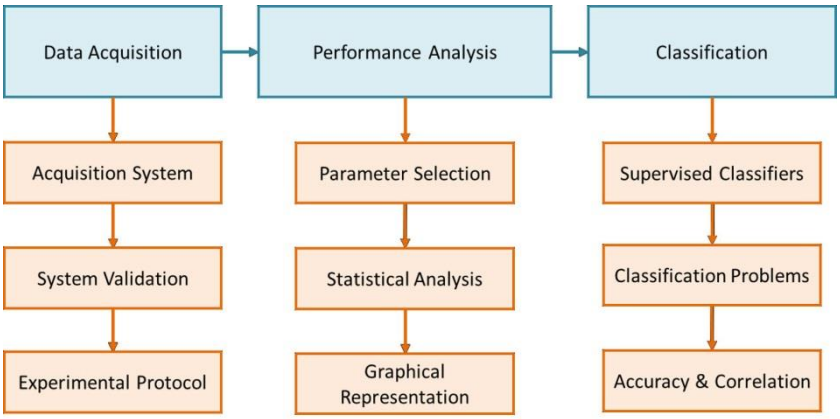

Figure 53: Schema of the proposed approach for the assessment of body movement

5.2 Data Acquisition

5.2.1. The Acquisition System

The implemented acquisition system is a 3D vision system which consists of both hardware and software components that are not only related to motion capture, but also to image and video processing.

The *hardware component* consists of the Microsoft Kinect v.2, an RGB-Depth camera that provides RGB and DEPTH streams at about 30 frame/sec, with a resolution of 1920×1080 pixels and 512×424 pixels respectively. The operating functionality is optimized for "long range mode": the device can physically and reliably perceive distances and calculate depth up to 10 meters, although in case of body detection and tracking, it is safer to limit the maximum operating distance to no more than 4.5 meters. The RGB-Depth camera is connected via an USB port to a processing unit, which can be a mini-pc (as the Intel NUC i7) or a laptop or desktop. The processing unit can be connected to a monitor or TV screen via a VGA or HDMI connection on which the visual feedback of body movement is displayed. One of the typical system configurations is shown in [Figure 54].

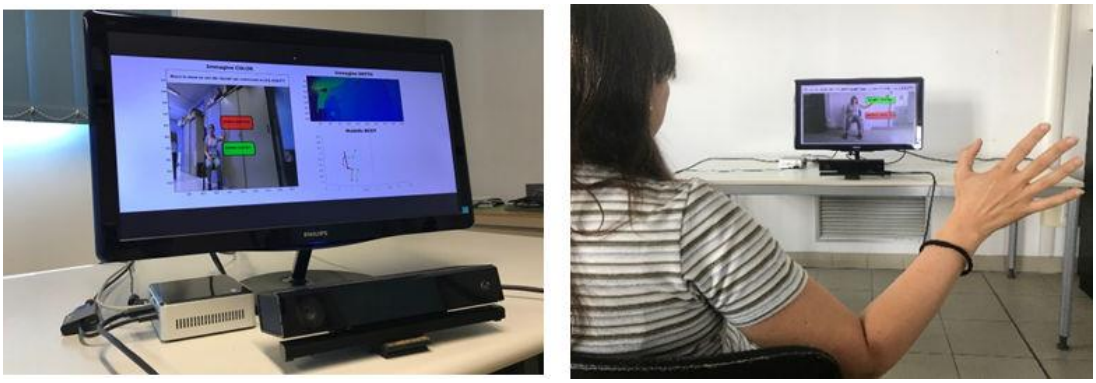

Figure 54: The system configuration with mini-pc (left) and the visual feedback on monitor (right)
[Image source: Paper 2]

An important element of this solution is the skeletal model provided by the SDK of the device, which consists of 25 joints that approximately correspond to anatomical points on the body. Each joint is characterized by both a 2D position (coordinates on the image) and a 3D position (coordinates in real space). The joints of the skeletal model are shown in [Figure 55]: to make the image clearer, all the 3D joints are represented except the hands, thumbs and finger tips; on the color image, only the 2D positions of joints relative to trunk, arms and legs are represented.

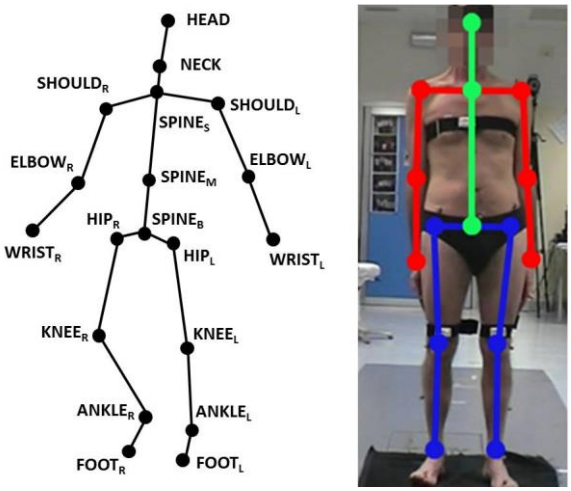

Figure 55: Position of 3D joints in real space (Left); position of 2D joints on color image (Right)
[Image source: Paper 2]

The *software component* consists of custom C++ and MATLAB scripts that run on the processing unit. Several functionalities are implemented by the software component: tracking of body movement based on the skeletal model provided by the device SDK; real-time interaction by a Human Computer Interface (HCI) based on joints tracking and processing; the analysis and characterization of body movements from the trajectories of the 3D joints; automated assessment of motor performance through supervised classifiers.

It is important to note that the acquisition and processing of skeletal model data in real time is critical to ensure reliable human-machine interaction based on simple gestures or actions such as positioning, raising or moving of some parts of the body.

Estimation of body Center of Mass

In this work, particular attention was paid to the analysis of postural stability, estimated from the movement of body's Center of Mass (CoM). Recently, the strong correlation between postural sway and balance dysfunctions has been demonstrated by several studies[158,159,160]: the postural sway corresponds to the movements of body CoM activated to maintain balance and is generally estimated through posturography which quantifies the displacements of the Center of Pressure (CoP) in steady standing (stationary condition) and in presence of external perturbation (dynamic condition)[161]. The CoP and CoM movements are closely related: CoP is the reaction force to maintain balance when postural sways can be observed through the CoM movements. CoP analysis is traditionally preferred because it is difficult to estimate CoM out of clinical or research facilities[162,163].

In stationary or not very dynamic conditions, the center of mass of the body can be approximated by means of the skeletal model provided by the body tracking algorithms, adopting a method similar to the biomechanical approaches (called Segmentation method) which involves more or less body segments, taking into account their length and mass relative to total body mass[164,165]. In particular, a simplified model, based on six body segments derived from the skeletal model, was considered for this study: due to the semi-static condition of postural tasks, it was not necessary to consider separately, for example, the thigh and lower part of the leg. The center of mass of the body (CoM_{body}) has been calculated as indicated in Equation 8, or the weighted average of the center of mass (CoM_i) of the six body segments. The position of each CoM_i (Equation 9) was estimated from the 3D coordinates of its proximal and distal extremities (i.e., joints of the skeletal model), while the percentage weight (w_i) was set on the basis of standard anthropometric tables that refers to the Dempster studies in 1955[166]. Segments and parameters for estimating CoM_{body} are shown in Table 14[167].

$$CoM_{body} = \frac{1}{6}\sum_{1}^{6} CoM_i * w_i \qquad (8)$$

$$CoM_{segment} = \frac{perc_{prox} * joint_{prox} + perc_{dist} * joint_{dist}}{perc_{prox} + perc_{dist}} \qquad (9)$$

SEGMENTS	JOINTS OF SKELETAL MODEL (FIG. 55)	WEIGHT FACTOR	LENGTH FACTOR [a]
Head	HEAD - $SPINE_S$	0.081	P: 1.000, D: 0.000
Trunk	$SPINE_S$ - $SPINE_B$	0.497	P: 0.500, D: 0.500
Total Left Arm	$SHOULD_L$ - $WRIST_L$	0.050	P: 0.530, D: 0.470
Total Right Arm	$SHOULD_R$ – $WRIST_R$	0.050	P: 0.530, D: 0.470
Total Left Leg	HIP_L - $ANKLE_L$	0.161	P: 0.447, D: 0.553
Total Right Leg	HIP_R – $ANKLE_R$	0.161	P: 0.447, D: 0.553

Table 14: Segments, joints and anthropometric data for CoM body estimation

a) Length Factor indicate the position of segment CoM with respect to Proximal and Distal extremities

It is important to consider that CoM_{body} is a 3D point, but only the components in the horizontal plane (X and Z components in the reference system of the RGB-Depth sensor) were considered for the analysis of the postural stability. The position of 3D joints, CoM_{body} and CoM_i (for each segment) are shown in Figure 56.

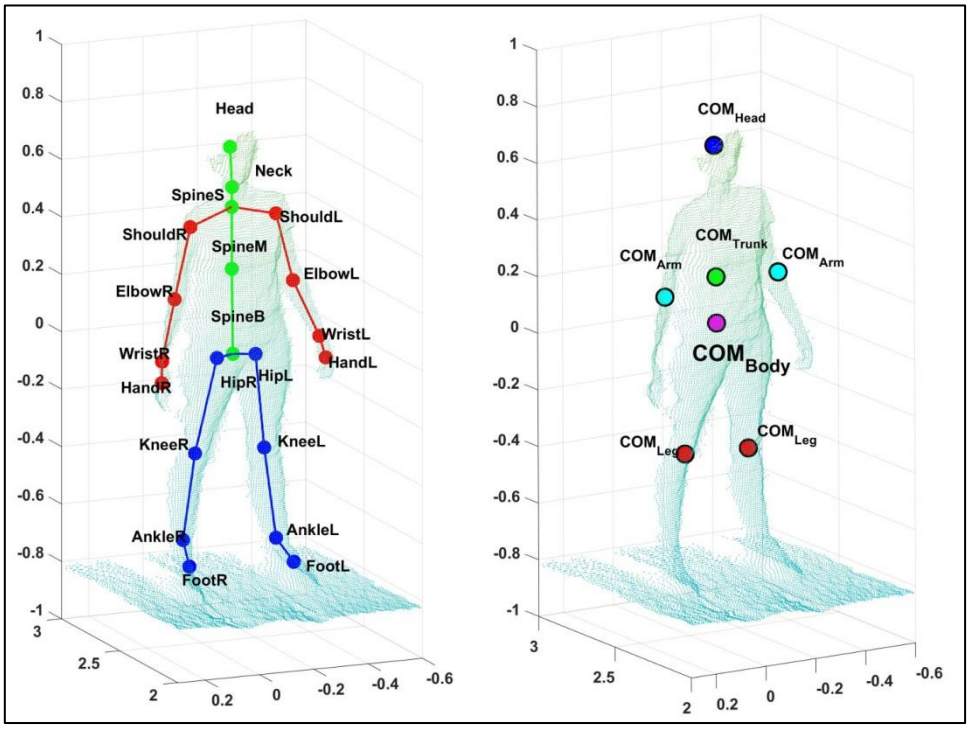

Figure 56: 3D position of joints (left) and CoM_{body} (right) on point cloud (3D reconstruction of body) The position of each CoM_i is also displayed: head (blue), trunk (green), arms (light blue), legs (red) [Image source: Paper 2]

5.2.2. System Validation

The acquisition system and the body tracking algorithm were subjected to a *validation procedure* with the aim of evaluating the performance of the proposed system (in terms of tracking accuracy and robustness) compared to a gold-reference system. In particular, a BTS SMART DX400 optoelectronic system with 8 TVC and an acquisition rate of about 100 fps

(BTS Bioengineering, Milan, Italy) was used for this purpose. An experimental setup was defined to allow the two systems to simultaneously acquire body movements while performing specific motor tasks. The UPDRS tasks for lower limb and postural (i.e., Leg Agility, Arise from Chair, Posture, Posture Stability) used for the experimental protocol were considered also for system validation (see section 5.2.3).

To allow the optoelectronic system to capture body movements, a series of reflective markers were applied to the lower and upper body, according to Davis-Helen Hayes[101] and a simplified Plug In Gait[168] biomechanical models respectively. For the upper body model, the focus was on the chest, shoulders and spine. Three additional markers were applied to the head (M_{HEAD}) and wrists (MR_{WRS} and ML_{WRS}) to allow for head posture analysis, CoM_{body} estimation and data synchronization between the two systems involved in the validation procedure. The position of the body markers, relevant for this study, is shown in [Figure 57].

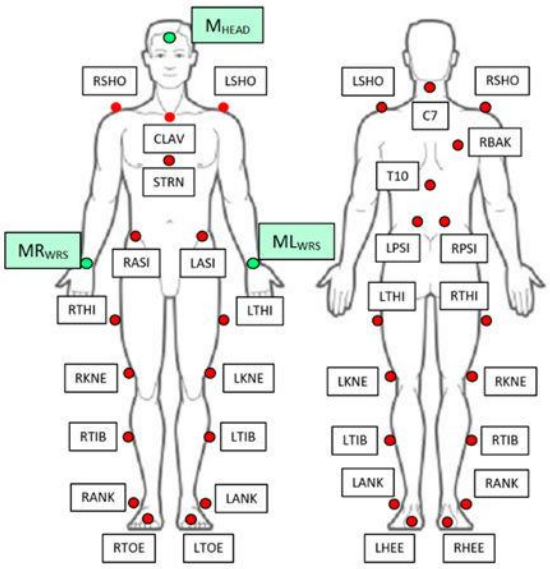

Figure 57: Markers configuration for validation procedure
[Image source: Paper 2]

Several tests were performed in which the 3D trajectories of joints and markers were acquired simultaneously. In post-processing, the trajectories of the joints have been aligned, both in space and time, to be compared correctly since the two systems have different time bases, acquisition rates and reference systems: a low-pass filter with a cut-off frequency of 10 Hz was used to reduce noise, while a resampling procedure was used to remove the typical sample rate jitter and to fit the sampling rate of the optoelectronic system.

Angular and linear measurements (Table 15) have been defined to estimate the accuracy of the body tracking on each test through the Pearson's correlation coefficient: considering that the points of the skeletal model do not coincide with the positioning of the markers, it is

not possible to proceed with a direct comparison of the trajectories as for the upper limbs. The tracking accuracy is shown in Table 16: the correlation coefficients indicate a good to strong correlation for all the defined measures from which the objective functional parameters will be then estimated.

MEASURE	SKELETAL MODEL SEGMENTS	OPTOELECTRONIC SYSTEM SEGMENTS
ANG_{KNEE} (L/R)	HIP_L–$KNEE_L$- $ANKLE_L$ HIP_R–$KNEE_R$-$ANKLE_R$	LASI–LKNE-LANK RASI-RKNE-RANK
ANG_{TRUNK}	$SPINE_S$ - $SPINE_B$	C7-MeanPSI
$ANG_{FORHEAD}$	HEAD- $SPINE_S$	M_{HEAD}-C7
$ANG_{LATHEAD}$	HEAD- $SPINE_S$	M_{HEAD}-C7
$CoM_{AP/ML}$	HEAD- $SPINE_S$ $SHOULD_R$ – $WRIST_R$ $SHOULD_L$ – $WRIST_L$ $SPINE_S$ - $SPINE_B$ HIP_R – $ANKLE_R$ HIP_L – $ANKLE_L$	M_{HEAD}-C7 RSHO-MR_{WRS} LSHO-ML_{WRS} C7-MeanPSI[a] RASI-RANK LASI-LANK

Table 15: Correspondence between skeletal model and markers

MEASURE	PEARSON'S CORRELATION COEFFICIENT *R*	
	MEAN ± STD. DEV.	P-VALUE (< 0.05)
ANG_{KNEE}	0.94 ± 0.07	$9.09e^{-03}$
ANG_{TRUNK}	0.87 ± 0.10	$6.72e^{-03}$
$ANG_{FORHEAD}$	0.73 ± 0.20	$3.98e^{-02}$
$ANG_{LATHEAD}$	0.71 ± 0.23	$3.57e^{-02}$
CoM_{AP}	0.84 ± 0.11	$3.18e^{-03}$
CoM_{ML}	0.90 ± 0.09	$8.94e^{-03}$

Table 16: Mean and standard deviation of correlation coefficients

This result indicates that the body tracking algorithm is accurate for capturing body movements, showing a performance comparable to the gold-reference system for all the measures considered. The robustness of the tracking algorithm can be verified by comparing the angular measurements after the data alignment procedure: in [Figure 58], an example of ANG_{KNEE} and ANG_{TRUNK} trajectories is shown. The trajectories are correctly aligned in time and even the smallest movements have been detected: the minimal residual difference between the trajectories is due to the non-coincident position of joints and reflective markers which produces slight different angular values.

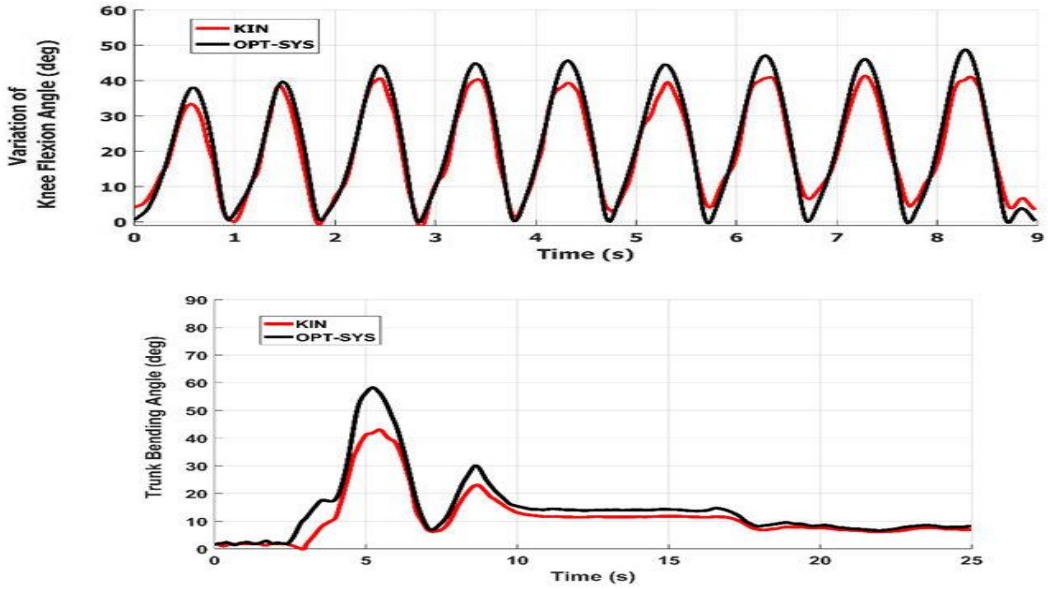

Figure 58: Example of ANG_{KNEE} and ANG_{TRUNK} trajectories estimated from skeletal model (red) and biomechanical protocols (black) [Image source: Paper 2]

5.2.3. Experimental Protocol

The experiment involved two group of subjects. The first group consisted of 14 subjects with Parkinson's disease (referred as PD group) whose main personal and pathological characteristics are indicated in [Table 17]. The following inclusion criteria were met: no previous neurosurgical procedure, tremor severity < 1 (according to UPDRS assessment), no cognitive impairment (Mini-Mental State Examination > 27/30). The other group consisted of 12 healthy controls (referred as HC group) with no history of neurological, motor or cognitive disorders: the HC group was selected to roughly match the PD group in age and gender.

	PD GROUP	HC GROUP
Number (M/F)	14 (8/6)	12 (6/6)
Age (years) range	53-80	55-75
Mean Hohen & Yahr Score (min, max)	2.1 (1,3)	-
Disease duration (years) range	3-10	-

Table 17: Characteristics of PD and HC groups

According to the experimental protocol, PD subjects were assessed on five standard UPDRS tasks: Leg-Agility (item 3.8), Arise from Chair (item 3.9), Gait (item 3.10), Postural Stability with standard retro-pulsing test (item 3.12), Posture (item 3.13). Each performance was clinically evaluated to assign a severity score: for Leg Agility, the two legs were evaluated independently. For the analysis of postural stability, another score was considered:

the Postural Instability and Gait Difficulty (PIGD) score, a subscale of UPDRS, which is the sum of Arise from Chair, Gait, retro-pulsing test and Posture standard UPDRS tasks[169].

During the experimental tests, all the subjects were instructed to perform the sequence of UPDRS tasks: each performance was supervised by neurologists and simultaneously captured by the 3D vision system. Subjects were either in standing or sitting position, depending on the motor task, in front of the RGB-Depth sensor, approximately at 2m-2.5m from it to allow the acquisition of total body movement. Two acquisition sessions were scheduled, with an interval of 30 minutes to allow for a short period of rest and recovery from the effort: PD subjects performed the five UPDRS tasks (considering Leg Agility for left and right legs) to allow the evaluation of PIGD; HC subjects performed only four tasks (Leg Agility for the two legs, Arise from Chair, Posture).

Since the retro-pulsing test (item 3.12) cannot be proposed for the home setting because it could be risky for the safety of the individual, one of the objectives of this study was to evaluate the alterations of postural stability by CoM_{body} movements, analyzing the correlation with the PIGD score considered as an indicator of postural instability in static and dynamic conditions. To this end, the Posture task (item 3.13) was divided into two phases in which the CoM_{body} movements were analysed separately: Phase 1, in which a normal standing posture was maintained for ten seconds; and Phase 2, in which an improved standing posture was maintained for other ten seconds. The second phase can be considered a kind of secondary and more challenging task for postural stability.

The motor performances of subjects with PD fall into three UPDRS levels of motor impairment (as assessed by the involved neurologists): 1 (slightly impaired performance), 2 (mildly impaired performance), 3 (moderately impaired performance) according to the qualitative criteria of UPDRS guidelines. No performance was rated as 0 (normal performance) or 4 (severely impaired performance) possibly due to initial subject selection.

Human Computer Interaction and Graphical User Interfaces

In the perspective of using the 3D vision-system in home environment to monitor the body motor function, the body tracking ability has also been used for the natural interaction with the system based on gestures and visual feedback. This makes the system easy to use and self-managed through graphical user interfaces (GUIs) that guide the user through the test session. The GUIs were designed to provide video and text suggestions and to make choices by selecting interactive objects displayed using Augmented Reality (AR), as shown in [Figure 59].

Figure 59: Examples of GUIs to select tasks and legs
[Image source: Paper 2]

5.3 Performance Analysis

Regarding the upper limbs, the clinical assessment of the severity of motor impairment is based on the observation of performance during UPDRS tasks (see Chapter 2, Figure 8), taking into account some physical quantities as required by the UPDRS evaluation criteria: in this case, kinematic and postural parameters related to the angles and movements of CoM_{body}. Using the proposed 3D vision system, kinematic and postural parameters are estimated from the 3D joints of the skeletal model captured by the body tracking algorithm.

Characterization of movement from joints of skeletal model

The characterization of the motor tasks is mainly based on the angles between body segments (that are defined by distal and proximal joints of the skeletal model) and CoM_{body} movements with respect to the starting position of the body. In particular, the characterization of the Leg Agility (LA), Arise from Chair (AC) and Posture (Po) tasks is based on the ANG_{KNEE} and ANG_{TRUNK} measures (for Po task, $ANG_{FORHEAD}$ and $ANG_{LATHEAD}$ are also considered). With reference to [Figure 60], these measures are used for:

- *LA task*: ANG_{KNEE} that is the knee angle between segments A-B and B-C ($A=HIP_R$, $B=KNEE_R$, $C=ANKLE_R$ for right side; $A=HIP_L$, $B=KNEE_L$, $C=ANKLE_L$ for left side)
- *AC task*: ANG_{KNEE}, as above. ANG_{TRUNK} is the angle between D-E segment ($D=SPINE_S$, $E=SPINE_B$) and the vertical direction
- *Po task*: ANG_{KNEE} and ANG_{TRUNK} , as above. $ANG_{FORHEAD}$ and $ANG_{LATHEAD}$ are the components of the angle between D-E ($SPINE_S$ and $SPINE_B$) and HEAD-$SPINE_S$ segments, on the sagittal and frontal body planes respectively

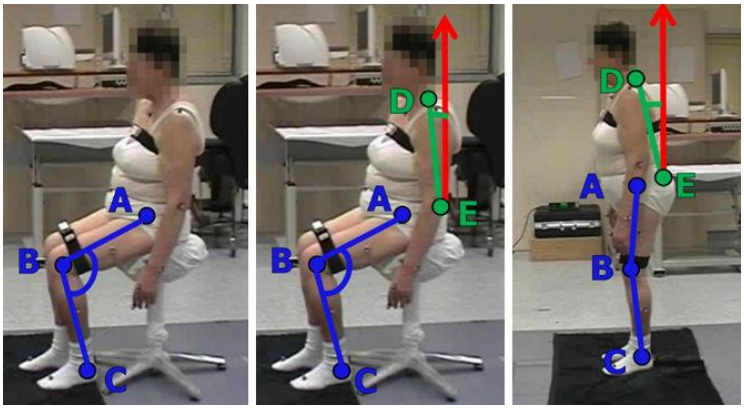

Figure 60: Segments involved in angular measures for LA, AC and Po tasks
[Image source: Paper 2]

Postural Stability (PS_{COM}) is evaluated by the movements of CoM_{body} (Equation 8) estimated both in $Phase_1$ and $Phase_2$ to highlight the effects of secondary tasks. The kinematic and postural parameters are obtained from the measures previously defined as follows:

- *LA task*: the ANG_{KNEE} signal is segmented into a sequence of flexion/extension movements (referred as cycles) from which various kinematic parameters are extracted. As for the upper limbs, *mean* (Equation 1) and *coefficient of variation* (Equation 2) are used as estimators of the global measurements. The kinematic parameters are related to the amplitude, speed, duration of the cycles, and number of "poor movements" defined as cycles whose amplitude and duration are less than 25% of the corresponding average values. The number of "poor movements" increases as the severity of the impairment increases, therefore detecting cycles with hesitations or very low amplitude
- *AC task*: the kinematic parameters are extracted from ANG_{TRUNK} signal, which is segmented into a sequence of forward/backward bending movements (referred as cycles) by finding the minimum-maximum-minimum sequences in the signal amplitude. Normally, there is only one peak (and consequently one cycle) to complete the task, but hesitations or instability can generate other clinically relevant peaks (NPeaks). Other parameters relating to task duration, speed and maximum bending angle are extracted from the main cycle
- *Po task*: the postural parameters are estimated from the ANG_{TRUNK} signal, by evaluating the *mean* (Equation 1) and *coefficient of variation* (Equation 2) of the flexion angles of the spine and head (forward and lateral) in $Phase_1$ and their variations in $Phase_2$

- *PS_{COM} task*: the kinematic parameters are estimated from the CoM_{body} signal (Equation 8), taking into consideration only the components along the Antero-Posterior (AP) and Medio-Lateral (ML) axes. The kinematic parameters are related to range, speed, total length and total area of CoM_{body} movements and are calculated with respect to the starting position of the body

Unlike the upper limbs, the kinematic and postural parameters are estimated only on the total duration of the tasks, since only for LA it would be possible to identify sub-periods in which to perform a local analysis.

5.3.1. Parameter Selection and Statistical Analysis

Initially, four groups of kinematic parameters were defined for the characterization of the motor tasks. These parameters were closely related to the physical quantities implicitly considered by neurologists to score each motor performance as indicated by UPDRS: the aim was to ensure that the objective parameters had a clinical relevance. Each initial group of parameters consisted of about ten parameters, deriving from the previously described signal analysis, but some of them turned out to be irrelevant, redundant or simply less important from a clinical point of view. One of the most interesting aspects of kinematic analysis, especially for Parkinson's disease, is to identify the most significant parameters, i.e. the parameters most related to the standard UPDRS assessment.

The same analysis procedure for the upper limbs was applied to select the most significant parameters. The average value of each parameter was calculated by grouping the subjects into classes indicated as *CTRL* (for healthy subjects) and *$UPDRS_1$..$UPDRS_3$* for PD subjects based on the severity score assigned to each motor performance. The PIGD score was considered for PS_{COM} task. As for the upper limbs, the analysis revealed that some parameters have a *direct relationship* with the UPDRS score, while others have an *inverse relationship*. Furthermore, for each parameter the Spearman Correlation Coefficient was evaluated with respect to the clinical evaluations: the parameters with an absolute correlation coefficient greater than 0.3 ($\rho < 0.01$) were considered as significant parameters. The statistical significance of the parameters in discriminating between HC and PD groups was also estimated using the Mann-Whitney U test ($p < 0.05$).

The parameter selection procedure and statistical analysis led to the definition of four groups of significant kinematic and postural parameters that show a good correlation with

standard clinical assessments. The list of the selected parameters is shown in [Table 18], [Table 19],[Table 20], [Table 21].

		Mann-Whitney U Test				Spearman Correlation	
Parameter Name	**Meaning (Unit)**	**Median HC**	**Median PD**	**Z**	**p-value**	**ρ**	**p-value**
MKA_m	Mean of Maximum Knee Angle (deg)	32.41	25.02	1.93	$5.37e^{-02}$	-0.72	$9.99e^{-06}$
MKA_v	Var. [1] of Maximum Knee Angle (-)	0.07	0.13	1.81	$7.03e^{-02}$	0.49	$6.72e^{-03}$
TD_m	Mean of movement Duration (s)	0.26	0.42	2.88	$3.95e^{-03}$	0.43	$1.98e^{-02}$
TD_v	Var. [1] of movement Duration (-)	0.10	0.12	1.68	$9.19e^{-02}$	0.43	$2.07e^{-02}$
SP_m	Mean movement Speed (deg/s)	114.8	64.20	3.00	$2.66e^{-03}$	-0.84	$8.18e^{-09}$
PM	Num. of poor movements (#)	0.00	1.00	1.99	$4.69e^{-02}$	0.74	$3.94e^{-06}$

Table 18: Significant parameters for LA task (with respect to Leg Agility scores)

		Mann-Whitney U Test				Spearman Correlation	
Parameter Name	**Meaning (Unit)**	**Median HC**	**Median PD**	**Z**	**p-value**	**ρ**	**p-value**
MBA	Maximum Bending Angle (deg)	17.50	31.26	3.18	$1.44e^{-03}$	0.75	$4.00e^{-07}$
TD	Total movement Duration (s)	0.90	2.42	2.86	$4.17e^{-03}$	0.80	$1.08e^{-08}$
SP_m	Mean movement Speed (deg/s)	21.85	12.92	2.76	$5.84e^{-03}$	-0.69	$6.26e^{-06}$
NPeaks	Num. of Bending Peaks (#)	1.00	1.00	1.13	$2.59e^{-01}$	0.63	$5.65e^{-05}$

Table 19: Significant parameters for AC task (with respect to Arise from Chair scores)

		Mann-Whitney U Test				Spearman Correlation	
Parameter Name	**Meaning (Unit)**	**Median HC**	**Median PD**	**Z**	**p-value**	**ρ**	**p-value**
FTB	Forward Trunk Bending (deg)	0.38	-5.69	2.71	$9.88e^{-04}$	-0.70	$1.36e^{-04}$
FTB_Δ	Var.[1] Forward Trunk Bending (deg)	0.35	0.27	0.18	$8.55e^{-01}$	0.43	$5.54e^{-02}$
FHB	Forward Head Bending (deg)	-1.83	-6.86	1.92	$5.23e^{-02}$	-0.78	$5.90e^{-06}$
FHB_Δ	Var. [1] Forward Head Bending (deg)	0.46	0.53	0.22	$8.17e^{-01}$	0.27	$3.62e^{-01}$
LHB	Absolute Lateral Head Bending (deg)	2.05	3.02	0.53	$6.07e^{-01}$	0.59	$2.39e^{-03}$
LHB_Δ	Var. [1] Lateral Head Bending (deg)	0.19	0.43	1.53	$1.25e^{-01}$	0.43	$6.54e^{-02}$

Table 20: Significant parameters for Po task (with respect to Posture scores)

		Mann-Whitney U Test				Spearman Correlation	
Parameter Name	**Meaning (Unit)**	**Median HC**	**Median PD**	**Z**	**p-value**	**ρ**	**p-value**
AP_r	Range of CoM AP sway (cm)	0.59	1.13	1.80	$7.20e^{-02}$	0.59	$3.24e^{-03}$
AP_t	Total CoM AP sway (cm)	1.49	3.28	2.23	$2.50e^{-02}$	0.65	$2.54e^{-02}$
ML_t	Total CoM ML sway (cm)	0.98	3.48	2.24	$2.53e^{-02}$	0.48	$1.88e^{-02}$
AP_v	Speed of CoM AP sway (cm/s)	0.72	1.32	1.86	$6.34e^{-02}$	0.56	$4.92e^{-02}$
ML_v	Speed of CoM ML sway (cm/s)	0.48	1.49	2.24	$2.53e^{-02}$	0.42	$4.25e^{-02}$
SwayArea	Area of CoM sway (cm^2)	0.30	0.85	1.58	$1.13e^{-01}$	0.59	$2.92e^{-03}$

Table 21: Significant parameters for PS_{COM} task (with respect to PIGD scores)

[1] Variability is the coefficient of variation CV, i.e. ratio of standard deviation (σ) and mean (μ), CV = σ /μ

The type of relationship between parameters and clinical evaluations is confirmed by Spearman Correlation Coefficients, where negative values correspond to *inverse relationships.* It should be noted that the number of anomalies (PM parameter for LA and NPeaks parameter for AC) and all PS_{COM} parameters increase with greater severity of the impairment (higher scores). For Po task, the absolute value of lateral flexion of the head (LHB parameter) was considered because only the magnitude and not the side of the flexion is relevant.

5.3.2. Graphical Representation

As for the upper limbs, the same graphical representation using radar charts was adopted to provide an immediate indication on the performance. Considering that some parameters show a direct relationship and others an indirect relationship, the parameters with indirect relationship have been reversed before the graphical representation, so that all parameters have the same trend with respect to the clinical evaluation: increasing values indicate a worsening in performance, highlighted by a corresponding expansion of the relative radar chart.

Furthermore, to avoid biases due to the different scaling of the parameters, the average values of the parameters relating to the PD subjects were normalized with respect to HC subjects (Equation 5) and then represented in the range [0-1] (where 0 corresponds to the best average parameter and 1 to the worst average parameter) to enhance the differences between the severity of the impairment.

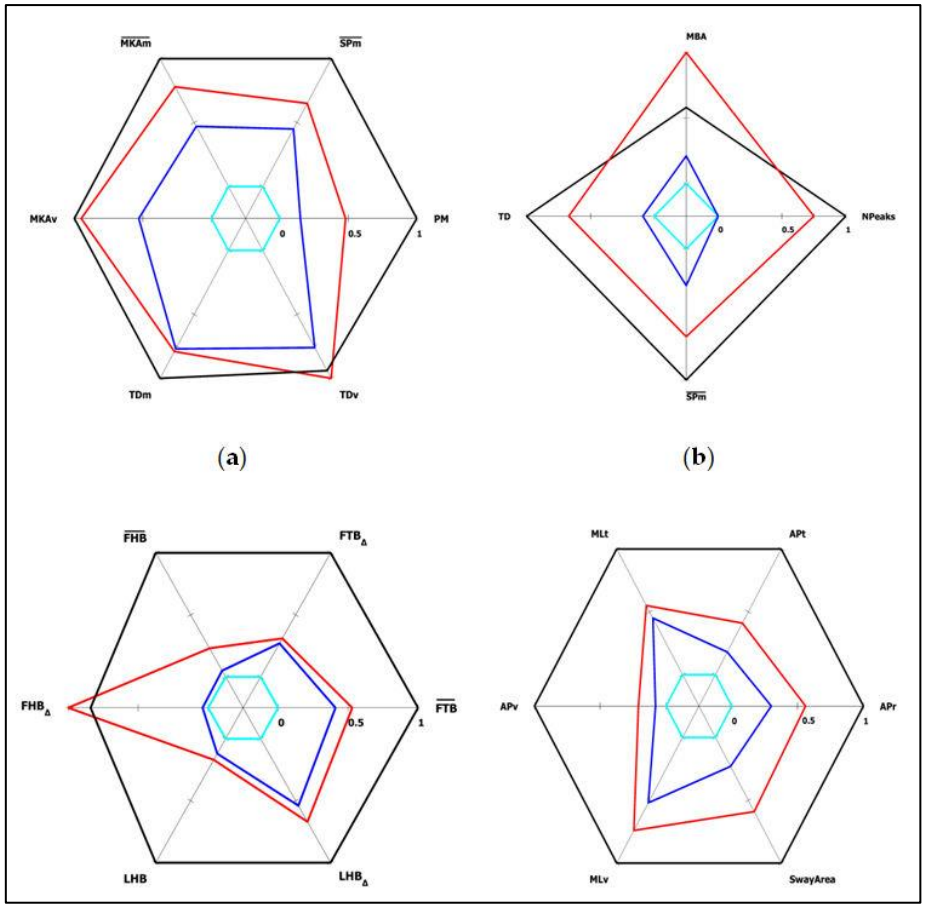

Figure 61: Radar charts of normalized kinematic parameters for LA (a), AC (b), Po (c) and PS_{COM} (d)
In light blue: HC; in blue $UPDRS_1$; in red $UPDRS_2$; in black $UPDRS_3$ [Image source: Paper 2]

Almost all parameters are able to discriminate the severity classes and the worsening of the UPDRS score for all motor tasks: the increasing severity of the impairment is evidenced by monotonically increasing values and broader radar without overlapping. The exceptions concern those parameters that do not seem to well-discriminate the more severe classes ($UPDRS_2$ and $UPDRS_3$), creating partial overlaps between the radars. This could be due to possible subclasses of Parkinsonian subjects that differ in some features but not in others: this point requires further investigation, on a larger reference sample of subjects.

5.4 Classification

5.4.1. Supervised Classifiers

Also for this study and on the basis of the previous experience on the upper limbs, a Machine Learning approach was used with supervised classifiers for the automatic assessment of motor performance. The dataset of the motor performance of HC and PD subjects was the training set for the supervised classifiers. Each motor performance was clinically evaluated according to UPDRS and analyzed by the system to estimate the

significant functional parameters. Pairs of "functional parameters – clinical evaluation" were used for the training phase of the supervised classifiers. In this way, the trained supervised classifiers will be able to assign a probabilistic score to a new motor performance expressed only by the functional parameters provided as input.

The output of the supervised classifiers are the *predictive score* (i.e., the estimated UPDRS severity score) and the associated *output probability* which indicates the probability with which the input parameters refer to a performance belonging to the predicted class. In general, the predicted class is the one with the highest associated probability. Once again, the classifiers provide an array of probabilities associated with each of the classes used during the training phase. Considering the small size of the reference dataset, it is however premature to use these probabilities for the definition of a UPDRS-like score, as for the upper limbs, pending consolidation of the data with further observations.

5.4.2. Classification problems

Three types of supervised classifiers were considered for the automatic assessment of each motor task: Multinomial Logistic Regression (MLR)[133], K-Nearest Neighbors (KNN)[134] and Support Vector Machine (SVM)[135]. The "significant parameters – clinical evaluation" pairs for each motor performance of the reference datasets, evaluated and analyzed, were used as input for the training phase of classifiers: in this way the classifiers learn to evaluate a new and unknown motor performance only on the basis of its functional parameters. As for the upper limbs, the Leave One Out and the 10-fold Cross Validation methods were considered to evaluate classification performance both in terms of accuracy and generalization ability. The PS_{COM} classifiers were trained using PIGD subscale scores as clinical assessments.

The supervised classifiers were used in two distinct classification problems: *binary classification* problem, used to discriminate the performance of HC and PD subjects regardless of the severity score; *multiclass classification* problem (three classes based on the three PD severity scores) to discriminate performance based on the severity score. The second classification problem was designed taking into account the severity scores assigned to parkinsonian performance, which are essentially distributed among slight ($UPDRS_1$), mild ($UPDRS_2$) and moderate ($UPDRS_3$) impairment. As shown in [Table 22], the severity scores were sufficiently balanced between classes for all tasks, that is one of the important requirements for supervised classifiers.

	UPDRS Severity Scores		
UPDRS Task	**$UPDRS_1$ (slight)**	**$UPDRS_2$ (mild)**	**$UPDRS_3$ (moderate)**
LA	16	22	18
AC	12	11	5
Gait	12	8	8
$PS_{(retro\text{-}pulsing)}$	8	6	14
Po	14	8	6

Table 22: Distribution of severity UPDRS scores for PD subjects

For the *binary classification* problem, only two labels (or classes) were matched to the significant parameters and used for the training phase: label "0" for HC subjects; label "1" for PD subjects. In the *multiclass classification* problem, three labels were matched to the significant parameters and used for the training phase: label "1" for PD subjects with $UPDRS_1$ score; label "2" for PD subjects with $UPDRS_2$ score; label "3" for PD subjects with $UPDRS_3$ score. For PS_{COM}, only the CoM_{body} parameters (Table 21) relating to $Phase_1$ were used for the training phase of the classifiers: the parameters relating to $Phase_2$ were used as testing sets as described into Section 5.5.

5.4.3. Accuracy and correlation: results

Table 23 shows the classification results on the reference dataset consisting of the motor performance of HC and PD subjects in the four UPDRS tasks (LA: Leg Agility, AC: Arise from Chair, Po: Posture, PS_{COM}: Postural Stability using PIGD and CoM_{body} parameters of $Phase_1$). The same type of classifiers have been trained and tested using LOOCV and 10-Fold Cross Validation methods: in the latter case, the accuracy reported is the average of 100 classifier runs due to the nondeterminism of this cross validation method.

		HC vs PD		UPDRS severity	
Task	**Classifier**	**LOOCV**	**10-Fold CV**	**LOOCV**	**10-Fold CV**
LA	SVM	**95.6**	**96.5**	**68.9**	**73.6**
	KNN	94.5	**96.5**	51.7	58.0
	MLR	89.6	89.6	**68.9**	70.5
AC	SVM	88.2	88.2	66.3	69.9
	KNN	86.0	88.2	60.0	67.5
	MLR	**94.1**	**96.8**	**70.5**	**73.3**
Po	SVM	91.6	93.5	68.0	68.2
	KNN	**95.8**	**95.0**	**70.8**	**68.9**
	MLR	83.3	81.7	62.5	58.8
PS_{COM}	SVM	95.2	93.2	**58.3**	**59.6**
	KNN	92.8	**95.7**	41.6	45.8
	MLR	**95.8**	91.9	50.0	52.1

Table 23: Accuracies of classifiers for binary (Healthy vs PD) and multiclass (UPDRS severity) problems

Accuracies for binary classification are higher than multiclass classification: this behavior was not unexpected because, in general, classifier performance deteriorates as the number of classification labels (i.e., classes) increases. In general, SVM and MLR perform better than KNN, both in binary and multiclass classification with the exception of the Po task where KNN performance is slightly higher than SVM. In multiclass classification, the classification error of KNN and MLR is often greater than 1 UPDRS class: considering the absolute classification error (*ec*), as defined in Equation 8, the *ec* for KNN and MLR is consequently greater than for SVM, even when the average accuracy is better than for SVM classifiers. For these reasons, the SVM classifier was chosen for automatic assessment of motor performance for lower limb and postural tasks.

In this study, the reliability of automatic versus clinical assessment was evaluated using the Intra Class Correlation (ICC)[170], a commonly accepted reliability measure in the context of clinical evaluation. The $ICC_{N\text{-}SY}$ was evaluated between clinical and automatic assessments (i.e., the scores predicted by classifies), considering the system as a "virtual" rater. The results for $ICC_{N\text{-}SY}$, shown in Table 24, indicate good agreement between clinical (consensus between reference neurologists) and automatic assessments for all tasks: in fact, the average ICC is greater than 0.7, in line with the inter-rater reliability among reference neurologists.

RELIABILITY/ TASK	LA	AC	PO	PS_{COM}
$ICC_{N\text{-}SY}$	0.77	0.80	0.74	0.65

Table 24: ICC between system and neurological assessment

The lower result is for PS_{COM} task in which parameters have been correlated to PIGD: considering that PIGD involves also dynamic tasks (such as Gait), CoM parameters estimated under static or semi-static conditions could affect multiclass classification performance and consequently the agreement with clinical evaluations. Despite this, the results are good and suggest that the analysis of postural stability using CoM_{body} parameters could be a valid alternative to evaluate postural stability compared to the test with retro-pulsing test, especially in environments not directly supervised by healthcare personnel.

5.5 Focus on the analysis of postural stability

In this study, particular attention was paid to the analysis of postural stability using parameters related to CoM_{body} movements, both in natural standing posture and in the presence of a more complex motor task or a secondary task. According to the experimental protocol, the secondary motor task was obtained by asking the subjects to assume and

maintain a more correct posture for 10 seconds (the $Phase_2$ of the Posture task), with the aim of stressing the onset of instability with a more challenging condition.

Figure 62 (on the left) shows an example of CoM_{body} trajectories measured simultaneously by the 3D vision system (green line) and the reference optoelectronic system (black line): the graphs concern the validation procedure of the PS_{COM} task, the variant of the postural stability task based on the movements of the body center of mass. The shapes of the two trajectories are quite similar: this confirms the feasibility of the developed solution in the acquisition of CoM_{body} in accordance with the gold standard system. There is a slight scaling and offset between the trajectories measured by the two systems, due both to the different position of reflective markers and joints of the skeletal model (that are not on the same "physical" point of the body), and to the different algorithms used to estimate the 3D position of CoM_{body}. The CoM_{body} trajectories during $Phase_1$ (cyan line) and $Phase_2$ (red line) of the Po task (which constitute the PS_{COM} task), as measured by the reference optoelectronic system (central image) and the 3D vision system (on the right) confirm this behavior. In any case, both the systems detected an increase on postural instability during $Phase_2$, in particular along the antero-posterior direction as expected for the type of secondary task that is characterized by greater stability along ML direction: according to the experimental protocol, subjects had to stand upright with feet apart to ensure greater lateral balance. This supports the initial hypothesis that secondary motor tasks (as in $Phase_2$), which is a common condition during daily activities, can actually impair balance and produce a degradation of postural stability.

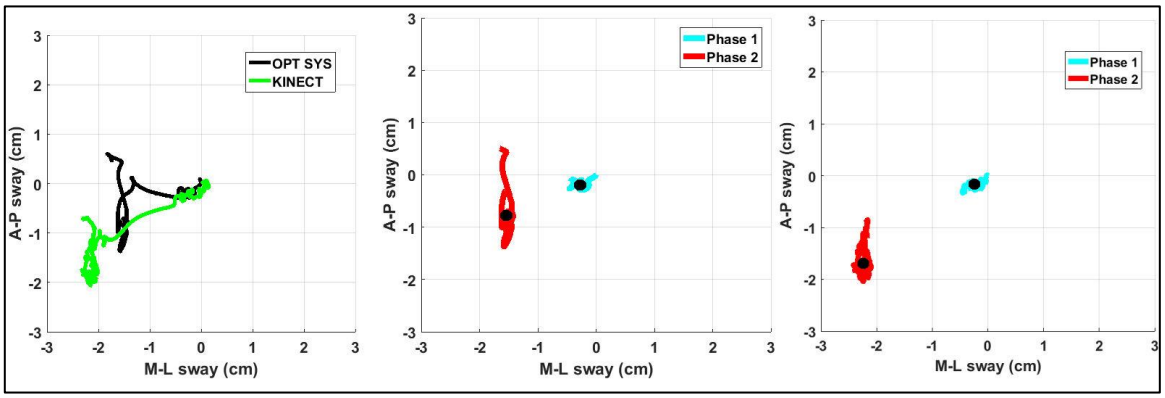

Figure 62: Example of CoM_{body} trajectories during the $Phase_1$ and $Phase_2$ of Po task (i.e., PS_{COM})

The analysis of the parameters related to CoM_{body} (Table 21), estimated for $Phase_1$, shows the ability to discriminate HC and PD subjects and a good correlation with standard clinical evaluation. From the analysis of the same parameters estimated for $Phase_2$, two other important results were found:

- CoM_{body} parameters worsen for both HC and PD subjects, suggesting that the secondary motor task, in any case, affects the postural stability (Figure 63)
- the average difference between HC and PD subjects widens compared to $Phase_1$, confirming the initial hypothesis of greater instability in subjects with PD in the presence of more complex and concurrent tasks (Table 25)

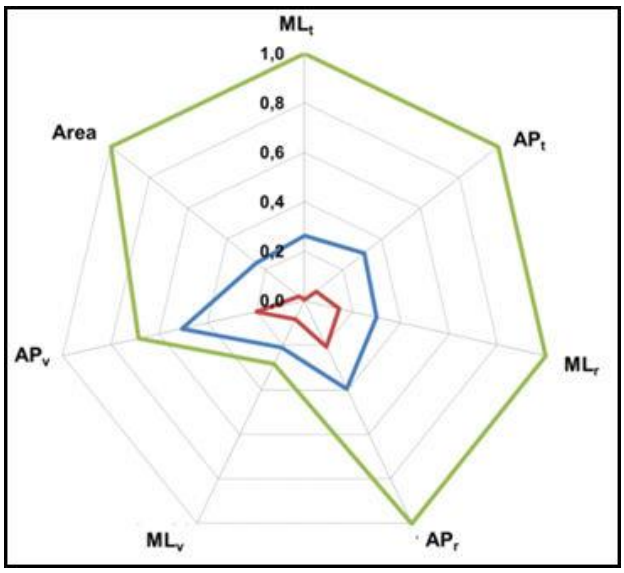

Figure 63: Worsening of CoM_{body} parameters between $Phase_1$ and $Phase_2$ for HC subjects (red line), PD subjects (blue line) and the worst PD subject (green line)

	MANN-WHITNEY U TEST			
Parameter Name	**Median HC**	**Median PD**	**Z**	***p*-value**
AP_r	0.47	1.17	2.69	7.24×10^{-3}
ML_r	0.48	1.12	2.30	2.13×10^{-2}
AP_t	0.94	4.73	2.23	2.58×10^{-2}
ML_t	0.29	1.72	2.27	2.33×10^{-2}
AP_v	0.68	1.72	2.68	7.12×10^{-3}
ML_v	0.67	1.31	2.15	3.44×10^{-2}
SwayArea	0.35	1.43	2.50	1.24×10^{-2}

Table 25: Average difference of postural parameters between $Phase_1$ and $Phase_2$ for HC and PD subjects

The $Phase_2$ condition clearly increases the average values of CoM_{body} parameters (in fact, all the differences in Figure 63 are positive), indicating a worsening of postural stability compared to the $Phase_1$ condition. This deterioration was also detected by supervised classifiers using the CoM_{body} parameters estimated for $Phase_2$ as input for the trained classifiers on the $Phase_1$ parameters. The worsening of postural stability was successfully detected by the trained classifiers as a shift to a "worse" severity class for PD subjects or as an increasing probability associated to the same class predicted for $Phase_1$ with a consequent

redistribution of other probabilities towards "worse" severity classes (average increase in probability associated with the predicted class: +10%, min: +5%, max: +23%). This good result suggests that supervised classifiers are able to detect worsening in postural stability automatically using CoM_{body} estimated parameters, making the PS_{COM} task a possible alternative to quantify the postural stability (and instability) in home setting. In any case, a more in-depth investigation is necessary to consolidate the data with further analysis.

5.6 Limitations

Certainly, this study would require further investigations to consolidate the results achieved but also to explore new interesting aspects. First of all, the number of subjects analyzed should be increased in order to obtain a more robust characterization of each task and better accuracy in the automated assessments. A new aspect to investigate could concern the recognition of Parkinsonian phenotypes, in practice verifying whether different functional parameters would be able to characterize and identify different motor patterns associated with specific parkinsonian phenotypes. Finally, an aspect that should be strengthened concerns postural instability. At present, it was considered a single standing task. However, many studies in the literature have investigated balance problems in PD using dedicated clinical reference scales such as the Berg Balance Scale. A subset of tasks, derived from the Berg scale and suitable to be performed also in home setting, could be defined and evaluated through the proposed 3D vision system, in order to broaden the analysis relating to postural instability that is closely related to the risk of falls, one of the most frequent causes of injury with the progression of the disease.

Finally, considering a purely technical point of view and as explained in Chapter 3, the RGB-Depth sensor used for this 3D vision system was discontinued two years ago and this can be considered the main limitation of this study. However, other commercial alternatives are currently available, such as the new Microsoft Kinect Azure, as well as other body tracking algorithms and deep learning approaches that can certainly lead to even better results in the near future. Recent studies have already demonstrated the better accuracy of Microsoft Kinect Azure than its predecessor used for this study: this bodes well for the opportunity to work just as well with the new device.

5.7 Summary and Discussion

The aim of this study was the development of 3D vision system for the objective and automatic assessment of lower limb and postural tasks (Leg Agility, Arise from Chair,

Posture and Postural Stability) defined in standard UPDRS clinical rating scale. In particular, Postural Stability was analyzed through the movement of body center of mass. The core of the system is a low-cost RGB-Depth camera suitable for long-range motion capture for the acquisition of full body movement. The body tracking algorithm is provided by the SDK of the optical device: it is based on a Machine Learning approach in which the depth image is used to map, in real time, the body movements onto a skeletal model consisting of 25 joints which approximately correspond to anatomical points of the body. The accuracy and robustness of the implemented solution were verified in experimental tests against an optoelectronic system, considered the gold standard in motion analysis. The motor performance of healthy subjects and subjects with Parkinson's disease were evaluated by neurologists according to UPDRS. At the same time, each motor performance was objectively characterized by groups of functional parameters estimated from the 3D trajectories of joints and body segments. The initial sets of parameters, one for each task, have been reduced in size by selecting the most significant parameters, i.e. the parameters more correlated to standard clinical evaluations. For the analysis of Postural Stability, the PIGD sub-score was considered as a reference clinical evaluation for the analysis of the movements of body center of mass, which was estimated from the skeletal model by adopting a biomechanical approach (Segmentation model). Different methods have been used for the parameter selection procedure leading to the definition of the same groups of significant parameters. To give an immediate and intuitive indication about the motor performance, a graphical representation of the selected parameters has been adopted, using radar charts in which worst motor performances are associated with radar charts with wider shapes. The selected parameters were then used to train supervised classifiers, adopting a machine learning approach, to obtain an automatic assessment of motor performance correlated to standard clinical assessments. Different classifiers were compared on the basis of the reference datasets of motor performance available for each motor task: considering the global performance, in terms of classification accuracy and classification errors, SVM classifiers have been considered the best classifiers for automated assessment. The predicted scores assigned by the classifiers show very good agreement with standard clinical assessments. The 3D vision system has also been equipped with a natural human machine interface, designed to make the system easy to use in the perspective of remote monitoring applications at patients' home.

Significant results were obtained from the analysis of postural stability, in particular relating to the worsening of postural stability when secondary or concurrent tasks are

performed, a situation typical of daily activities. The analysis of CoM_{body} parameters showed an overall degradation of postural stability, both for the healthy controls but in particular for the PD subjects: the difference between the two groups is greater than in the single task condition as shown by the radar charts of the corresponding CoM_{body} parameters.

The results obtained are very promising, but must be consolidated from two points of view: by increasing the size of the reference dataset for each motor task and by increasing the number of neurologists who perform clinical assessments, in order to overcome any inter-rater reliability issue.

Finally, from a technical point of view, the 3D vision system will have to be adapted to the most recent RGB-Depth devices, and in particular to Microsoft Kinect Azure, to be successfully used in the next experimental tests of remote monitoring.

Chapter 6

New perspectives in management of neurological diseases

This chapter presents the third main study concerning one of the secondary objectives of the PhD project and in particular the application of the solution implemented for the upper limbs to remote monitoring in home environment. This was the first experimental test of autonomous use of the 3D vision system in the patient's home, with a view to new strategies for managing Parkinson's disease and, more generally, neurological diseases characterized by motor dysfunctions. The aim of this experimental test was to analyze any significant changes in daily motor performance related to fluctuations in response to drug therapy or other events.

This study led to the paper "*Home-based automated assessment of upper limb motor function in Parkinson's Disease*", referred as Paper 3, which was published in 2019 on the Journal of Advances in Life Sciences (IARIA).

6.1 Technology at "patient's home"

The solution implemented for the characterization of the upper limbs was integrated into a home monitoring platform, with the aim of moving disease management to patient's home through remote monitoring applications.

This could generate many benefits for patients, reducing the inconvenience of reaching healthcare facilities and allowing motor assessment in familiar environments with a very positive emotional and psychological impact. On the other hand, the advantages could be also for clinicians, that can follow patients more frequently and act promptly in the presence of functional alterations automatically detected by the remote monitoring system and which, otherwise, could be detected during scheduled visits and, in any case, in longer times.

The hypothesized general infrastructure (Figure 64) of the remote monitoring platform is a network made up of a number of *Patient subsystems*, *Clinician subsystems* and *Administrator subsystems*. Each Patient subsystem consists of the 3D vision system for the characterization of the motor function of the upper limbs and it is located at patient's home. Each Clinician subsystem consists of a simple PC or notebook, placed in a hospital or outpatient environment, from which the clinician can access the data collected by the Patient subsystems. Each Administrator subsystem is a technical workstation from which to manage

any technical problems of the 'infrastructure. Each element of the infrastructure has been equipped with specially developed application software, consisting of a Graphical User Interface (GUI), which takes into account both the type of user and the primary function of each subsystem.

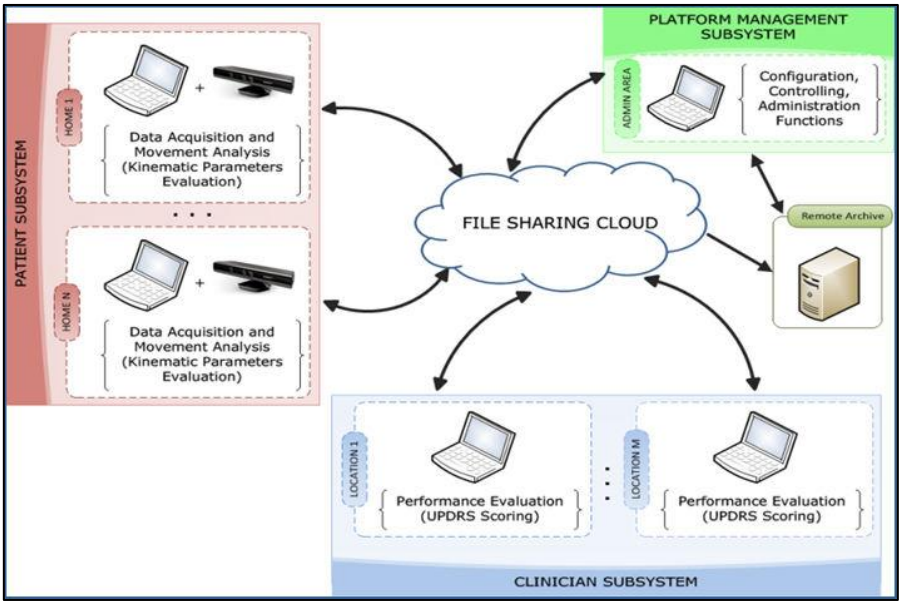

Figure 64: Infrastructure of the remote-monitoring platform

6.1.1. The Patient subsystem

Within the monitoring platform, the *role* of the Patient subsystem is to automatically capture and analyze the motor function of the upper limbs in home environment. The *user* of this subsystem is a person suffering from Parkinson's disease, mainly elderly, characterized by forms of motor impairment and, generally, with poor technological skills. It is therefore clear that, in this context, one of the most challenging aspects is making the system easy-to-use and self-managing: for this purpose, the natural HCI of the 3D vision system, described in Chapter 4, has been further simplified and the GUI has been specially designed to be suitable for remote monitoring. The GUI consists of several *program windows* that are displayed on the system monitor and provide visual feedback on hand movements and allow to trigger actions and make selections.

The *main window* of the Patient subsystem ([Figure 65]) is automatically activated a few seconds after the system is switched on: this is to avoid the user having to search and launch the main program from desktop using the keyboard and mouse. During the activation phase, all the initial checks are performed to correctly configure the acquisition system, including the checks of the RGB-Depth sensor, internet connection, and the presence of any messages for the user (that are shown in the bottom area of the main window). In addition, continuous

messages are displayed on the top area of the main window to inform the user about the progress and status of the checks: in the event of *simple failures*, suggestions are provided to solve the problem; in the event of *complex failures*, an immediate warning is raised and sent to the Administrator subsystem which, if possible, operates remotely to solve the problem.

Figure 65: The main window of the Patient subsystem
Messages of preliminary checks (top area); messages to patient from clinician (bottom area)

In addition, other windows have been designed to enter some useful and clinically relevant information, regarding for example the drug intake, the self-perceived health status and the self-perceived level of dyskinesia: information is entered through a gestural interaction before starting the acquisition session in order to allow the subsequent statistical and correlation analysis with motor performance (Figure 66).

Figure 66: The GUI window to enter time of drug intake (left) and the perceived dyskinesia level (right)

Finally, the sequence of motor tasks to be performed is automatically proposed by the system in a predefined order (*guide mode*) for a peer comparison between the test sessions.

The default order consists of Finger Tapping, Hand Movement and Pronation-Supination tasks with the least affected limb, followed by the same sequence of tasks performed with the most affected limb. The elements of the window (Figure 67) are updated at the end of each task performed to indicate the next and the progress of the acquisition session.

Figure 67: Guided mode window with list of tasks to be performed

The system also supports the subject with text messages, both during the acquisition session and the interaction with the system, and videos that can be activated to show how to perform each motor task correctly.

As mentioned in Chapter 4, the system locally saves marker trajectories and videos of motor performance to be remotely supervised by clinicians. At the end of the acquisition session, each performance is analyzed and evaluated (as described in Chapter 4) by a standalone MATLAB (EXE) program, automatically activated by the software scheduler running on the system, to estimate kinematic parameters, evaluate the motor performance and generate a PDF report which in turn is saved locally. Then, at the end of the *analysis phase*, all the data stored locally are also transferred, appropriately anonymized, to the remote archive indicated in Figure 64 as *file sharing cloud*.

It is important to consider that the analysis and the data transfer phases are automatically activated and managed by the software scheduler, without any further involvement or action by the user: at the end of data transfer, the automatic shutdown of the system has been planned as a further simplification.

6.1.2. The Clinician subsystem

Within the monitoring platform, the *role* of the Clinician subsystem is the clinical management and remote supervision of the patients. The user of this subsystem is a

neurologist, with experience in movement disorders, who works in hospital or outpatient settings and usually uses computers or tablets, therefore with good technological skills in interacting with devices and software. In this context, the GUI was designed adopting a more complex structure, with widgets and features capable of supporting remote monitoring activities and with an interaction based on mouse and keyboard. The GUI is organized in a hierarchy of *program windows* that activate specific functionalities: access to collected data is guaranteed only to authorized clinicians by a preliminary authentication procedure with personal accounts.

The *main window* of the Clinician subsystem (Figure 68) allows the selection of a particular patient's session from the repository in which all the collected sessions have been archived by each Patient subsystem: videos, parameters, reports and information relating to the session selected are then displayed in dedicated fields to be analyzed and evaluated clinically. Videos are handled via standard video player features (as start, stop, pause, rewind) for detailed inspection of motor performance.

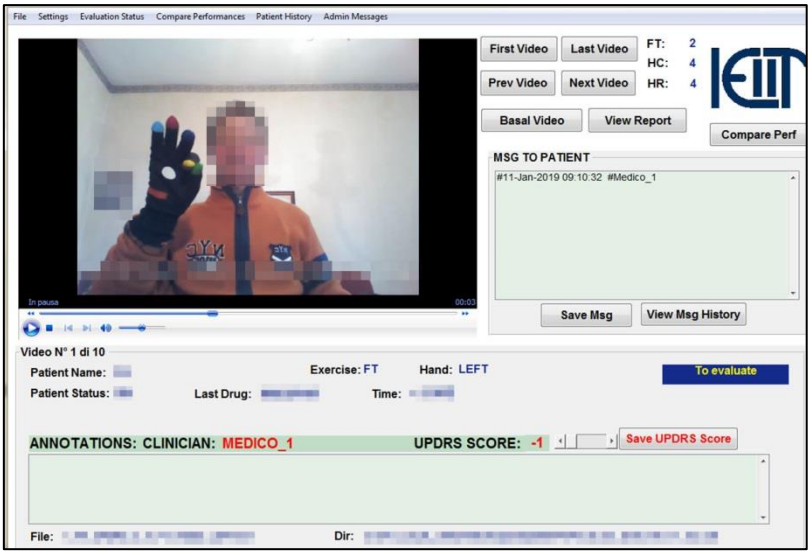

Figure 68: Main window of Clinician subsystem
[Image source: Paper 3]

The bottom area is dedicated to the clinical evaluation of motor performance which consists of useful annotations in addition to the simple standard clinical assessment according to UPDRS: this information is then archived as part of the session examined for future consultations. The "MSG TO PATIENT" area is used to write and send messages or communications that will be displayed in the main window of the Patient subsystem before starting a new acquisition session. Other windows (and therefore associated functionalities) can be activated from the menu bar of the main window for specific analysis: for example, to

compare the performance of the left and right hand in the same acquisition session; compare performance in different acquisition sessions; monitor the evolution of parameters over time.

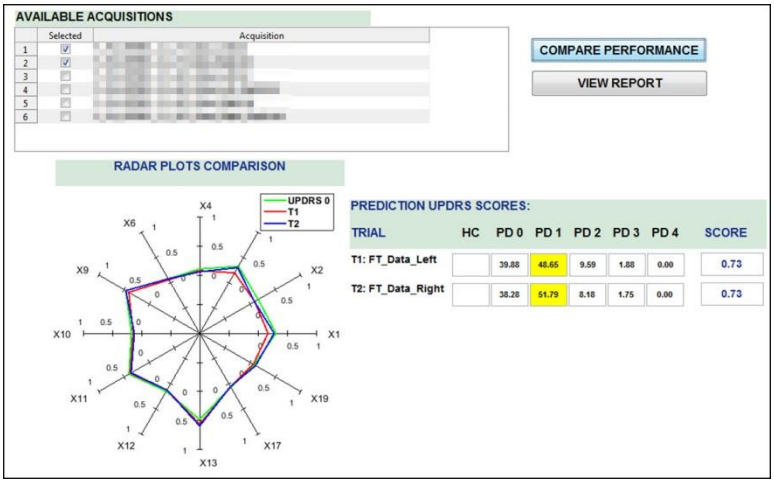

Figure 69: Comparison between left and right hand (in the same acquisition session)
[Image source: Paper 3]

The comparison between left and right hand (Figure 69) aims to highlight different motor behaviour between the two hands: the radar charts (in the bottom-left area of the window) give an immediate indication on the major differences in the selected kinematic parameters, also with respect to the reference performance displayed in green; while the table provides the prediction of the supervised classifier, with the predicted severity classes and probability associated highlighted in yellow, and the UPDRS-like scores automatically estimated.

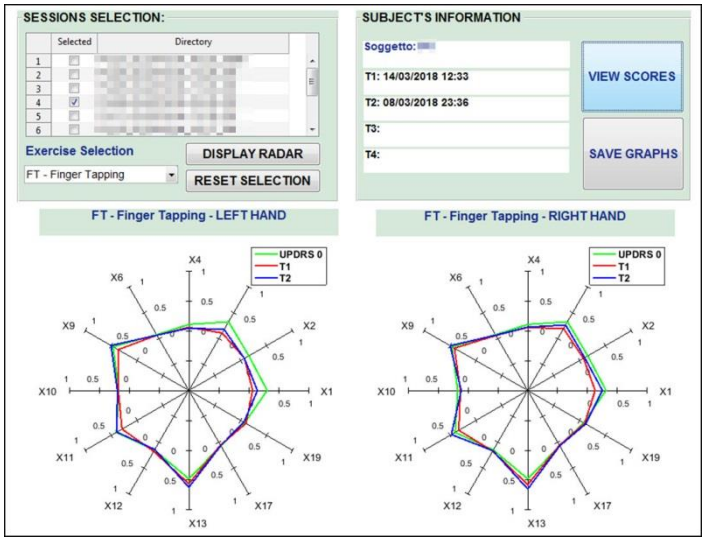

Figure 70: Comparison over time between left and right hands performance (different acquisition sessions)
[Image source: Paper 3]

The window shown in Figure 70 has the purpose of highlighting the different motor behaviour over time and between the left and right hand by comparing different acquisition sessions: the radar charts (in the bottom area of the window) provide an immediate indication

on the major variations of kinematic parameters between the selected sessions, also with respect to the reference performance displayed in green: the predictions of the supervised classifier and the scores automatically assigned are displayed using the "VIEW SCORES" button.

To monitor the evolution of the kinematic parameters over time, the window displayed in [Figure 71] is used to provide the trend of each individual parameter considering all the acquisition sessions available into the repository relating to the selected subject: this is particularly useful for a global overview of motor behavior, for example based on a personalized experimental protocol and to detect particular motor patterns hidden in similar performance scores.

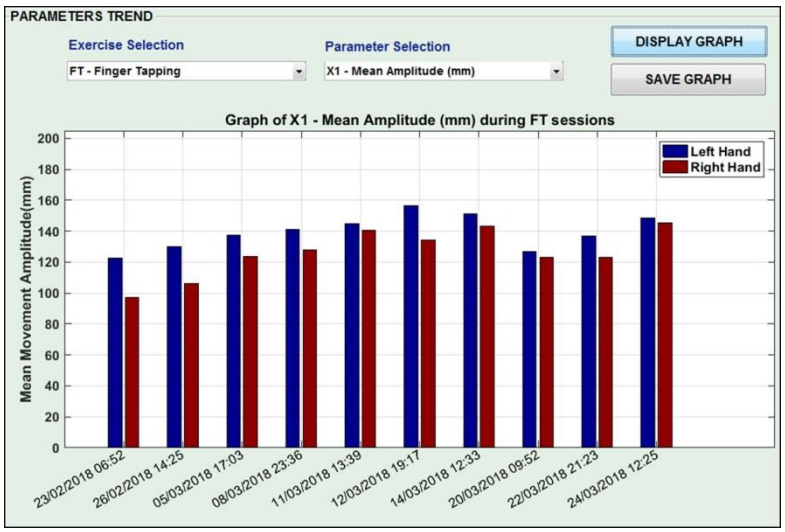

Figure 71: Trend of kinematic parameters over time
[Image source: Paper 3]

6.2 Experimental Protocol

The first experiment, to evaluate the feasibility of the home monitoring system, involved a single volunteer ($Subject_0$) who self-managed the system at home for 5 weeks, carrying out daily and multiple acquisition sessions on the same day (morning, afternoon and evening) . $Subject_0$ was previously instructed on how to interact and use the system by clinical and technical staff. The goal of this first experiment was to receive direct feedback on usage issues and make functional changes (mainly focused on the GUI) to improve usability.

Subsequently, a second experiment involved a small group of participants (4 subjects, including $Subject_0$) that used the system for one week. Again, participants were instructed to perform motor tasks each day of the week, at different times after taking the drug (after 30 min, 1.5, 2.5 and 3.5 hours). The goal of this second experiment was to evaluate the potential fluctuations in motor performance in the post-drug period.

Thanks to the storage, analysis and transmission capacity of the Patient subsystem, the data of each acquisition session were consulted, analyzed and clinically evaluated remotely by the reference neurologist through the Clinician subsystem. For this experiment, the agreement between the automatic scores assigned by the system and the UPDRS scores assigned by the neurologist (based on motor performance videos) was evaluated using the Intra Class Correlation (ICC) coefficient: ICC values were evaluated for each task, collecting the daily scores throughout the week for all participants. The results, displayed in Table 26, are compliant with the inter-rater reliability between neurologists[98,99], indicating that the system behaves as a "virtual" rater.

	MOTOR TASK		
	FT	**OC**	**PS**
$ICC_{N\text{-}SY}$	0.80	0.61	0.58

Table 26: ICC values between the scores of reference neurologist from videos (N) and system (SY)

6.3 Usability

Good usability and acceptability are important requirements for remote and self-managed monitoring, especially in case of pathological elderly such as individuals with PD.

Different tools were used for the analysis of characteristics and feedback from the participants: in particular, all the subjects who interact with the 3D vision system (including those of the study described in Chapter 4) were interviewed at the end of the acquisition session or the planned period of remote monitoring, to evaluate the global level of technological skills, the ability to wear gloves, the level of satisfaction by presenting them with a series of qualifying "positive and negative" adjectives attributable to the system.

The technological skills were assessed by a questionnaire with 18 items, concerning the previous use of computers and technologies, any difficulties in using the system, the need for a supervisor to understand activities and actions to be carried out during the acquisition session. The sum of the "yes/no" answers attributed to each item was considered to generate a final score corresponding to 4 levels of technological skills (identified as none, basic, intermediate, advanced). The percentage breakdown for the 4 levels is shown in [Table 27]: most of the subjects interviewed (> 73.0%) had no or had poor technological skills, but nevertheless they were all able to use and interact with the system.

TECHNOLOGICAL SKILLS			
NONE	**BASIC**	**INTERMEDIATE**	**ADVANCE**
55.2%	18.0%	16.8%	10.0%

Table 27: Results of the questionnaire on the technological skills

The ability to wear gloves was evaluated in 3 levels: impossibility to wear, wearable with help (for example, by the supervisor or caregiver), wearable without help.

ABILITY IN WEARING GLOVES		
IMPOSSIBILITY TO WEAR	WEARABLE WITH HELP	WEARABLE WITHOUT HELP
3%	5%	92%

Table 28: Results on the ability to wear gloves

Finally, the usability of the system was assessed by the standard Post-Study System Usability Questionnaire (PSSUQ)[171]. It is a questionnaire of 19 items, to which ordinal scores are assigned based on 7-point Likert scales[172], which addresses the six main components of the user's satisfaction in using a system: ease of use, ease of learning, simplicity, effectiveness, information and user interface. Subjects were asked to answer the 19 questions by assigning a score, from 1 (corresponding to absolute agreement) to 7 (corresponding to absolute disagreement), to express their positive or negative opinion on the experience. The results are shown in [Figure 72]: the 19 items are ordered from the first (on the left) to the last question (on the right) and, for each question, the average score on all participants is reported. The analysis shows that PD participants rated the usability of the system with an overall "agreement" score of 2.16 (±0.58) on the PSSUQ. The highest "disagreement" scores were assigned to items 9 and 10, which refer to the recovery from failure conditions: this suggested to enhance the GUI (in particular, messages to user) providing clearer and more effective indications for managing fault conditions. But the results also confirmed that the participants were satisfied with the experience, appreciating the possibility of home monitoring of their health status.

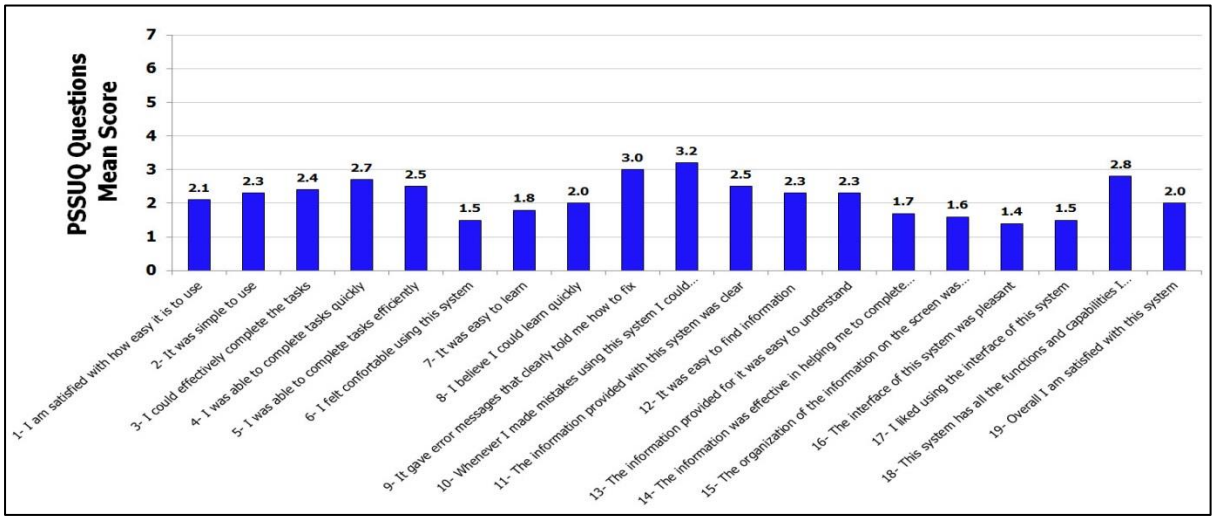

Figure 72: Results of the PSSUQ questionnaire on the system usability
[Image source: Paper 3]

6.4 Main results of the first experimental test: analysis of aggregated data

The first experimental test involved a male subject, 65 years old and diagnosed with PD for 5 years, with no evidence of fluctuations and with slightly more severe motor impairment on the right side. The experimental protocol, defined by the reference neurologist, provided for acquisition sessions distributed throughout the day (in the morning, afternoon, evening or more than one) considering the work commitments of the participant. The 3D vision system was used for 5 weeks (excluding Saturdays and Sundays). The first week was considered as a *training week* to become familiar with the system and to solve technical problems mainly related to the optimal positioning of the RGB-Depth sensor in home environment; the other weeks was used to collect significant data and provide feedback of the experience.

All the motor performances were automatically analyzed and evaluated by the system that produced an automatic score (i.e., W score as defined in Equation 6), and clinically evaluated from video by the reference neurologist according to the UPDRS evaluation criteria. For the first experiment, global statistical analysis was performed, by aggregating data for week, time slot of acquisition and time elapsed from drug intake. For the second experiment, analysis on daily behavior was also performed.

As mentioned above, in the first experiment, some sessions of the training week were discarded due to external factors (such as ambient light conditions or interference with objects). Statistical analysis shows that the failure rate decreased over the next weeks as a result of remote support (Table 29). Each session consisted of the three upper limb motor tasks, performed with the left and right hand. The table indicates the largest number of acquisition sessions occurred during the second week, while fewer sessions were performed in the last two weeks to some work commitments.

DISTRIBUTION OF ACQUISITION SESSIONS FOR WEEK (5 DAYS)					
	1° WEEK	2° WEEK	3° WEEK	4° WEEK	5° WEEK
%FAILURE	30.0%	2.5%	1.0%	0.0%	0.0%
N° VALID SESSIONS	10	16	10	8	8

Table 29: Failure rate and number of valid sessions for week

The statistical analysis of aggregated data "per week" denotes an improvement in performance over the weeks for Finger Tapping task (Figure 73): the average values of W scores were evaluated considering the left and right hand performances grouped by week (solid lines). The same was estimated considering the clinical UPDRS scores assigned to each performance from the recorded videos (dashed lines). The two trend lines show the same behavior, denoting a decrease in automatic and clinical scores associated with improved

motor performance over the weeks. Furthermore, the scores assigned to right hand are, on average, higher than the left hand, confirming greater impairment of the right side as indicated by the subject's clinical picture. Finally, the trend lines of automatic scores (W) are within the trend lines of clinical scores: it is important to remember that while clinical scores refer to a discrete scale of values (UPDRS), automatic scores refer to a continuous scale of values (UPDRS-like score), therefore able to evaluate motor performance more finely. The same trend was also observed for Hand Movements and Pronation Supination tasks.

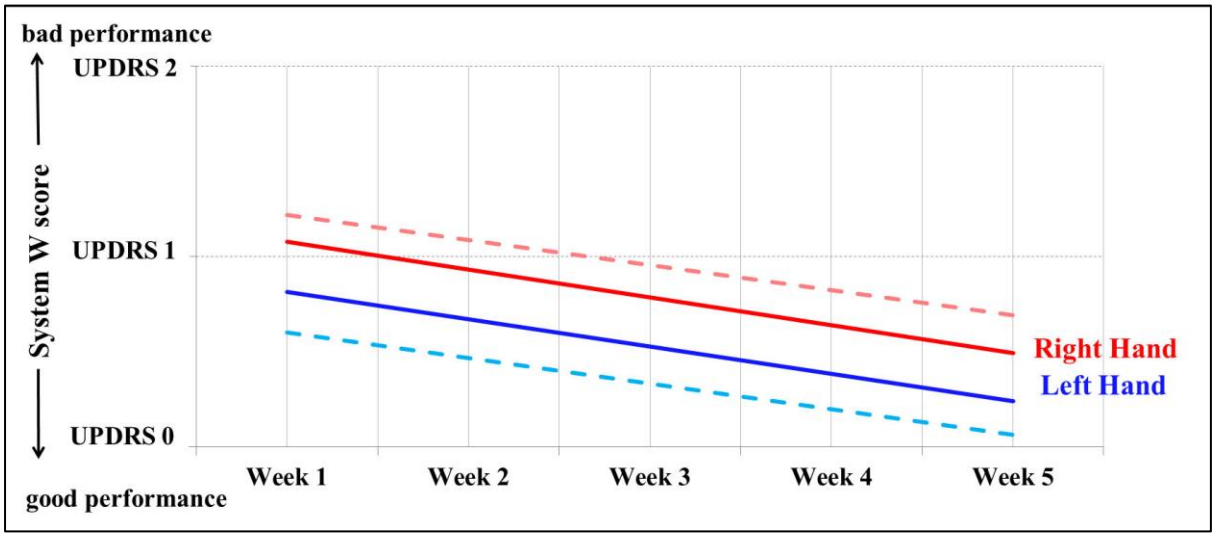

Figure 73: Linear trends of "per week" data aggregation (Finger Tapping task)
Left hand average system scores (solid blue); right hand average system scores (solid red); left hand average clinical scores (dashed blue); right hand average clinical scores (dashed red)

The analysis of the aggregated data for acquisition "time bands" provides other interesting information on the variations of motor performance. All sessions were grouped according to four acquisition time bands (6 a.m.-10 a.m.; 10 a.m.-14 p.m.; 14 p.m.-18 p.m.; 18 p.m.-24 p.m.) to analyze the performance trends during the day. Once again, the analysis confirmed more impairment on the right hand, which resulted in higher automatic and clinical scores for all tasks.

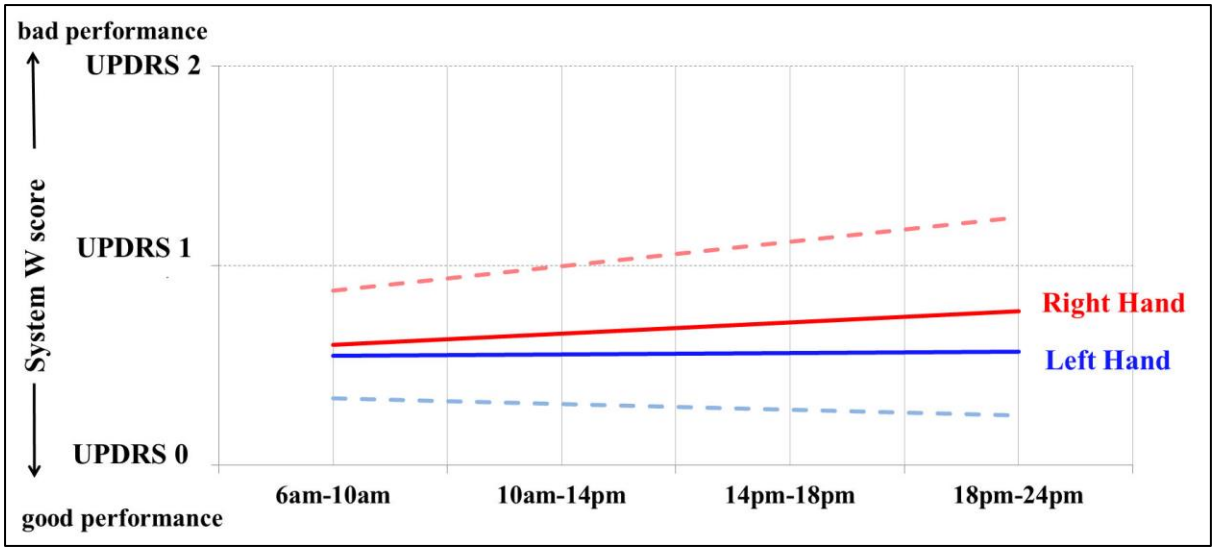

Figure 74: Linear trends for "time bands" data aggregation (Finger Tapping task)
Left hand average system scores (solid blue); right hand average system scores (solid red); left hand average clinical scores (dashed blue); right hand average clinical scores (dashed red)

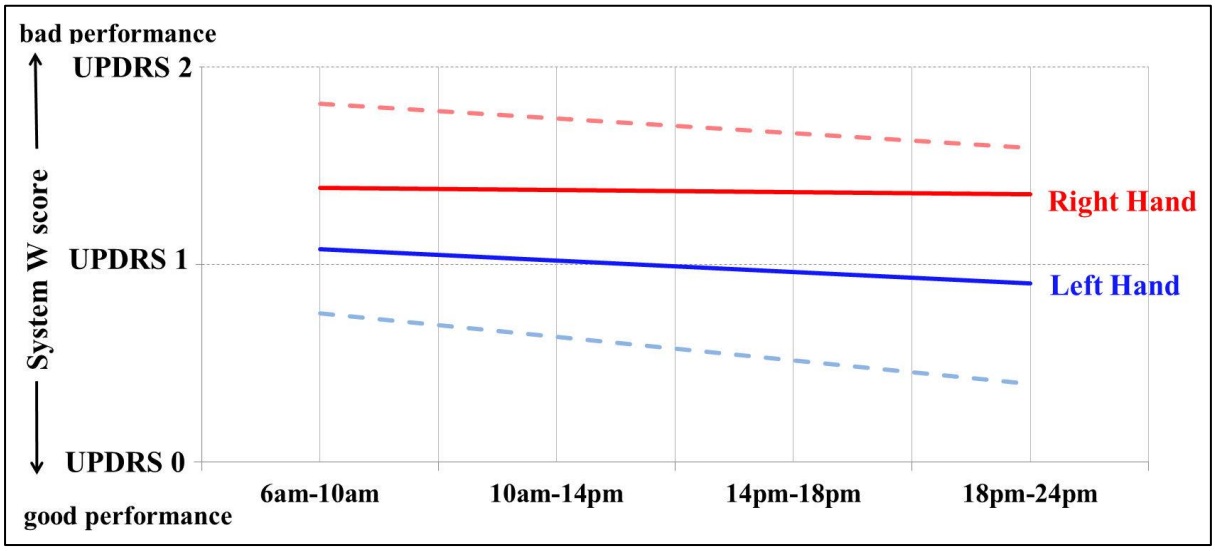

Figure 75: Linear trends for "time bands" data aggregation (Hand Movements task)
Left hand average system scores (solid blue); right hand average system scores (solid red); left hand average clinical scores (dashed blue); right hand average clinical scores (dashed red)

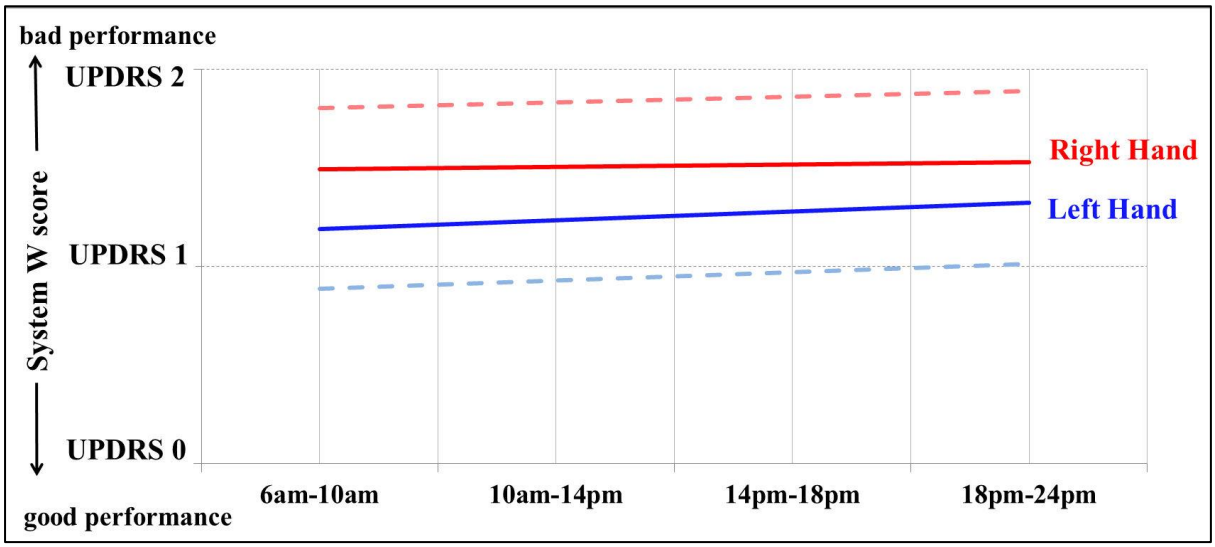

Figure 76: Linear trends for "time bands" data aggregation (Pronation Supination task)
Left hand average system scores (solid blue); right hand average system scores (solid red); left hand average clinical scores (dashed blue); right hand average clinical scores (dashed red)

In addition, higher scores were obtained for the tasks of Hand Movements (Figure 75) and Pronation Supination (Figure 76) compared to Finger Tapping task (Figure 74), indicating greater difficulty in performing this type of movement. Regarding the variations during the day, the performance of the right hand, on average, deteriorates slightly in the evening; while the performance of the left hand has a different behavior depending on the motor task. As previously pointed out, the acquisition sessions were carried out on the basis of the subject's work commitments: in fact, the analysis of the distribution of the acquisition sessions in the time bands showed that 34% was performed in the 10-14 band; 25% in 18-24 band; 22% in the 6-10 band and 19% in the 14-18 band. This imbalance condition could partially influence the results obtained, especially since the analysis did not consider the correlation between the time of the acquisition session and the time of drug intake. Nevertheless, the previous graphs demonstrate that, on the basis of an analysis by aggregate data, the system is able to provide an indication of the overall trend during the observation period in line with clinical one.

6.5 Main Results of the second experimental test: anomalies and fluctuations

In addition to the analysis by aggregate data, the experimental tests made it possible to accurately highlight the trend in motor performance during the day. In particular, the second experiment, that involved 4 participants (including the subject of the first experimental test), was aimed at evaluating the daily motor performance at different times from taking the drug dose. The experimental protocol required to start an acquisition session after thirty minutes

(0.5h), one and half hours (1.5h), two and half hours (2.5h), three and half hours (3.5h). Each participant performed the acquisition sessions according to the experimental protocol, every day of the week. Due to the limited observation period, in this case, it was preferred to consider the daily performance trend of each subject instead of proceeding with an aggregate analysis on all the data collected as in the previous experimental test. This type of analysis allowed to focus on two aspects: the presence of abnormalities with respect to habitual motor behavior and the presence of fluctuations in motor performance. By way of example, some interesting results of the analysis on $Subject_0$ are reported.

Regarding the detection of anomalies, Figure 77 shows an example of abnormal motor behavior detected during the Pronation-Supination task performed with the most compromised hand (right hand). The radar charts refer to two consecutive days (indicated as DAY_1 and DAY_2) but at the same evening time (21:23 p.m. for DAY_1 and 21:25 p.m. for DAY_2): the two performance were therefore acquired under the same pharmacological condition. The radar graph (red line) on the right, which refers to DAY_2, covers a larger area than the one (red line) on the left which refers to DAY_1: it is evident that the parameters, selected for the PS task (see Chapter 4), have increased their values (amplitude of hand rotation, speed and regularity of movement), clearly denoting a different motor behavior in DAY_2 and, in particular, a worsening of the motor performance due to greater impairment in performing the same task (radar chart expands outwards). In addition, the radar chart for DAY_1 also shows a slight deterioration compared to the reference performance (green line) which refers to the best performance of $Subject_0$ with right hand.

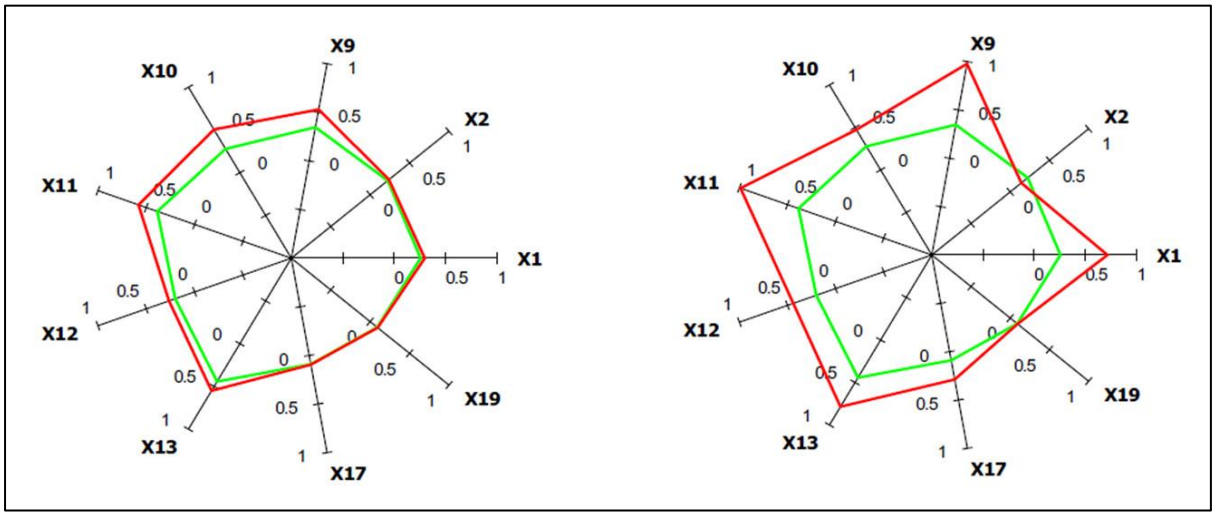

Figure 77: Example of abnormal behaviours during Pronation-Supination task with right hand
Left: DAY_1 performance at 21:23 p.m. (red line); Right: DAY_2 performance at 21:25 p.m. (red line).
Reference best right hand performance (green line)

This behavior was confirmed by the reference neurologist by observing the motor performance recorded by the system: the abnormal behavior in DAY_2 was due to the limited rotation of the hand (indicated by X1 parameter), to the reduced speed (indicated by X9-X13 parameters) and to the irregularity of movement duration (indicated by X17-X19 parameters). The cause was a form of rigidity and dystonic attitude of the right hand that does not occur in other days. The automatic assessment was able to capture the difference in motor performance, in accordance with the standard clinical evaluation, as shown in the table below, highlighting this difference both in the predicted and automatic "W" scores.

	DAY_1	**DAY_2**
CLINICAL EVALUATION (UPDRS SCORE)	2	3
SYSTEM EVALUATION (PREDICTED SCORE)	2 (47.2%)	3 (79.1%)
AUTOMATIC SCORE (UPDRS-LIKE SCORE)	1.56	2.78

With regard to fluctuations or alteration in motor performance, in Figure 78, Figure 79 and Figure 80 there are examples of daily assessment performed by the system and by the reference neurologist (from recorded videos) for the three upper limbs tasks referred to $Subject_0$, whose clinical picture indicated more severe impairment on the right and non-fluctuating condition. These figures show an almost constant difference between the two hands and how this difference changes in relation to the time elapsed between the treatment and the execution of tasks. In addition, further detailed information on motor performance can be extracted from this analysis. First of all, the analysis confirmed more severe impairment on the right hand which achieves higher clinical and instrumental scores, on average, than the left hand. Then, greater difficulty in performing CO and PS tasks which achieve higher clinical and instrumental scores, on average, than the FT task. For FT task, performance appears to improve 1.5 hours after drug intake, with progressive degradation for both hands beyond 2.5 hours, where the difference between the two hand performances increases. For CO task, the performance seems to improve 2.5 hours after drug intake with a progressive degradation for both hands over 3.5 hours: also in this case, the difference between the performances of the two hands increases. As for CO, the PS task performance improves after 2.5 hours from taking drugs with a progressive degradation for both hands over 3.5 hours: also in this case, the difference between the performances of the two hands increases even if there is, on average, less difference between them.

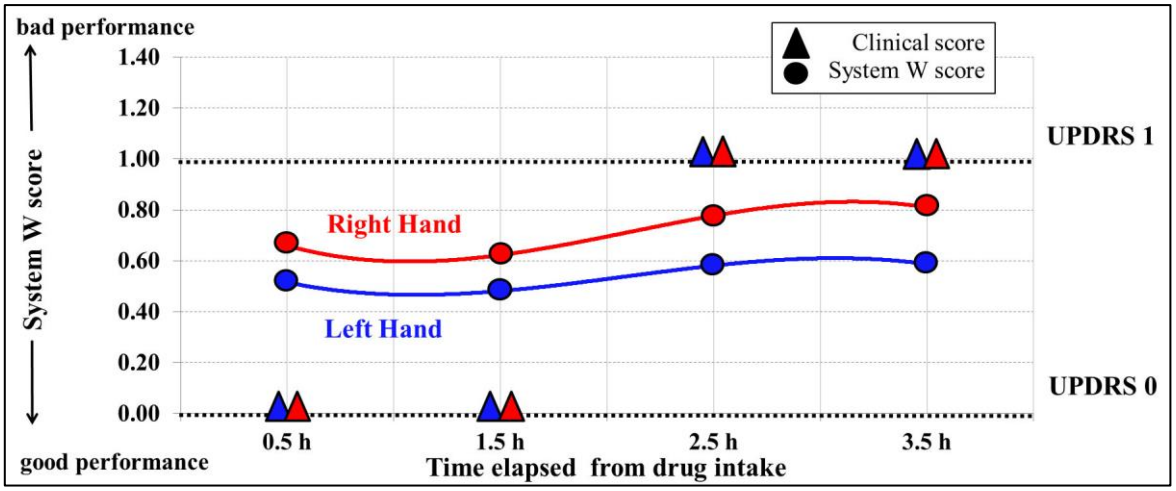

Figure 78: Example of clinical and instrumental assessment for FT task left hand (blue) and right hand (red) at different times from drug intake

[Image Source: Paper 3]

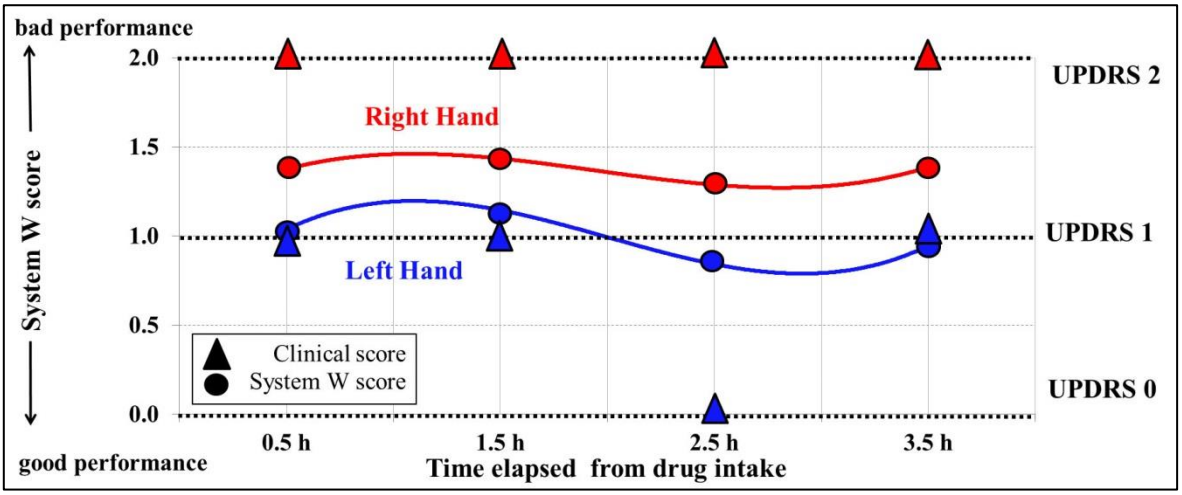

Figure 79: Example of clinical and instrumental assessment for CO task left hand (blue) and right hand (red) at different times from drug intake.

[Image Source: Paper 3]

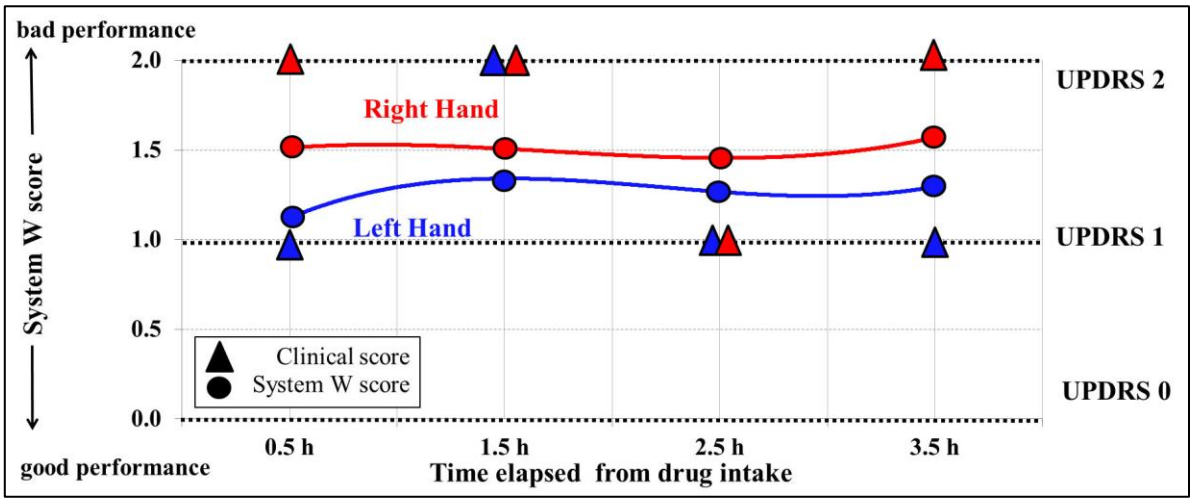

Figure 80: Example of clinical and instrumental assessment for PS task left hand (blue) and right hand (red) at different times from drug intake.

[Image Source: Paper 3]

Finally, it is important to note that this analysis revealed a change in motor performance, related to the time elapsed since taking the therapy, even though the subject was identified as non-fluctuating. Furthermore, the good agreement between the system and the neurological scores was confirmed: the system can evaluate tasks on a continuous scale compared to the standard discrete UPDRS, allowing to detect even minimal alterations in motor performance. This feature can certainly open up the possibility of investigating the interaction between drugs and motor effects with an objective approach also suitable for home environment, allowing to promptly detect and report any alterations in motor performance with respect to usual behavior.

6.6 Summary and Discussion

The purpose of this study was to integrate the 3D vision system for the upper limbs into the home monitoring platform, carrying out the first experimental tests of autonomous use of the acquisition system at patient's home. The Patient subsystem was equipped with a new human-computer interaction to facilitate the system management by means of a gestural interface that makes the acquisition system suitable for users with motor impairment. To allow for remote clinical supervision, the Clinician subsystem provides secure access to all relevant clinical data (videos, reports with automated scores and information entered by the subject) that can be viewed and analyzed by clinicians. The usability of the system has been also evaluated: the results confirm its suitability for the home monitoring of people with Parkinson’s disease.

The results obtained seem to be very promising, in particular thanks to the ability to detect anomalies and slight variations in motor performance, both considering the aggregation of data or single daily assessments, and the possibility of more frequent assessments of motor performance, impossible in clinical setting. Nevertheless, the results need to be consolidated by increasing the number of subjects involved and including other UPDRS tasks aimed at obtaining a comprehensive assessment of the neuro-motor status of people with PD. In any case, this study represents an example of how new strategies for Parkinson’s disease can improve clinical management and patient's quality of life.

Chapter 7

Conclusions and Future Work

In this chapter, the thesis contributions are summarized and the proposals for future extensions of this dissertation are presented.

7.1 Thesis Contributions

In this thesis, non-invasive and cost-effective solutions for the quantitative analysis of movement disorders in Parkinson's disease have been developed. The aim was to support standard clinical assessment of symptom severity and disease progression with objective functional parameters, estimated from the 3D trajectories of human body movements that are acquired with dedicated 3D vision systems based on RGB-Depth optical devices. Secondary objective was to make the implemented solutions easy to use, self-manageable and suitable for remote monitoring of patients at home, in order to improve the effectiveness of treatments and the quality of life through more frequent assessments of motor performance. This last point is fundamental for defining new clinical management strategies for the disease and patients, which ensure prompt action in case of deviations from normal motor behavior due to external factors or to a worsening of the symptoms.

First, a solution for the analysis of the UPDRS tasks related to the upper limbs was presented. In this case, the 3D vision system was based on RGB-Depth sensors suitable for “near-range” motion capture and was equipped with light gloves with color markers. A custom hand tracking algorithm was developed to recognize and track the 3D trajectories of hand and fingers using Computer Vision techniques. A set of kinematic parameters was initially defined, correlated to some physical quantities implicitly considered during the standard clinical evaluation as required by the qualitative evaluation criteria established by UPDRS. Different features selection procedures were considered to determine the most significant parameters, that is, the most correlated to standard clinical evaluations: the results show that the selected parameters have a good correlation with standard clinical evaluations and are able to discriminate severity classes, as also demonstrated by the radar charts representation, for each of the tasks considered. A Machine Learning approach, based on supervised classifiers, was then used to obtain the automatic assessment of motor performance starting from the selected functional parameters: several supervised classifiers

were considered and their performance were compared both in binary classification problems (healthy vs parkinsonians) and in multiclass classification problems (healthy vs UPDRS severity). The results indicate the good classification accuracy and a very low average classification error for all three motor tasks. In addition, a new UPDRS-like score was defined as the linear combination of the output probabilities of the best classifiers: this score shows greater correlation with clinical evaluations and the ability to detect slight alterations in motor performance since it is expressed on a continuous scale of values.

Second, a solution for the analysis of UPDRS tasks related to lower limbs, posture and postural instability was presented. In this case, the 3D vision system was based on RGB-Depth sensors suitable for "long range" motion capture. The manufacturer's body tracking algorithm was used to recognize and track the 3D trajectories of the joints of the skeletal model using a Machine Learning approach. The goal was to integrate the analysis of the upper limbs with these tasks to provide a more complete assessment of the motor status of subjects with PD. In addition, a new methodology for the analysis of postural instability, based on the sway of the body center of mass estimated from the skeletal model, was defined and analyzed. For each of the tasks examined, sets of kinematic and postural parameters were defined: also in this case, the feature selection procedures made it possible to determine the most significant parameters with respect to the standard clinical assessments. The methodology for the objective and automatic evaluation was the same used for the upper limbs and, also in this case, the results on correlation and classification accuracy were in line with what was previously obtained. In addition, the results indicate that the evaluation of postural instability using movements of the body center of mass is strictly related to clinical instability sub-score (PIGD) and can be proposed as an alternative to the standard UPDRS retro-pulsion test, impractical in unsupervised settings. Finally, the analysis of postural instability also confirmed the initial hypothesis of worsening in the presence of secondary or concomitant tasks, both in healthy subjects but in particular in subjects with PD: the detection of these alterations is essential to prevent the risk of falls during daily activities in which dual activities are very common.

Third, the results of the experimental home monitoring test were presented. The goal was to test the suitability and usability of the upper limb solution in home setting to monitor fluctuations or changes in motor performance throughout the day. The participants managed and interacted with the system autonomously using a gestural human-computer interaction to control the system functionalities, to make selections and to enter data through dedicated GUIs based on the hand tracking algorithms. The experimental test involved four participants

who used the system for observation periods during which they performed several daily acquisition sessions. The system was able to detect anomalies, changes in motor performance and to confirm the clinical picture of participants, in terms of impairment severity as assessed by the reference neurologists. With regards of usability, a series of questionnaires and interviews were administered to evaluate the satisfaction in the experience of using the system. The good results demonstrate the satisfaction and usability of the system, even in the presence of subjects with poor or no technological skills: this is an important point, especially in the perspective of the delivery and acceptance of technology at home, paving the way for new opportunities for patients and disease management.

7.2 Future Work

The future work related to the doctoral thesis will address the following topics:

- **Analysis of other UPDRS tasks**: in particular, the preliminary analysis of Gait will be enhanced and completed. Subsequently, the tremor and facial impairment will be considered to automatically and quantitatively evaluate further important effects of the symptoms of Parkinson's disease using the same technology in order to provide patients with a solution capable of performing a comprehensive assessment of the neuro-motor status
- **Rehabilitation:** the same technology and methodology is also applicable to motor and cognitive rehabilitation, in Virtual environments and using exergames, rehabilitation exercises designed as videogames to be more stimulating and engaging, which lead the patient to complete the rehabilitation plan while having fun
- **Application to other pathologies:** the same technology and methodology is also applicable to other pathological and neurological conditions characterized by movement disorders, such as post-stroke, normal pressure hydrocephalus, extrapyramidal disorders.

Most of these activities will be carried out in REHOME – Soluzioni ICT per la riabilitazione motoria e cognitiva nelle patologie neurologiche", a research project funded by Regione Piemonte (POR-FESR 2014-2020) that started in May 2019 and which will be completed in May 2022. The objective is to create a motor-cognitive monitoring and

rehabilitation platform for neurological diseases (Parkinson's disease, Stroke and MCI) with the aim of evaluating the effects of the rehabilitation treatments performed at patient's home.

7.3 The future of Telemedicine

The recent COVID-19 pandemic highlighted the need to enhance telemedicine and remote healthcare services: many of the clinics have been closed for months or have been reorganized to cope with the health emergency. The time between scheduled outpatient visits has increased, even more than before, to reduce access to hospital facilities. It is therefore clear how much telemedicine plays and will play a fundamental role in guaranteeing care and assistance especially in emergency conditions. The activities described in this PhD thesis were developed with this aim and point precisely in this direction, carrying out a first experimentation of remote monitoring service for PD. The initial goal was to monitor some of the UPDRS motor tasks using 3D vision systems and optical approaches: the results obtained and presented demonstrate the feasibility of this service. However, the use of this system for exclusively indoor, non-ubiquitous and non-continuous monitoring could make it limiting and not exhaustive with respect to all clinical aspects.

Just think of gait freezing (FOG), one of the most typical signs in advanced PD: due to its sudden onset during walking, episodes of FOG may only be detected by continuous monitoring and also outdoors monitoring, through for example wearable sensors or smartphones. The same is true, for example, for monitoring the motor fluctuations and complications in advanced PD, such as the percentage of hours in the OFF state, which would require continuous monitoring during daily activities.

It is therefore clear that each technological solution is focused on a specific need, but it is almost certainly complementary to other solutions that address different needs in the same context. The future of telemedicine will evolve precisely on this direction: the integration of different sensing technologies to cover multiple aspects of clinical interest, overcoming the intrinsic limits of each single system and expanding the potentiality of care and assistance services. After all, we have always been told that “unity is strength”.

References

1. United Nations - Department of Economic and Social Affairs Population Division, United Nations (2017). *World Population Ageing 2017 – Highlights (ST/ESA/SER.A/397).* Available online: http://www.un.org/en/development/desa/population/publications/pdf/ageing/WPA2017_Highlights.pdf
2. Bloom DE, Canning D, Lubet A (2015). *Global Population Aging: Facts, Challenges, Solutions & Perspectives*. Daedalus, 144(2), pp.80-92
3. World Health Organization (2015). *World Report on Ageing and Health*. ISBN 978-92-4-156504-2
4. Béjot Y, Yaffe K (2019). *Ageing Population*: *A Neurological Challenge*. Neuroepidemiology, 52, pp.76-77
5. European Commission (2018). *Silver Economy Study: How to stimulate the economy by hundreds of millions of Euros per year.* Available on line: https://ec.europa.eu/digital-single-market/en/news/silver-economy-study-how-stimulate-economy-hundreds-millions-euros-year
6. European Commission (2018). *The 2018 Ageing Report. Economic & Budgetary Projections for the 28 EU Member States (2016-2070).* European Economy. ISBN 978-92-79-77460-7
7. World Health Organisation (2011). *Global Health and Aging*. National Institutes of Health. Publication n. 11-7737
8. Hazra NC, Gulliford M (2017). *Evolution of the "fourth stage" of epidemiologic transition in people aged 80 years and over: population-based cohort study using electronic health records.* Population Health Metrics, 15 (18)
9. Harper K, Armelagos G (2010). *The Changing Disease-Scape in the Third Epidemiologic Transition.* International Journal of Environmental Research and Public Health, 7(2), pp.675-697
10. GBD 2016 Parkinson's disease Collaborators (2018). *Global, regional and national burden of Parkinson's disease 1990-2016: a systematic analysis for the Global Burden of Disease Study 2016*. The Lancet Neurology, 17(11), pp. 939-953
11. Shulman LM, Gruber-Baldini AL, Anderson KE, et al. (2008). *The evolution of disability in Parkinson disease.* Movement Disorders, 23(6), pp. 790-796
12. Tabish SA, Nabil S. (2015). *Future of Healthcare Delivery: Strategies that will Reshape the Healthcare Industry Landscape.* International Journal of Science and Research, 4(2), pp.727-758
13. Scott RE, Mars M. (2015). *Telehealth in the developing world: current status and future prospects.* Smart Homecare Technology and Telehealth, 3, pp.25-37
14. World Health Organization. (2010). *Telemedicine: opportunities and developments in the member states.* Report on the second global survey. ISBN 978-9-241564144
15. Boucenna S, Narzisi A, Tilmont E, et al. (2014). *Interactive Technologies for Autistic Children: A Review.* Cognitive Computation, 6, 722-740
16. Khan F, Amatya B, Kesselring J, Galea M. (2015). *Telerehabilitation for persons with multiple sclerosis.* Cochrane Database of Systematic Reviews, 4 (CD010508)
17. Pinto-Bruno AC, Garcia-Casal AJ, Csipke E, et al. (2017). *ICT-based applications to improve social health and social participation in older adults with dementia. A systematic literature review.* Aging & Mental Health, 21, pp. 58-65

18. Kolb B, Whishaw IQ (2001). *An Introduction to Brain and Behaviour*. ISBN 978-07-16-75169-0, Worth Publishers Inc., U.S., 576 pages, Chapter 10 – How Does the Brain Produce Movement?
19. Augustine JR (2008) *Human Neuroanatomy*. ISBN 978-0470961612, Blackwell Pub, 2nd Edition, 415 pages, Chapter 15 - 15.1 Regions Involved in Motor Activity
20. Chakravarthy VS, Joseph D, Bapi RS. (2010). *What do the basal ganglia do? A modeling perspective.* Biological Cybernetics, 103(3), pp. 237–253
21. Knudson DV, Morrison CS (2002) *Qualitative Analysis of Human Movement.* ISBN 0-7360-3462-5, Human Kinetics, 2nd Edition, 252 pages, Chapter 1 – Interdisciplinary Nature of Qualitative Analysis
22. Winter DA (2009) *Biomechanics and Motor Control of Human Movement.* ISBN 978-0-470-39818-0, John Wiley & Sons, Inc., 4th Edition, 370 pages.
23. Salter N, Darcus HD (1953) *The amplitude of forearm and of humeral rotation.* Journal of Anatomy, 87(4), pp. 407-418
24. Thomas DP, Whitney RJ (1959) *Postural Movements during normal standing in man.* Journal of Anatomy, 93(4), pp. 524-539
25. Murray MP, Seireg A, Scholtz RC (1967) *Center of gravity, center of pressure and supportive forces during human activities*. Journal of Applied Physiology, 23(6), pp. 831-838
26. Ramsey JD (1968) *The quantification of human effort and motion for the upper limbs.* International Journal of Production Research, 7(1), pp. 47-59
27. Polo O, Brissaud L, Sales B et al. (1968) *The validity of static charge sensitive bed in detecting obstructive sleep apneas.* European Respiratory journal, 1(4), pp. 330-336
28. Angel RW, Alston W, Higgins JR (1970) *Control of Movements in Parkinson's Disease*. Brain, 93, pp.1-14
29. Salzer M (1972) *Three-dimensional tremor measurements of the hand*. Journal of Biomechanics, 5(2), pp. 217-221
30. Winter DA, Greenlaw RK, Hobson DA (1972) *Television-Computer Analysis of Kinematics of Human Gait*. Computer and Biomedical Research, 5, pp.498-504
31. Lamoreux LW (1971) *Kinematic measurements in the study of human walking*. Bulletin of Prosthetic Research, 10(15), pp.3.84
32. Velasco F, Velasco M (1973) *A quantitative evaluation of the effects of L-Dopa on Parkinson's Disease*. Neuropharmacology, 12, pp.89-99
33. Morris JRW (1973) *Accelerometry – A technique for the measurement of human body movements*. Journal of Biomechanics, 6(6), pp. 733-736
34. Ackmann JJ, Sances A, Larson SJ, Baker JB (1977) *Quantitative Evaluation of Long-Term Parkinson Tremor*, IEEE Transactions on Biomedical Engineering, 24(1), pp. 49-56
35. Stern GM, Franklyn SE, Imms FJ, Prestidge SP (1983) *Quantitative assessments of gait and mobility in Parkinson's disease.* Journal of Neural Transmission (Supplementum), 19, pp. 201-214
36. Colyer SL, Murray E, Cosker DP, Salo AIT (2018) *A Review of the Evolution of Vision-Based Motion Analysis and the Integration of Advanced Computer Vision Methods Towards Developing a Markerless System*. Sports Med Open, 4(1), 24
37. Cimolin V, Galli M, Grugni G, et al. (2010) *Gait Patterns in Prader-Willi and Down syndrome patients.* Journal of NeuroEngineering and Rehabilitation, 7, 28
38. Grecco LAC, Carvalho Duarte N, Mendoza ME, et al. (2014) *Transcranial direct current stimulation during treadmill training in children with cerebral palsy: A randomized controlled double-blind clinical trial*. Research in Developmental Disabilities, 35(11), pp. 2840-2848

39. Lempereur M, Brochard S, Mao L, et al. (2012) *Validity and reliability of shoulder kinematics in typically developing children and children with hemiplegic cerebral palsy*. Journal of Biomechanics, 45(11), pp. 2028-2034
40. Vismara L, Menegoni F, Zaina F, et al. (2010) *Effect of obesity and low back pain on spinal mobility: a cross sectional study in women*. Journal of NeuroEngineering and Rehabilitation, 7, 3
41. Tsarouhas A, Iosifidis M, Kotzamitelos D, et al. (2010) *Three-Dimensional Kinematic and Kinetic Analysis of Knee Rotational Stability After Single and Double-Bundle Anterior Cruciate Ligament Reconstruction.* Arthroscopy: The Journal of Arthroscopic & Related Surgery, 26(7), pp. 885-893
42. Zhang Z (2012) *Microsoft Kinect and its effect*. IEEE Multimedia, 19(2), pp. 4-10
43. Mousavi Hondori H, Khademi M (2014) *A Review on Technical and Clinical Impact of Microsoft Kinect on Physical Therapy and Rehabilitation*. Journal of Medical Engineering, 846514
44. Otte K, Kayser B, Mansow-Model S, et al (2016) *Accuracy and Reliability of the Kinect Version 2 for Clinical Measurement of Motor Function*. PlosOne, 11(11), e0166532
45. Clark RA, Pua YH, Ritchie C, et al. (2012) *Validity of Microsoft Kinect for assessment of postural control.* Gait & Posture, 36(3), pp. 372-377
46. Galna B, Barry G, Mhiripiri D, et al. (2014) *Accuracy of the Microsoft Kinect sensor for measuring movement in people with Parkinson's disease.* Gait & Posture, 39(4), pp. 1062-1068
47. Chang YJ, Chen SF, Huang JD (2011) *A Kinect-based system for physical rehabilitation: A pilot study for young adults with motor disabilities*. Research in Developmental Disabilities, 32(6), pp. 2566-2570
48. Metcalf CD, Robinson R, Malpass AJ, et al. (2013) *Markerless Motion Capture and Measurement of Hand Kinematics: Validation and Application to Home-Based Upper Limb Rehabilitation.* IEEE Transactions on Biomedical Engineering, 60(8), pp. 2184-2192
49. Olesh EV, Yakovenko S, Gritsenko V (2014) *Automated Assessment of Upper Extremity Movement Impairment due to Stroke*. PlosOne, 9(8), e104487
50. Webster D, Celik O (2014) *Systematic review of Kinect applications in elderly care and stroke rehabilitation.* Journal of NeuroEngineering and Rehabilitation, 11, 108
51. Springer S, Seligmann G (2016) *Validity of the Kinect for Gait Assessment: A Focused Review*. Sensors, 16(2), 194
52. Ibanez R, Soria A, Teyseyre A, Campo M (2014) *Easy gesture recognition for Kinect.* Advances in Engineering Software, 76, pp. 171-180
53. Lun R, Zhao W (2015) *A survey of Applications and Human Motion Recognition using Microsoft Kinect.* International Journal of Pattern Recognition and Artificial Intelligence, 29(5), 1555008
54. Mukhopadhyay SC (2015) *Wearable Sensors for Human Activity Monitoring: A Review.* IEEE Sensors Journal, 15(3), pp. 1321-1330
55. Patel S, Park H, Bonato P, et al (2012) *A review of wearable sensors and systems with application in rehabilitation*. Journal of Neuroengineering and Neurorehabilitation, 9, 21
56. Heikenfeld J, Jajack A, Rogers J, et al. (2018) *Wearable Sensors: Modalities, Challenges, and Prospects.* Lab Chip, 18(2), pp. 217-248
57. Long X, Yin B, Aarts RM (2009) *Single-Accelerometer-based daily physical activity classification.* Proceedings of 31st Annual International Conference of IEEE Engineering in Medicine and Biology Society (EMBC 2009), 2-6 September 2009, Minneapolis, Minnesota, USA

58. Nam Y, Roo S, Lee C (2013) *Physical* Activity *Recognition using multiple sensors embedded in a wearable device.* ACM Transactions on Embedded Computing Systems, 12(2), 26
59. Gravina R, Alinia P, Fortino G, et al (2016) *Multi-Sensor Fusion in Body Sensor Networks: State-of-the-art and research challenges*. Information Fusion, 35, pp. 68-80
60. Parisi F, Ferrari G, Giuberti M, et al (2015) *Body-Sensor-Network-Based Kinematic Characterization and Comparative Outlook of UPDRS Scoring in Leg Agility, Sit-to-Stand, and Gait Tasks in Parkinson's Disease*. IEEE Journal on Biomedical and Health Informatics, 19(6), pp. 1777-1793
61. Reyes-Ortiz JL (2015) *Smartphone-based Human Activity Recognition*. Springer Theses, ISBN 978-3-319-14273-9, Chapter 2 – Background, pp. 9-35
62. Capela NA, Lemaire ED, Baddour N (2015) *Feature Selection for Wearable Smartphone-Based Human Activity Recognition with Able bodied, Elderly, and Stroke Patients*. PloS One, 10(4), e0124414
63. Mellone S, Tacconi C, Chiari L (2012) *Validity of Smartphone-based instrumented Timed Up and Go*. Gait & Posture, 36(1), pp. 163-165
64. Ong AA, Gillespie MB (2016) *Overview of smartphone applications for sleep analysis.* World Journal of Otorhinolaryngology-Head and Neck Surgery, 2(1), pp. 45-49
65. Ellis RJ, NG YS, Zhu S, et al. (2015) *A Validated Smartphone-Based Assessment of Gait and Gait Variability in Parkinson's Disease.* PloS One, 10(10), e0141694
66. Abbate S, Avvenuti M, Bonatesta F, et al. (2012) *A smartphone-based fall detection system.* Pervasive and Mobile Computing, 8(6), pp. 883-899
67. Kos A, Tomazic S, Umek A (2016) *Suitability of Smartphone Inertial Sensors for Real-time Biofeedback Applications*. Sensors, 16(3), 301
68. Parkinson J (1817) *An essay on Shaking Palsy*. London, Sherwood, Neely and Jones.
69. Goetz CG (2011) *The History of Parkinson's Disease: Early Clinical Descriptions and Neurological Therapies*. Cold Spring Harbor Perspectives in Medicine, 1(1), a008862
70. Charcot JM (1862) *De la paralysie agitante*. Ouvres Complètes, Leçons sur le maladies du système nerveux, pp. 155-188
71. Richer P, Meige H (1895) *Etude morphologique sur le maladie de Parkinson.* Novelle Iconographie de la Salpêtrière, 8, pp. 361-371
72. Babinski J (1921) *Kinésie Paradoxale*. Rev Neurol, 37, pp. 1266-1270
73. Foix MC, Nicolesco J (1925) *Les noyaux gris centraux et la région mésencéphale-sous-optique.* Masson, Paris.
74. Brissaud E (1925) *Leçon sur les maladies nerveuses*. Masson, Paris.
75. Greenfield JG, Bosanquet FD (1953) *The brain-stem lesions in Parkinsonism.* Journal of Neurology, Neurosurgery & Psychiatry, 16(4), pp. 216-226
76. Hoehn MM, Yahr MD (1967) *Parkinsonism: Onset, progression and mortality.* Neurology, 17(5), pp. 427-442
77. Von Campenhausen S, Bornschein B, Wick R, et al (2005) *Prevalence and Incidence of Parkinson's disease in Europe*. European Neuropsychopharmacology, 15, pp. 473-490
78. Associazione Italiana Parkinsoniani, *Carta dei Diritti del Parkinsoniano*. Available online: https://www.parkinson.it/archivio-documenti/send/9-varie/177-carta-dei-diritti-del-parkinsoniano.html (Last access: April 2020)
79. https://clinicalgate.com/the-basal-ganglia/#bib11 (Last access: April 2020)
80. https://www.kenhub.com/en/start/neuroanatomy (Last access: April 2020)
81. Jankovic J (2008) *Parkinson's disease: clinical features and diagnosis*. J Neuro Neurosurg Psychiatry, 79(4), pp. 368-376

82. Massano J, Bhatia KP (2012) *Clinical Approach to Parkinson's disease: Features, Diagnosis, and Principles of Management.* Cold Spring Harb Perspect Med, 2(6), a008870
83. Hughes AJ, Daniel SE, Kilford L, Lees AJ (1992) *Accuracy of clinical diagnosis of idiopathic Parkinson's disease: a clinical and pathological study of 100 cases.* J Neurol Neurosurg Psychiatry, 55(3), pp. 181-184
84. Connolly BS, Lang AE (2014) *Pharmacological treatment of Parkinson's disease: a review.* Jama, 311(16), pp. 1670-1683
85. Pedrosa DJ, Timmerman L (2013) *Review: Management of Parkinson's disease.* Neuropsychiatr Dis Treat, 9, pp. 321-340
86. Oertel WH (2017) *Recent advances in treating Parkinson's disease.* F1000Res, 6, 260
87. Schapira AHW, Emre M, Jenner P, Poewe W (2009) *Levodopa in the treatment of Parkinson's disease.* European Journal of Neurology, 16(9), pp. 982-989
88. The National Collaborating Centre for Chronic Conditions (2006) *Symptomatic pharmacological therapy in Parkinson's disease.* London: Royal College of Physicians, ISBN 978-1-86016-283-1, pp. 59-100
89. Weaver FM, Follett KA, Stern M, et al (2012) *Randomized trial of deep brain stimulation for Parkinson's disease.* Neurology, 79(1), pp. 55-65
90. Keus S, Munneke M, Graziano M, et al (2014) *European Physiotherapy Guideline for Parkinson's Disease*. Available on line: https://www.parkinsonnet.nl/app/uploads/sites/3/2019/11/eu_guideline_parkinson_guideline_for_pt_s1.pdf (Last access: May 2020)
91. Abbruzzese G, Marchese R, Avanzino L, Pelosin E (2016) *Rehabilitation for Parkinson's disease: Current outlook and future challenges.* Parkinsonism & Related Disorders, 22(Suppl. 1), pp. S60-S64
92. Opara J, Malecki A, Malecka E, Socha T (2017) *Motor Assessment in Parkinson's disease.* Ann Agric Environ Med, 24(3), pp. 411-415
93. Hoehn M, Yahr M (1967) *Parkinsonism: onset, progression and mortality*. Neurology, 17(5), pp. 427–442
94. Goetz CG, Poewe W, Rascol O, et al (2004) *Movement Disorder Society Task Force Report on the Hoehn and Yahr Staging Scale: Status and Recommendations. The Movement Disorder Society Task Force on Rating Scales for Parkinson's Disease*. Movement Disorders, 19(9), pp. 1020–1028
95. Zhao YJ, Wee HL, Chan YH, et al (2010) *Progression of Parkinson's disease as evaluated by Hoehn and Yahr stage transition times*. Mov Disord, 25(6), pp. 710–716
96. Fahn S, Elton R (1987) *The Unified Parkinson's Disease Rating Scale.* Recent developments in Parkinson disease, pp. 153-163
97. Goetz CG, Fahn S, Martinez-Martin P, et al (2007) *Movement Disorder Society-sponsored revision of the Unified Parkinson's Disease Rating Scale (MDS-UPDRS): Process, format, and clinimetric testing plan*. Mov Disord, 22(1), pp. 41–47
98. Richards M, Marder K, Cote L, Mayeux R (1994) *Interrater reliability of the Unified Parkinson's Disease Rating Scale motor examination.* Mov Disord, 9(1), pp. 89-91
99. Goetz CG, Stebbins GT, Chmura TA, et al (1995) *Teaching Tape for the Motor Section of the Unified Parkinson's Disease Rating Scale*. Mov Disord, 10(3), pp. 263-266
100. Van der Kruk E, Rejine MM (2018) *Accuracy of human motion capture systems for sport applications: state-of-the-art review.* European Journal of Sport Science, 8(6), pp. 806-819
101. Davis RB, Ounpuu S, Tyburski D, Gage JR (1991) *A gait analysis data collection and reduction technique*. Human Movement Science, 10(5), pp. 575–587

102. Ferrari A, Benedetti MG, Pavan E (2008) *Quantitative comparison of five current protocols in gait analysis.* Gait & Posture, 28(2), pp. 207-216
103. Aggarwal JK, Cai Q (1999) *Human Motion Analysis: A Review*. Computer Vision & Image Understanding, 73(3), pp. 428-440
104. Erol A, Bebis G, Nicoluscu M, et al (2007) *Vision-based hand pose estimation: A review*. Computer Vision and Image Understanding, 108(1), pp. 52-73
105. Poppe R (2007) *Vision-based human motion analysis: an overview.* Computer Vision & Image Understanding, 108(1,2), pp. 4-18
106. Zalevsky Z, Shpunt A, Maizels A, Garcia J (2007) *Method and System for object reconstruction.* Patent, WO2007043036
107. Kinect for Windows Programming Guide . Available online https://www.slideshare.net/katsudream/kinect-for-windows-sdk-programming-guide (Last Access: July 2020)
108. Shotton J, Fitzgibbon A, Cook M, et al (2011) *Real-time human pose recognition in parts from single depth images*. IEEE Conference on Computer Vision and Pattern Recognition, Providence, RI, US, June 2011
109. Kinect for Window SDK 2.0 – Available online: https://developer.microsoft.com/it-it/windows/kinect/ (Last Access: July 2020)
110. Intel RealSense D415 – Available online: https://www.intelrealsense.com/depth-camera-d415/ (Last Access: July 2020)
111. Intel RealSense D435 – Available online: https://www.intelrealsense.com/depth-camera-d435/ (Last Access: July 2020)
112. Astra series – Available online: https://orbbec3d.com/product-astra-pro/ (Last Access: July 2020)
113. Nuitrack SDK – Available online: https://nuitrack.com/ (Last Access: July 2020)
114. Leap Motion – Available online: https://developer.leapmotion.com/ (Last Access: July 2020)
115. Microsoft Kinect Azure – Available online: https://azure.microsoft.com/it-it/services/kinect-dk/ (Last Access: July 2020)
116. OpenPose – Available online: https://github.com/CMU-Perceptual-Computing-Lab/openpose (Last Access: July 2020)
117. Zago M, Luzzago M, Marangoni T, et al (2020) *3D Tracking of Human Motion Using Visual Skeletonization and Stereoscopic Vision.* Front. Bioeng. Biotechnol., 00181
118. Votta V (2020) *Evaluation of low-cost optical motion capture systems for the assessment of parameters in neurologic rating scales*. Master's Thesis in Biomedical Engineering, Politecnico di Torino
119. Heldman DA, Giuffrida JP, Chen R, et al (2011) *The modified bradykinesia rating scale for Parkinson's disease: Reliability and comparison with kinematic measures.* Mov Disord, 26, pp. 1859-1863
120. Taylor Tavares AL, Jefferis GS, Koop M, et al (2005) *Quantitative measurements of alternating finger tapping in Parkinson's disease correlate with UPDRS motor disability and reveal the improvement in fine motor control from medication and deep brain stimulation.* Mov Disord, 20, pp. 1286-1298
121. Espay AJ, Beaton DE, Morgante F, et al (2009) *Impairments of speed and amplitude of movement in Parkinson's disease : A pilot study.* Mov Disord, 24, pp. 1001-1008
122. Stamatakis J, Ambroise J, Cremers J, et al (2013) *Finger Tapping Clinimetrics Score Prediction in Parkinson's Disease Using Low-Cost Accelerometers.* Comput. Intell. Neurosci., 717853

123. Oess NP, Wanek J, Curt A. (2012) *Design and evaluation of a low-cost instrumented glove for hand function assessment.* J Neuroeng. Rehabil., 9(2)
124. Khan T, Nyholm D, Westin J, et al (2014) *A computer vision framework for finger-tapping evaluation in Parkinson's disease.* Artif. Inttell. Med., 60, pp. 27-40
125. Jobbagy A, Harcos P, Karoly R, et al (2005) *Analysis of finger-tapping movement.* J. Neurosci. Methods, 141, pp. 29-39
126. Butt AH, Rovini E, Dolciotti C, et al (2017) *Leap Motion evaluation for assessment of upper limb motor skills in Parkinson's disease.* Proceedings of ICORR 2017, London, UK, July 2017, pp. 116-121
127. Bank JMO, Marinus J, Meskers CGM, et al (2017) *Optical Hand Tracking: A novel Technique for the Assessment of Bradykinesia in Parkinson's Disease.* Mov. Disord. Clin. Pract, 4, pp. 875-883
128. Dror B, Yanai E, Frid A, et al (2014) *Automatic assessment of Parkinson's Disease from natural hands movements using 3D depth sensor*. Proceedings of IEEEI 2014, Eliat, Israel, December 2014
129. Guttman L (1944) *A Basis For Scaling Qualitative Data*. American Sociological Review, 9(2), pp. 139-150. Published by American Sociological Association.
130. Radar Chart - Available online: https://en.wikipedia.org/wiki/Radar_chart (Last Access: August 2020)
131. McCallum A (2019) *Graphical Models, Lecture2: Bayesian Network Represention* – Available online: https://people.cs.umass.edu/~mccallum/courses/gm2011/02-bn-rep.pdf (Last Access: August 2020)
132. McLachlan GJ (2004) *Discriminant Analysis and Statistical Pattern Recognition*. Wiley Interscience
133. Cramer GS (2003) *The origins and development of logit model*. Cambridge.org
134. Altman NS (1991) *An introduction to Kernel and Nearest-Neighbor Non-Parametric Regression*. The American Statistician, 4(3), pp. 175-185
135. Cortes C, Vapnik V (1995) *Support Vector Networks.* Machine Learning, 20, pp. 273-297
136. Fawcett T (2015) *The basic of classifiers evaluation: Part 1* – Available online: https://www.svds.com/the-basics-of-classifier-evaluation-part-1 (Last access: August 2020)
137. Espay AJ, Bonato P, Nahab FB, Maetzler W, et al (2016) *Technology in Parkinson's disease: Challenges and opportunities*. Mov. Disord., 31, pp. 1272–1282
138. Rovini E, Maremmani C, Cavallo F (2017) *How Wearable Sensors Can Support Parkinson's Disease Diagnosis and Treatment: A Systematic Review*. Front. Neurosci.,11, 555
139. Ossig C, Antonini A, Buhmann C, Classen J, et al (2016) *Wearable sensor-based objective assessment of motor symptoms in Parkinson's disease.* J. Neural Transm.,123, pp. 57–64.
140. Parisi F, Ferrari G, Giuberti M, et al (2015) *Body-sensor-network-based kinematic characterization and comparative outlook of UPDRS scoring in leg agility, sit-to-stand, and Gait tasks in Parkinson's disease.* J. Biomed. Heal Inf.,19, pp. 1777–1793
141. Patel S, Lorincz K, Hughes R, Huggins N, et al (2009) *Monitoring motor fluctuations in patients with Parkinson's disease using wearable sensors*. IEEE Trans. Inf. Technol. Biomed.,13, pp. 864–873
142. Boroojerdi B, Ghaffari R, Mahadevan N et al. (2019) *Clinical feasibility of a wearable, conformable sensor patch to monitor motor symptoms in Parkinson's disease*. Parkinsonism Relat. Disord.,61, pp. 70–76

143. Schlachetzki JCM, Barth J, Marxreiter F, Gossler J et al. (2017) *Wearable sensors objectively measure gait parameters in Parkinson's disease.* PlosOne, 0183989
144. Silva de Lima AL, Evers LJW, Hahn T, et al. (2017) *Freezing of gait and fall detection in Parkinson's disease using wearable sensors: a systematic review*. J Neurol., 264, pp. 1642-1654
145. Phan D, Horne M, Pathirana PN, Farzanehfar P (2018) *Measurement of Axial Rigidity and Postural Instability Using Wearable Sensors*. Sensors, 18(2), 495
146. Linares-del Reyal M, Vela-Desojo L, Cano-de la Cuerda R (2019) *Mobile phone applications in Parkinson's disease: a systematic review*. Neurologia, 34(1), pp. 38-54
147. Zhan A, Mohan S, Tarolli C et al. (2018) *Using Smartphones and Machine Learning to Quantify Parkinson Disease Severity*. JAMA Neurology, 75(7), pp. 876-880
148. Capeccia M, Pepa L, Verdini F, Ceravolo MG (2016) *A smartphone-based architecture to detect and quantify freezing of gait in Parkinson's disease*. Gait & Posture, 50, pp. 28-33
149. Pepa L, Verdini F, Spalazzi L (2017) *Gait parameter and event estimation using smartphones.* Gait & Posture, 57, pp. 217-223
150. Clark RA, Pua YH, Oliveira CC, Bower KJ, et al. (2015*) Reliability and concurrent validity of the Microsoft Xbox One Kinect for assessment of standing balance and postural control*. Gait Posture,42, pp. 210–213
151. Müller B, Ilg W, Giese MA, Ludolph N (2017) *Validation of enhanced Kinect sensor based motion capturing for gait assessment*. PlosOne,12,0175813
152. Mishra AK, Skubic M, Willis BW, Guess TM, et al. (2017) *Examining methods to estimate static body sway from the Kinect V2. 0 skeletal data: Implications for clinical rehabilitation*. Proceedings of 11th EAI International Conference on Pervasive Computing Technologies for Healthcare, Barcelona, Spain, 23–26 May 2017; pp. 127–135.
153. Li Q, Wang Y, Sharf A, Cao Y, Tu C, et al. (2018) *Classification of gait anomalies from kinect.* Vis. Comput.,34, pp. 229–241
154. Kähär H, Taba P, Nõmm S, Medijainen K (2017) *Microsoft Kinect-based differences in lower limb kinematics during modified timed up and go test phases between men with and without Parkinson's disease.* Acta Kinesiologiae Universitatis Tartuensis 2017
155. Knippenberg E, Verbrugghe J, Lamers I, et al. (2017) *Markerless motion capture systems as training device in neurological rehabilitation: A systematic review of their use, application, target population and efficacy*. J. Neuroeng. Rehabil.,14, 61
156. Ejupi A, Brodie M, Gschwind YJ, Lord SR, et al. (2016) *Kinect-Based Five-Times-Sit-to-Stand Test for Clinical and In-Home Assessment of Fall Risk in Older People*. Gerontology, 62(1), pp. 118-124
157. Dehbandi B, Barachant A, Smeragliuolo AH, et al. (2017) *Using data from the Microsoft Kinect 2 to determine postural stability in healthy subjects: A feasibility trial*. PlosOne, 0170890
158. Frenklach A, Louie S, Koop MM, Bronte-Stewart H (2009) *Excessive postural sway and the risk of falls at different stages of Parkinson's disease*. Mov Disord, 24(3), pp. 377-385
159. Ozinga SJ, Machado AG, Miller Koop M, et al. (2015) *Objective assessment of postural stability in Parkinson's disease using mobile technology*. Mov Disord., 30(9), pp. 1214-1221
160. Mancini M, Horak FB, Zampieri C, et al. (2011) *Trunk accelerometry reveals postural instability in untreated Parkinson's disease*. Parkinsonism Relat Disord., 17(7), pp. 557-562
161. Johnson L, James I, Rodrigues J, et al (2013) Clinical and posturography correlates of falling in Parkinson's disease. Mov Disord., 28(9), pp. 1250-1256

162. Hasan SS, Robun DW, Szurkus DC, et al. (1996) *Simultaneous measurement of body center of pressure and center of gravity during upright stance*. Part I: Methods, Gait and Posture, 4(1), pp. 1-10

163. Leach JM, Mancini M, Peterka RJ, et al. (2014) *Validating and calibrating the Nintendo Wii balance board to derive reliable center of pressure measures*. Sensors, 14(10), pp. 18244-18267

164. Lafond D, Duarte M. Prince F (2004) *Comparison of three methods to estimate the center of mass during balance assessment*. J. Biomech., 37, pp. 1421–1426

165. González A, Hayashibe M, Bonnet V, et al. (2014) *Whole Body Center of Mass Estimation with Portable Sensors: Using the Statically Equivalent Serial Chain and a Kinect*. Sensors, 14, pp. 16955–16971

166. Clauser CE, McConville JT, Young JW (1971) *Weight, Volume, and Center of Mass Segments of the Human Body*. J. Occup. Med, 13(5), 270

167. Winter A (2009) *Biomechanics and motor control of human body*. 3rd Edition, Wiley & Sons.

168. Gutierrez EM, Bartonek A, Haglund-Akerlind Y, et al. (2003) *Centre of mass motion during gait in person with myelomengocele*. Gait Posture, 18, pp. 37–46.

169. Jankovic J, McDermott M, Carter J, Gauthier S, et al. (1990) *Variable expression of Parkinson's disease: A base-line analysis of the DATATOP cohort. The Parkinson study group*. Neurology, 40, pp. 1529–1534

170. Richards M, Marder K, Cote L, Mayeux R. (1994) *Interrater reliability of the Unified Parkinson's Disease Rating Scale motor examination*. Mov. Disord., 9, pp. 89–91

171. Lewis JR (2002) *Psychometric evaluation of the PSSUQ using data from five years of usability studies*. International Journal of Human-Computer Interaction, 14(3-4), pp. 463-488

172. Likert R (1932) *A Technique for the Measurement of Attitudes.* Archives of Psychology, 140, pp. 1-55